Medical Image Analysis 88 (2023) 102869

Contents lists available at ScienceDirect

Medical Image Analysis

journal homepage: www.elsevier.com/locate/media

Survey paper

Multi-modality cardiac image computing: A survey

Lei Li [a,*], Wangbin Ding [c], Liqin Huang [c], Xiahai Zhuang [b,1], Vicente Grau [a,1]

[a] Department of Engineering Science, University of Oxford, Oxford, UK
[b] School of Data Science, Fudan University, Shanghai, China
[c] College of Physics and Information Engineering, Fuzhou University, Fuzhou, China

ARTICLE INFO

Keywords:
Multi-modality imaging
Cardiac
Registration
Fusion
Segmentation
Review

ABSTRACT

Multi-modality cardiac imaging plays a key role in the management of patients with cardiovascular diseases. It allows a combination of complementary anatomical, morphological and functional information, increases diagnosis accuracy, and improves the efficacy of cardiovascular interventions and clinical outcomes. Fully-automated processing and quantitative analysis of multi-modality cardiac images could have a direct impact on clinical research and evidence-based patient management. However, these require overcoming significant challenges including inter-modality misalignment and finding optimal methods to integrate information from different modalities.

This paper aims to provide a comprehensive review of multi-modality imaging in cardiology, the computing methods, the validation strategies, the related clinical workflows and future perspectives. For the computing methodologies, we have a favored focus on the three tasks, i.e., registration, fusion and segmentation, which generally involve multi-modality imaging data, *either combining information from different modalities or transferring information across modalities*. The review highlights that multi-modality cardiac imaging data has the potential of wide applicability in the clinic, such as trans-aortic valve implantation guidance, myocardial viability assessment, and catheter ablation therapy and its patient selection. Nevertheless, many challenges remain unsolved, such as missing modality, modality selection, combination of imaging and non-imaging data, and uniform analysis and representation of different modalities. There is also work to do in defining how the well-developed techniques fit in clinical workflows and how much additional and relevant information they introduce. These problems are likely to continue to be an active field of research and the questions to be answered in the future.

1. Introduction

Cardiovascular diseases (CVDs) remain one of the leading causes of mortality worldwide. Non-invasive cardiac imaging techniques can provide anatomical and functional information on health and pathology, and have been developed and employed extensively for the diagnosis and treatment of CVDs. Several imaging modalities are used for cardiac assessment, including X-ray, computed tomography (CT), magnetic resonance imaging (MRI), echocardiography (Echo), positron emission tomography (PET), and single-photon emission computed tomography (SPECT) (Laczay et al., 2021). As Fig. 1 shows, each imaging modality manifests particular information, and a single modality may provide insufficient and/or ambiguous information regarding the condition of the heart that is a nonrigid and dynamic structure. Combining the complementary information from multi-modality cardiac images can be beneficial in establishing a more accurate diagnosis or assisting clinicians in the treatment management of CVDs (Valsangiacomo Buechel and Mertens, 2012; Olsen et al., 2016; Puyol-Antón et al., 2022).

However, automated cardiac image computing is particularly challenging on account of normal or pathologic deformation of the heart during the respiratory and cardiac cycle. Furthermore, there exist misalignment and intensity variations among different modalities, and the imaging phases, field-of-views (FOVs), and resolution of different acquisitions can vary significantly. Several research methods have been developed to process multi-modality cardiac images, including *registration*, *fusion*, and *segmentation* of multi-modality images. With multi-modality images, image registration aims to align the available measurements (shape, function, pathology, etc.) into the same anatomical Ref. Zhuang (2019). Image fusion intends to integrate several imaging modalities in an optimal way for visualization or decision-making. Image segmentation attempts to extract target regions by combining

* Corresponding author.
E-mail address: lei.li@eng.ox.ac.uk (L. Li).
[1] Both are co-senior authors and contribute equally.

https://doi.org/10.1016/j.media.2023.102869
Received 25 August 2022; Received in revised form 1 May 2023; Accepted 12 June 2023
Available online 16 June 2023

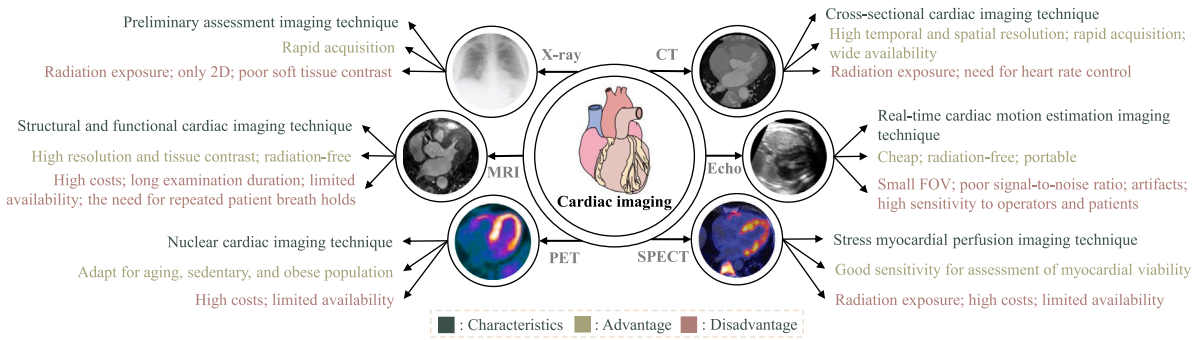

Fig. 1. Examples of cardiac imaging techniques from different modalities with their characteristics, advantages and disadvantages. CT: computed tomography; MRI: magnetic resonance imaging; Echo: echocardiography; PET: positron emission tomography; SPECT: single-photon emission computed tomography. Here, X-ray, PET and SPECT images adapted from Kholiavchenko et al. (2020), Quail and Sinusas (2017) and Klaassen et al. (2020) with permission, respectively.

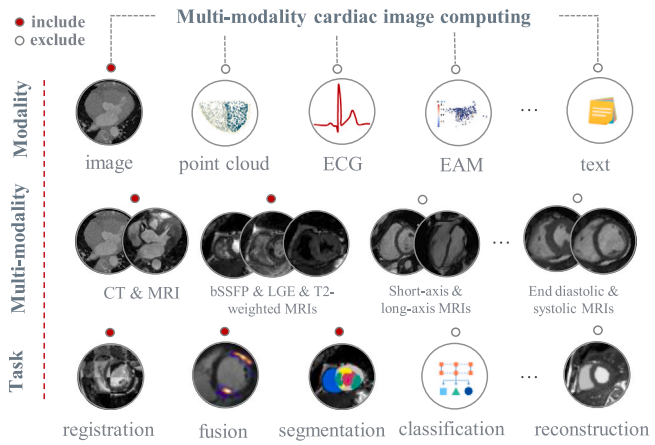

Fig. 2. The scope of this review. ECG: electrocardiogram; EAM: electroanatomical mapping; Here, the solid and hollow circles at the top of each category indicate inclusion and exclusion, respectively.

the complementary information from several imaging modalities. The three tasks exhibit overlap as well as distinct challenges. Specifically, their common issues are related to various sources of motion (patient, respiratory, and cardiac cycle). Unique challenges for registration and fusion may arise from the lack of a gold standard, which disables most current supervised learning-based models. The challenges associated with segmentation could originate from specific target regions, which can have large shape variations (e.g. the left atrium (LA)), can be small and/or diffuse (such as fibrotic regions and scars), or thin compared to image resolution (such as LA wall and coronary arteries). The proper selection of fusion techniques is complicated, as they should be easily interpretable in order to obtain traceable results. Also, the algorithms must satisfy several requirements, such as robustness to different acquisition conditions or tolerable computation times in a real-time system.

1.1. Study inclusion and literature search

In this work, we aim to provide readers with a survey of the state-of-the-art in multi-modality cardiac image computing techniques and the related literature. Fig. 2 illustrates the review scope of this survey. Note that in the computer vision area the modality might refer to text, audio and images, but in this work we restrict modality to imaging techniques. *We consider multi-modality cardiac computing to include studies that involve diverse modalities, either combining or transferring information between cardiac image modalities.* In the deep learning-based framework, different modalities may be present during training or more critically at the test phase at the same time. Therefore, we also include cardiac studies aiming at image translation or cross-modality domain adaptation, although different modality images may only appear separately in the training and test stages. Note that works that only test their methods in different cardiac imaging modalities for evaluation will not be included in this review. As for the cardiac computing tasks, we only consider the three major tasks at the current state of the art, i.e., registration, fusion, and segmentation. Image classification and object detection have also been applied in specific scenarios within CVD, such as identifying certain types of cardiac pathologies (Clough et al., 2019) and detecting specific anatomical landmarks (Zheng et al., 2009). However, they may not be sufficient to capture the intricacies of CVD, which normally involve multiple structures and functional aspects of the heart and blood vessels. Therefore, they are less commonly seen in CVD applications and also less usual to employ multi-modality imaging data. Current classification works within CVDs mainly integrate features from different cardiac signals, such as the electrocardiogram (ECG) and phonocardiogram (PCG), rather than imaging techniques (Kalidas and Tamil, 2016; Li et al., 2021d). There exist several cardiac image reconstruction works with the assistance of other modalities, mainly for cardiac motion correction (Polycarpou et al., 2021; Sang et al., 2021), which however is under-researched yet.

To ensure comprehensive coverage, we have screened publications mainly from the last 12 years (2010–2021) related to this topic. Our main sources of reference were Internet searches using engines, including Google Scholar, PubMed, IEEE-Xplore, Connected Papers, and Citeseer. To cover as many related works as possible, flexible search terms have been employed when using these search engines, as summarized in Table 1. Both peer-reviewed journal papers and conference papers were included here. In the way described above, we have collected a comprehensive library of 147 papers. Fig. 3 presents the distributions of papers in multi-modality cardiac image computing per year/task. Note that we picked the most detailed and representative ones for this review when we encountered several papers from the same authors about the same subject. Moreover, as multi-modality cardiac image fusion works are more likely to be driven by a clinical objective rather than technical development, we only select several representative studies here to cover as many modality combinations as possible. Also, the work of fusion or segmentation may involve a registration step, but we usually only regard this work as fusion or segmentation when counting the number of papers, since these are the final aims.

1.2. Existing survey from literature

Table 2 lists current review papers related to the topic, i.e., multi-modality cardiac image computing. One can see that the scopes of current review works are different from ours though with partial overlaps. For example, current review works on cardiac image registration

Table 1
Search engines and expressions used to identify potential papers for review.

Engine	Google scholar, PubMed, IEEE-Xplore, and Citeseer
Term	"Multi(-)modality/modal/sequence/source" or "cross(-)modality/modal/sequence" **and** "X-ray" or "computed tomography/CT" or "magnetic resonance/MR(I)" or "ultrasound/US" or "echocardiography/Echo" or "positron emission tomography/PET" or "single-photon emission computed tomography/SPECT" or "angiography" or "angiogram" **and** "Cardiac" or "heart" or "atri*" or "ventricl*" or "myocardi*" or "aort*" or "coronary artery" **and** "Regist*" or "fus*" or "integrat*" or "combin*" or "hybrid" or "overlay" or "segment*" or "domain adaptation"

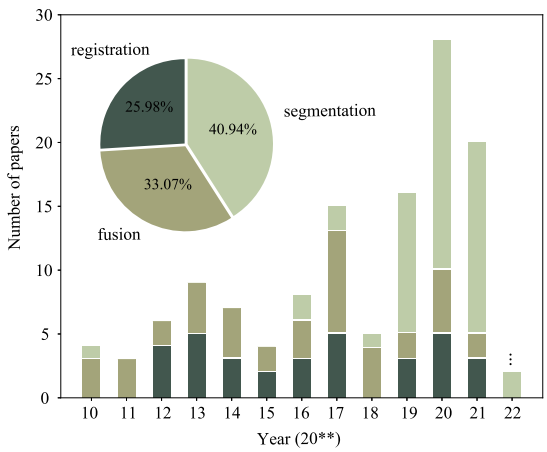

Fig. 3. The distributions of reviewed papers of multi-modality cardiac image computing per year and task.

only summarized conventional registration methods (Makela et al., 2002; Tavakoli and Amini, 2013), only revolved around specific modalities (Ming et al., 2015), or partially included multi-modality image registration (El-Gamal et al., 2016; Khalil et al., 2018). Cardiac image fusion survey works mainly focused on a specific CVD (Piccinelli and Garcia, 2013) or intra-modality fusion (Chauhan et al., 2021). Though there are several cardiac segmentation review works (Petitjean and Dacher, 2011; Zhuang, 2013; Peng et al., 2016; Chen et al., 2020a), they only concentrated on single-modality or single-structure cardiac imaging. In contrast, we provide a comprehensive review of multi-modality cardiac image analysis, excluding single-modality works.

1.3. Structure of this review

The rest of the survey is organized as follows. Section 2 summarizes widely used imaging modalities for cardiology. Section 3 covers the well-developed computing algorithms. In Section 4, publicly available datasets and performance evaluation measurements are listed. Discussion of current clinical applications, challenges and future perspectives of multi-modality cardiac image computing is given in Section 5, followed by a conclusion in Section 6.

2. Cardiac imaging

Many imaging techniques are available for cardiac analysis, as presented in Fig. 1. In general, these techniques either focus on the anatomical (wall thickness, volume, coronary artery morphology, etc.) or the functional (wall motion patterns, cardiac perfusion, etc.) aspects. This section briefly reviews the most commonly used imaging techniques for clinical investigation of the heart.

2.1. X-ray (fluoroscopy)

X-ray imaging captures a projection of a 3D structure on a 2D plane, with poor soft-tissue contrast but providing high contrast images of devices (Housden et al., 2012). It has an important role in the preliminary assessment of CVDs. For example, increased heart size and the presence of increased pulmonary vascular markings or pleural effusions in X-ray may suggest pulmonary congestion secondary to heart failure. X-ray angiography can provide information about coronary arteries (CA) and their stenosis, and therefore is a standard and popular assessment tool for medical diagnosis of coronary artery diseases (CADs) (Tayebi et al., 2015). It is however fundamentally limited by its 2D representation, as extensive 3D/4D information about the CA is lost. Though many 3D reconstruction methods have been proposed for CA reconstruction from 2D X-ray angiography, it remains a challenging and dynamic research area (Çimen et al., 2016). X-ray fluoroscopy is a real-time imaging technique that displays a continuous X-ray image on a monitor and is easy to use during interventions (Ma et al., 2010a; Faranesh et al., 2013). Therefore, it has been routinely utilized in patients to guide vascular and cardiac interventions. For example, it can visualize the blood flow through the CA for arterial occlusion detection (Ma et al., 2020), guide placement of pacemaker leads for cardiac resynchronization therapy (CRT) (Ma et al., 2010a) and enhance image guidance during cardiovascular interventional procedures (Faranesh et al., 2013). However, it is limited by exposure to ionizing radiation, poor soft tissue characterization and lack of quantitative functional information. Cardiac X-ray is often combined with CT, MRI, and Echo, leveraging its ability to provide real-time, two-dimensional images of the heart's size, shape, and position, to complement the detailed anatomical and functional information provided by other imaging modalities.

2.2. Computed tomography

Cardiac CT generates cross-sectional images of the human body, with excellent temporal and spatial resolution. It represents the X-ray attenuation properties of the tissue being imaged, where the measured attenuation can be employed to reconstruct the 3D heart structure. Moreover, contrast agents can be utilized in CT to enhance the 3D visualization of CA (Mylonas et al., 2014), the localization of the myocardial infarction (MyoI) (Bauer et al., 2010), the detection of LA appendage (LAA) thrombus in atrial fibrillation (AF) patients (Spagnolo et al., 2021), and the estimation of myocardial (Myo) blood flow (Alessio et al., 2019). CT angiography (CTA) can give complementary information (clear anatomical information) about the CA tree but without any functional information in cardiac imaging (Zhou et al., 2012). Cardiac CT is frequently combined with X-ray, MRI, Echo, and PET/SPECT, leveraging its ability to provide detailed cross-sectional images of the heart's anatomy and blood vessels, in addition to its fast acquisition time, to complement the information obtained from other imaging modalities, enabling a comprehensive evaluation of cardiac conditions with high spatial resolution and diagnostic accuracy.

2.3. Magnetic resonance imaging

Cardiac MRI is an imaging technique with high resolution as well as high tissue contrast for the assessment of heart chambers, cardiac valves, cardiac vessels, and surrounding structures such as the pericardium (Earls et al., 2002). It can also be used to study myocardial perfusion and viability, and permits the calculation of ventricular function parameters such as left ventricle (LV) ejection fraction, end diastolic/systolic volumes or LV mass. Compared to nuclear imaging (PET or SPECT), the dependence of MRI signal on regional hypoperfusion is minimal (Kang et al., 2012). Note that within MRI, various pulse sequences can attenuate different tissue features to identify anatomical and functional information, resulting in images of varying contrasts. For example, cine MRI (usually using bSSFP sequence) can provide

Table 2
Summary of the related representative review works. ML: machine learning; CAD: coronary artery disease; WH: whole heart; LA: left atrium; RV: right ventricle; DL: deep learning; TMI: IEEE Transactions on Medical Imaging; MedIA: Medical Image Analysis; CRP: Cardiology Research and Practice; CVIU: Computer Vision and Image Understanding; JBR: Journal of Biomedical Research; JHE: Journal of Healthcare Engineering; EIJ: Egyptian Informatics Journal; MAGMA: Magnetic Resonance Materials in Physics, Biology and Medicine; FCM: Frontiers in Cardiovascular Medicine; IPADCD: Image Processing for Automated Diagnosis of Cardiac Diseases; EP: EP Europace; CET: Cardiovascular Engineering and Technology; IET: IET Image Processing; FIP: Frontiers in Physiology; CCRR: Current Cardiovascular Risk Reports; EJNMMI: European journal of nuclear medicine and molecular imaging; JT: Jurnal Teknologi; CMIG: Computerized Medical Imaging and Graphics; JNM: Journal of Nuclear Medicine; CCIR: Current cardiovascular imaging reports. Note that here "single modality" refers to the methods designed for a single modality but they may be evaluated on several different modalities, separately.

Source	Venue	Scope	Inclusion
Makela et al. (2002)	TMI	Cardiac image registration	Partially includes multi-modality
Slomka and Baum (2009)	EJNMMI	Multi-modality image registration	Software based; partially includes heart
Tavakoli and Amini (2013)	CVIU	Cardiac image segmentation and registration	Single modality; shape-based methods
Ming et al. (2015)	JT	Cardiac US and CT registration	US and CT registration
El-Gamal et al. (2016)	EIJ	Medical image registration and fusion	Partially includes multi-modality or heart
Khalil et al. (2018)	CRP	Cardiac image registration	Partially includes multi-modality
Rischpler et al. (2013)	JNM	Cardiac PET and MRI fusion	Clinical review; PET/MRI fusion
Piccinelli and Garcia (2013)	JBR	Multi-modality cardiac image fusion	Clinical review; focus on CAD
Chauhan et al. (2021)	IPADCD	Cardiac image fusion	Partially includes multi-modality
Petitjean and Dacher (2011)	MedIA	Cardiac short-axis MRI segmentation	Single modality
Zhuang (2013)	JHE	WH segmentation	Single modality; conventional methods
Peng et al. (2016)	MAGMA	Cardiac MRI segmentation	Single modality
Pontecorboli et al. (2017)	EP	Fibrosis segmentation from LGE MRI	Single modality; thresholding methods
Jamart et al. (2020)	FCM	LA cavity segmentation from LGE MRI	Single modality; DL-based methods
Habijan et al. (2020)	CET	WH and chamber segmentation	Single-modality
Chen et al. (2020a)	FCM	DL-based cardiac segmentation	Single modality; DL-based methods
Ammari et al. (2021)	IET	RV segmentation from short-axis MRI	Single modality; RV segmentation
Wu et al. (2021)	FIP	Scar/fibrosis segmentation from MRI	Single modality; scar/fibrosis segmentation
Jia and Zhuang (2021)	CMIG	Learning-based vessel segmentation	Single modality; learning-based methods
Kwan et al. (2021)	CCRR	DL-based cardiac image segmentation	Partially includes multi-modality
Li et al. (2022b)	MedIA	LA-related segmentation from LGE MRI	Single modality; LA-related segmentation

clear structure and global ventricular performance via quantification of chamber volumes and function; late gadolinium enhanced (LGE) MRI provides fibrosis information by visually enhancing fibrosis regions; and T2-weighted images can be used to identify myocardial edema caused by inflammation or acute ischemia (Zhuang, 2019). In clinical practice, myocardial analysis of LGE/T2-weighted MRI is typically combined with bSSFP MRI considering the poor image quality of LGE/T2-weighed MRI (Kim et al., 2009). Similar to CTA, MR angiography is a standard technique for imaging the aorta and large vessels of CA (Mieres et al., 2007). Cardiac MRI is often combined with X-ray, CT, Echo, PET, and various MRI sequences such as cine, LGE, and T2-weighted imaging, to provide a comprehensive assessment of the heart's anatomy, function, tissue characteristics, and blood flow, enabling precise diagnosis and management of a wide range of cardiac conditions.

2.4. Echocardiography

Echo (or US of the heart) is a real-time cardiac imaging technique without irradiation, and its temporal resolution is excellent. Echo is the most widely used imaging technique in cardiology as it is relatively inexpensive, radiation-free and portable. Dynamic Echo is the gold standard modality to assess myocardial strain. The limitations of Echo include small FOV, poor signal-to-noise ratio, artifacts, and high sensitivity to operators and patients. There are various echocardiographic modalities, such as transthoracic Echo (TTE), transesophageal Echo (TEE), and intracardiac Echo (ICE) (Hascoët et al., 2016). TTE can be used to identify the great majority of cardiac causes of shock (de Bruijn et al., 2006), diagnose pulmonary embolism (Fields et al., 2017), and evaluate patients with suspected myocarditis (Goitein et al., 2009). TEE allows for high-quality color flow imaging, which can be utilized for visualizing the cardiac structures near the upper chambers and assisting device positioning and deployment during cardiac treatment procedures (Khalil et al., 2018). However, TEE is an invasive imaging technique, as it is acquired via a thin tube connected with an Echo probe through the mouth of patients into the esophagus. ICE is a catheter-based technique that presents imaging within the heart as well as aortic root images, with a larger view than TEE. Several research works have presented the superiority of 3D over 2D Echo alone in the catheterization laboratory (Martin et al., 2013; Hascoet et al., 2015). Unfortunately, 3D Echo is not widely available in clinical practice and is more expensive compared with 2D Echo. Echo is commonly integrated with X-ray, CT, and MRI to capitalize on its unique features of real-time, non-invasive, and dynamic imaging, which allows for the simultaneous assessment of the heart's structure, function, and blood flow.

2.5. Nuclear imaging

Cardiac PET is a nuclear medical imaging technique that can measure myocardial perfusion, metabolism and regional/absolute myocardial blood flow (Slomka et al., 2009; Angelidis et al., 2017). It is particularly suitable for obese patients and patients with multi-vessel diseases to confirm or exclude balanced myocardial ischemia (Dewey et al., 2020). Its spatial resolution (about 3–4 mm) is lower compared to cardiac MRI or CT (about 1 mm), so PET usually cannot provide clear anatomical information about the heart. Therefore, CT is usually utilized to perform attenuation correction for better resolution of PET images. Cardiac SPECT is the most commonly employed imaging technique for clinical myocardial perfusion, whereas PET is the clinical gold standard for myocardial perfusion quantification. With new detectors, SPECT can quantify myocardial blood flow and is suitable for patients with a high body mass index (BMI) (Dewey et al., 2020). SPECT can also be used to detect ischemia and viability in heart failure (Angelidis et al., 2017), assess the physiological relevance of coronary lesions and provide a high prognostic predictive value (Kaufmann and Di Carli, 2009). Moreover, compared with PET, SPECT can accurately assess myocardial viability and has a lower cost of equipment and less expensive radiotracers, but with lower resolution imaging prone to artifacts and attenuation (Partington et al., 2011). Cardiac PET/SPECT is commonly integrated with CT and MRI, capitalizing on its ability to provide functional and metabolic information on the heart, such as myocardial perfusion, glucose metabolism, and neurohormonal activity, in conjunction with the anatomical details obtained from CT and MRI, allowing for comprehensive assessment and diagnosis of cardiac conditions with enhanced sensitivity and specificity.

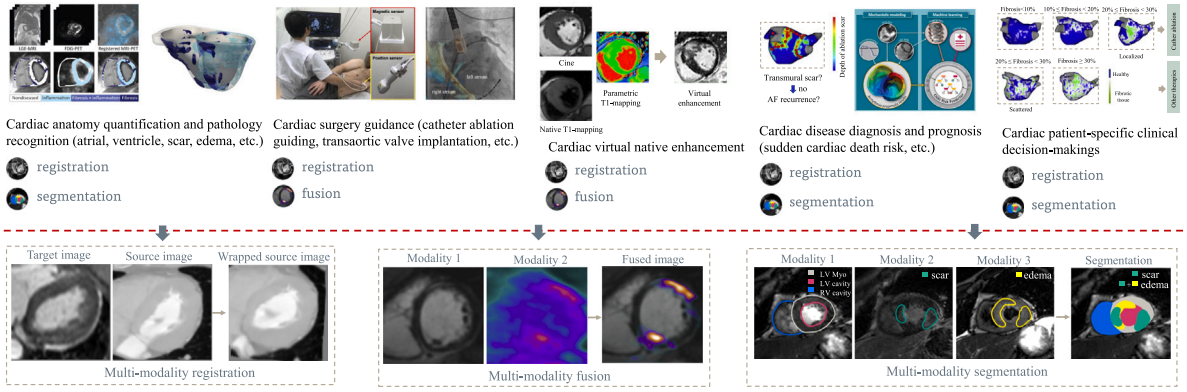

Fig. 4. Multi-modality cardiac image computing tasks motivated by corresponding clinical applications. Here, the images in the clinical application are adapted from Shade et al. (2021), Housden et al. (2012), Zhang et al. (2021a) and Siebermair et al. (2017) with permission; and the images in the multi-modality fusion and segmentation are adapted from Quail and Sinusas (2017) and Li et al. (2023b) with permission, respectively.

3. Multi-modality cardiac image computing

With these cardiac imaging techniques, one could combine their advantages for cardiac analysis in the clinic, such as cardiac pathology identification, cardiac surgery guidance, and cardiac disease diagnosis, treatment and prognosis. Fig. 4 provides five typical clinical applications which benefit from multi-modality cardiac image computing. Although the ultimate goal of the five applications is not the same, they all aim to use complementary information from different imaging modalities of one patient, providing a more detailed and comprehensive assessment of the heart's condition. However, in some cases, multi-modality cardiac image computing may involve using data from another patient's imaging modality to assist in the evaluation or treatment planning of the target patient. This could be mainly attributed to the limited data availability, especially single modality. Besides, one can standardize or normalize quantitative measurements of the target patient by referencing data from a larger population with different modalities. This can help to establish a more reliable and objective comparison of the target patient's data with a reference population, which may aid in more accurate assessment and monitoring of disease progression. In this section, we cover all these situations and summarize techniques for three multi-modality cardiac image computing tasks, i.e., multi-modality registration, fusion and segmentation.

3.1. Registration

Multi-modality image registration is a native way to propagate knowledge between modalities as well as a primary step in integrating information of multi-modality images. It can align images with respect to each other and typically involves several components, i.e., feature extraction (optional), geometrical transformation, similarity measure, and optimization. Accurate multi-modality image registration can offer additional crucial clinical relevant information, which may be unavailable in a single imaging modality. However, registration is an ill-posed problem with several challenges, such as anatomy variations, possible partial overlaps between images, and high variability of tissue appearance under different modalities that leads to the lack of robust similarity measures.

Cardiac image registration is particularly challenging due to respiration and mixed motions during the cardiac cycles. Furthermore, multi-modality cardiac images are normally inconsistent in the cardiac phases, slice thickness, dimension, and state (static or dynamic), which introduce additional challenges. For example, for multi-sequence MRI registration, T2 imaging generally only includes a few slices with larger thickness compared to bSSFP and LGE imaging (Zhuang, 2019). Echo/CT image registration frameworks usually consist of two major steps: temporal synchronization and spatial registration (Huang et al., 2009; Khalil et al., 2017a). Temporal synchronization allows the echocardiographic time-series data to be time-stamped to identify frames that are in a similar cardiac phase to the CT volume. Spatial registration aims at producing an interpolated cardiac CT image that matches the Echo image, which sometimes involves a challenging 2D-3D registration. Despite these challenges, there exist several promising solutions for multi-modality image registration. We have coarsely divided these methods into three categories, namely intensity based registration, structural/anatomical information based registration, and image synthesis/disentangle based registration. Note that these categories are not mutually exclusive, and some methods may utilize a combination of two or three categories. The works employed both intensity and structural/anatomical information for registration, in which case we categorized them as structural/anatomical information based registration. Once the methods involved image synthesis/disentangle, we categorized them as image synthesis/disentangle based registration. Table 3 provides a summary of the state-of-the-art cardiac multi-modality registration methods according to the categories.

3.1.1. Intensity based registration

A straightforward approach is to employ modality invariant similarity metrics, such as mutual information (MI) and its variants such as normalized MI (Pluim et al., 2003; Sandoval and Dillenseger, 2013). MI and its variations are well suited for multi-modality image registration, as they do not assume a linear relationship between intensities of different imaging modalities (Maes et al., 1997). Kullback–Leibler (KL) divergence has also been employed as a similarity metric for multi-modality cardiac image registration (Cremers et al., 2006; Guetter et al., 2005). It enforces the joint intensity distribution of the source and target images according to the priors of learned distributions from the pre-aligned images. The prior knowledge can be obtained from the expert knowledge of a physician who manually aligns the images. Also, one can leverage the fused imaging data acquired using dual-modality/hybrid scanners, which can offer extensive amounts of pre-registered data (Guetter et al., 2005). KL divergence (total correlation) can also combined with intensity-class MI for group-wise multi-modality image registration, referred as the $\mathcal{X}$-metric Luo and Zhuang (2022). Jensen–Shannon divergence provides a more suitable measure than KL divergence in quantifying histogram discrepancy (Liao et al., 2006). In addition, it is upper bounded and symmetric, facilitating its use for multi-modality image registration, and its weighted version can further ensure an organ-specific intensity co-occurrence (Guetter et al., 2007). However, such global intensity-based similarity measures often ignore the spatial information of the target, so they are unsuitable in some situations. For instance, the tissue presented in Echo is inherently characterized by a specific spatial distribution of speckles rather than a specific distribution of gray scales that exist in MRI and CT (Sandoval and Dillenseger, 2013).

Table 3
Summary of previously published works on the *multi-modality cardiac image registration*. reg: registration; seg: segmentation; MS-CMRSeg: paired cardiac bSSFP, T2-weighed, and LGE MRIs from Multi-sequence Cardiac MR Segmentation Challenge (Zhuang et al., 2019); X-rayAI: X-ray angiography image; CTA: CT angiography; CSA:coronary sinus angiogram; MI: mutual information; NMI: normalized MI; NCC: normalized cross correlation; CoR: correlation ratio; ECC: entropy correlation coefficient; LCC: local correlation coefficient; CoC: correlation coefficient; RMSE: root mean squared error; MSD: mean square distance; JE: joint entropy; PSMI: point similarity measure based on MI; WC: Woods criterion; SEMI: spatially encoded MI; VWMI: Viola-Wells MI; MMI: Mattes MI; SSD: sum of squared difference; WJS: weighted Jensen–Shannon; KL: Kullback–Leibler; MD: mean distance; ASD: average surface distance; LV: left ventricle; CA: coronary arteries; FFD: free-form deformation; Syn/Dis: image synthesis/disentangle based registration.

	Study	Modality	Target	Method	Similarity metric
Intensity based registration	Pauna et al. (2003)	MRI, PET	WH	Intensity-based rigid reg	MI, CoR, CoC
	Walimbe et al. (2003)	Echo, SPECT	Myo	Intensity-based temporal + 2D-3D reg	MI
	Guetter et al. (2005)	CT, PET	Myo	Intensity-based non-rigid reg	MI + KL divergence
	Cremers et al. (2006)	CT, PET	Myo	Intensity-based non-rigid reg	MI + KL divergence
	Guetter et al. (2007)	CT, SPECT	Myo	Intensity-based rigid reg	WJS divergence
	Huang et al. (2009)	CT, Echo	WH	Intensity-based temporal + 2D-3D rigid reg	MI
	Papp et al. (2009)	CT, PET, SPECT	Myo	Intensity-based reg	Triple NMI
	Marinelli et al. (2012)	CT, PET	Myo	Intensity-based rigid reg	MI
	Sandoval and Dillenseger (2013)	CT, Echo	WH	Intensity-based rigid + elastic reg	MI, NMI, ECC, JE, PSMI, CoR, WC
	Lamare et al. (2014)	CT, PET	Myo	Intensity-based affine + elastic reg	NMI
	Turco et al. (2016)	CT, PET	WH	Intensity-based rigid reg	NMI
	Khalil et al. (2017a)	CT, Echo	Aorta	Intensity-based temporal + rigid reg	NMI
	Puyol-Anton et al. (2017)	MRI, Echo	Myo	Intensity-based rigid reg + FFD	N/A
	Khalil et al. (2017c)	CT, Echo	LA	Intensity-based 2D-3D rigid reg	NMI
	Zhuang (2019)	MS-CMRSeg	Myo	Intensity (+shape prior)-based rigid reg + FFD	Likelihood function
	Li et al. (2020b)	bSSFP, LGE MRI	WH	Intensity-based affine reg + FFD	SEMI
	Luo and Zhuang (2022)	MS-CMRSeg	LV, RV, Myo	Intensity-based FFD	MI + KL divergence
Structural/anatomical information based registration	Zhang et al. (2006)	MRI, Echo	LV, RV, Myo	Local phase based affine reg	Phase MI
	Cordero-Grande et al. (2012)	Cine, LGE MRI	Myo	Local entropy based reg	NCC
	Oktay et al. (2015)	CT, Echo	LV, RV, Myo	PEM-based rigid + non-rigid reg	NCC, LCC
	Choi et al. (2016)	MRI, X-ray	LV	Normalized gradient field based rigid reg	NCC
	Kolbitsch et al. (2017)	MRI, PET	Myo	Motion field based affine reg + FFD	NCC
	Gouveia et al. (2017)	CT, X-ray	CA	Regression based rigid reg	N/A
	Atehortúa et al. (2020)	MRI, Echo	Myo	Salient image based Eulerian and nonrigid reg	NCC
	Gilardi et al. (1998)	PET, SPECT	Myo	Surface-based rigid reg	ASD
	Savi et al. (1995)	Echo, PET	Myo	Landmark-based rigid reg	MSD
	Mäkelä et al. (2003)	MRI, PET, Echo	LV, RV, Myo	Landmark and seg-based reg	Region energy
	De Silva et al. (2006)	MRI, X-ray	LV, RV, Myo	Landmark-based rigid reg	MSD
	Baka et al. (2013)	CT, X-ray	CA	Landmark-based rigid reg	2D-3D distance
	Aksoy et al. (2013)	CT, X-ray	CA	Landmark-based rigid reg	2D-3D distance
	Döring et al. (2013)	Echo, CSA	Myo	Landmark-based reg	N/A
	Smith et al. (2014)	PET, SPECT	Myo	Landmark-based reg	N/A
	Tayebi et al. (2015)	CT, X-rayAI	CA	Landmark-based affine reg	RMSE
	Faber et al. (1991)	MRI, SPECT	LV	Point set based rigid reg	MD
	Sinha et al. (1995)	MRI, PET	Myo	Point set based rigid reg	MSD
	Santarelli et al. (2001)	MRI, SPECT	Myo	Point set based non-rigid reg	MSD
	Sturm et al. (2003)	MRI, CTA	Myo	Point set based rigid reg	MSD
	Tavard et al. (2014)	CT, Echo, EAM	LV	Point set based temporal reg	SSD
	Peoples et al. (2019)	CT, Echo	WH	Point set based non-rigid reg	Likelihood function
	Scott et al. (2021)	CT, Echo	WH	Point set based rigid reg	N/A
	Mäkelä et al. (2001)	MRI, PET	Myo	Seg-based rigid reg	N/A
	Martinez-Möller et al. (2007)	CT, PET	Myo	Seg-based emission-driven correction	N/A
	Woo et al. (2009)	CT, SPECT	Myo	Seg-based rigid + nonrigid reg	SSD
	Betancur et al. (2016)	Cine/LGE MRI, Echo	LV	Seg-based temporal + intensity-based rigid reg	MSD, NCC, VWMI, MMI, NMI
	Courtial et al. (2019)	Cine MRI, CT	WH	Seg-based temporal + intensity-based rigid reg	NCC, NMI
	Ding et al. (2020)	MRI, CT	Myo	Seg-based non-rigid reg	Dice
	Luo and Zhuang (2020)	MS-CMRSeg	LV, RV, Myo	Seg-based rigid + non-rigid reg	Likelihood function
	Ding et al. (2021)	MRI, CT	Myo	Seg-based non-rigid reg	SEGI
	Guo et al. (2021a)	Cine, LGE MRI	Myo	Seg-based affine + non-rigid reg	N/A
Syn/Dis based registration	Shi et al. (2012)	Cine, tagged MRI	Myo	Pseudo-anatomical MRI based nonrigid reg	Weighed NCC
	Dey et al. (2012)	CT, SPECT	WH	Synthetic CT based rigid and non-rigid reg	SSD
	Li et al. (2013)	CT, Echo	LV	Synthetic CT based non-rigid reg	MI
	Chartsias et al. (2020)	bSSFP/LGE MRI	LV, Myo	Disentangled representation based affine reg	MI

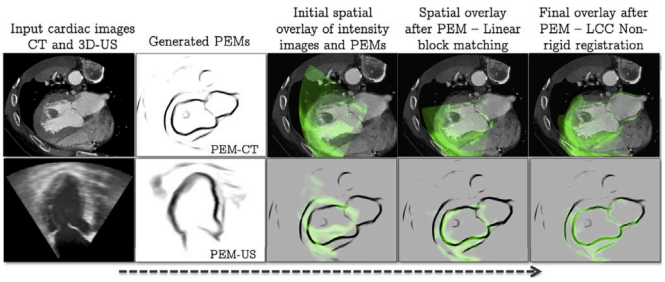

Fig. 5. An example of multi-modality cardiac image registration. Here, a generic and modality-independent image representation, namely probabilistic edge map (PEM), was proposed for cardiac CT and US registration. The PEM, by only highlighting the registration of relevant image structures, i.e., LV and atrial boundaries, is a more robust approach than registering every voxel in the images.
Source: Image adapted from Oktay et al. (2015) with permission.

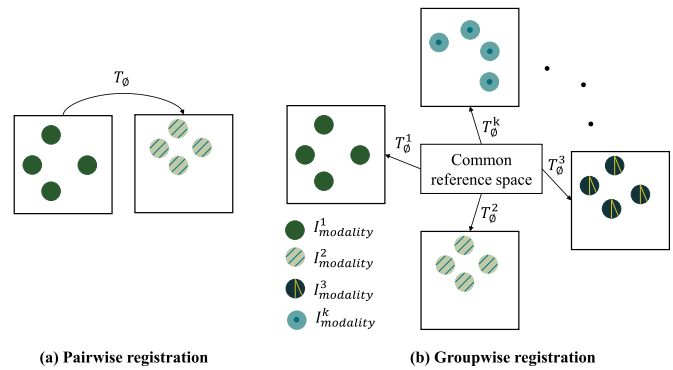

Fig. 6. Graphical illustration for (a) pairwise registration (b) groupwise registration. Here, T_ϕ is the adopted transformation, and $I^{1,2,3,\ldots,k}_{modality}$ refer to different imaging modalities. Here, each square box represents an image, the distribution of the circles in the box indicates the image anatomy, and the different textures of the circles represents different imaging modalities.

3.1.2. Structural/anatomical information based registration

Instead of directly employing image intensities, one could utilize structural information, which is supposed to be independent to modalities. In this way, the influence of appearance differences among various modalities can be mitigated, and a simple L1 or L2 distance can be used for the multi-modality image registration. One could extract image representations, namely structural representations, such as entropy, Laplacian images (Wachinger and Navab, 2012), local phase images (Zhang et al., 2006; Grau et al., 2007), and probabilistic edge maps (PEMs) (Oktay et al., 2015). Entropy images satisfy only certain requirements of a relaxed version of the theoretical properties, but they are computationally fast and lead to good alignment, facilitating its use as a practical solution. Laplacian images capture the intrinsic structure of imaging modalities, with the preservation of optimal locality. The local phase image can be a characterization of features detected in a signal, such as edges and ridges in a signal, so it has been shown appropriately for registration involving Echo images. In contrast to local phase representations, PEMs only highlight the image structures that are relevant for image registration, as presented in Fig. 5. Note that several anatomical structures that are visible in US images may not be visible in CT/MR images and vice versa, such as endocardial trabeculae (Oktay et al., 2015). Therefore, only registering the region of interest (ROI) can be more robust than registering every voxel in the images.

Modality-invariant anatomical landmarks, surfaces (contours or point clouds) or labels can also be used to define the transformation from one image to the other due to their inherent correspondences with original images. For example, Savi et al. (1995), Döring et al. (2013) and Smith et al. (2014) employed the landmarks being identified in multi-modality images for registration. Ding et al. (2020) predicted a dense displacement field (DDF) for cardiac CT and MRI registration by aligning the anatomical labels of MRI and CT instead. Nevertheless, these methods are highly sensitive to the accuracy of segmentation or landmark, so manual segmentation or landmark detection is usually required, which is impractical in image-guided intervention.

3.1.3. Image synthesis/disentangle based registration

An alternative way is to reduce the multi-modality registration into a mono-modality problem, where most existing mono-modality registration methods then can be applied (Li et al., 2013). One could either synthesize one modality from another one or transfer multiple modalities into a common domain (Chen et al., 2017; Arar et al., 2020). The main idea behind this is to mitigate the large appearance gap among different modalities. To achieve this, one can take advantage of prior knowledge of the physical properties of imaging devices (Roche et al., 2001) or capture their intensity relationships (Cao et al., 2017). As for mapping multiple modalities to a common space, these modalities need to share the same anatomical structure or features in order to build a meaningful correspondence. A major issue of current image synthesis based registration methods is that the image synthesis is normally performed in a single direction. Specifically, current image synthesis is often adapted from the imaging modality with rich anatomical details (e.g., MRI) to the imaging modality with limited anatomical details (e.g., CT/US). Note that it is quite challenging to achieve accurate local deformation prediction based on an imaging modality with limited anatomical details, especially in the presence of large local deformations in cardiac images. One could also disentangle the anatomy and modality information from images, and then a mono-modality registration can be adopted on the latent embedding space (Chartsias et al., 2020). A major issue with current disentanglement based methods is that they generally cannot explicitly impose the disentanglement, so the learned representations may be exposed to information leakage (Ouyang et al., 2021).

3.1.4. Discussion

Multi-modality cardiac image registration is a crucial step for further cardiac analysis, providing complementary information for cardiac image fusion (Section 3.2) and facilitating the cardiac image segmentation (Section 3.3). It allows for a more comprehensive analysis of the cardiac functions and pathologies, and has many applications in the clinic, such as monitoring the progression of diseases, quantifying the effectiveness of treatment mechanisms, surgery planning, and intra-operative navigation (Döring et al., 2013; Giannoglou et al., 2006; Khalil et al., 2017a). During the registration procedure, different combinations of dimensions, such as 2D-to-2D, 3D-to-3D, 2D-to-3D, and 3D-to-4D, may be involved, and they usually have different applications and optimization targets. For example, 2D-to-3D image registration is normally employed for establishing correspondence between X-ray and 3D volumes. Its main application is to facilitate image-guided surgery (Khalil et al., 2017b; Dori et al., 2011), so computational complexity must be minimized without compromising accuracy.

We have summarized various cardiac image registration methods according to the key elements of methodologies. One can see that structural/anatomical information based registration is the most popular for multi-modality cardiac image registration. This can be attributed to the fact that the structural/anatomical information is generally robust to changes in image intensity and contrast, and thus can handle images with different modalities, especially in modalities with well-defined anatomical structures, such as CT and MRI. Also, structural/anatomical information based registration can use simple similarity metrics instead of computationally expensive MI-based metrics, and thus accelerate the registration procedure. However, they may encounter difficulties

in extracting reliable structural or anatomical information from images with low contrast, noise, or artifacts, which can be an issue in modalities such as US, PET, and SPECT. In contrast, intensity based registration algorithms do not require additional information or features to be extracted from the images. They are robust to noise or artifacts, making them more suitable for modalities with lower image quality, such as PET and SPECT. However, they may not capture subtle differences in image content or structural changes between modalities, as they rely solely on intensity values. Image synthesis or disentangle based registration methods can generate or disentangle images from different modalities into single one modality. However, these methods may require additional training data and computational resources for model training and image synthesis. In general, the choice of similarity measure and registration strategy should be carefully considered based on the specific characteristics of the cardiac image modalities being registered, the clinical application, and the specific challenges associated with each modality. Pure rigid transformations have been applied in several works, but rigid cardiac image registration is generally not enough to describe the spatial relationship due to the existence of cardiac motion. Therefore, there is considerable research extending the transformation to the combination of rigid and non-rigid ones.

Conventional cardiac image registration basically is an iterative-based optimization procedure, which could be quite slow, especially for non-rigid image registration. DL-based registration procedures can be computationally efficient (Boveiri et al., 2020), and have been applied in multi-modality cardiac images (Gouveia et al., 2017; Ding et al., 2020; Luo and Zhuang, 2020). These methods generally require extensive anatomical labels for supervised network training. To solve this, Ding et al. (2021) investigated unsupervised DL-based cardiac multi-modality image registration by introducing a modality-invariant structural representation, i.e., spatially encoded gradient information. One can also exploit the image similarity analogous to conventional intensity-based image registration for unsupervised DL-based cardiac image registration (de Vos et al., 2019); or employ image disentangle learning to embed an image onto a domain-invariant latent space for the registration (Qin et al., 2019). Also, groupwise registration and combined computing have recently emerged and been applied for multi-modality registration and segmentation of cardiac images (Zhuang, 2019; Kouw and Loog, 2019; Luo and Zhuang, 2020, 2022). Compared to pairwise registration, groupwise registration is able to handle several imaging modalities simultaneously in an unbiased way (see Fig. 6). Therefore, DL-based multi-modality image registration can be further facilitated by introducing groupwise learning. Nevertheless, there are no general automatic methods due to the wide variety of modalities and clinical scenarios in cardiology.

3.2. Fusion

Multi-modality cardiac image fusion aims at integrating relevant information from several images into a single one, to obtain a more informative and representative integrated image, as presented in Fig. 7. The fusion process can improve image quality and reduce randomness and redundancy, in order to augment clinical accuracy and robustness of the analysis for an accurate diagnosis. For decades, images from different modalities have been used to develop image fusion frameworks either invasive or non-invasive, anatomical and functional, leading to the emergence of hybrid devices such as PET/MRI, PET/CT and SPECT/CT (Piccinelli, 2020), as shown in Fig. 8. Specifically in the field of cardiology, image fusion is mainly used to integrate functional imaging, such as SPECT or PET, and anatomical imaging, such as CT or MR. Also, it permits a combination of the advantages of each modality, such as excellent soft-tissue contrast and/or higher spatial resolution (CT or MRI) and high temporal resolution (X-ray fluoroscopy, Echo) for detailed real-time feedback. Among these hybrid cardiac imaging techniques, PET (or SPECT)/CT (CTA) is currently the most widespread (Lawonn et al., 2018). As cardiac MRI and CT are both high-resolution images,

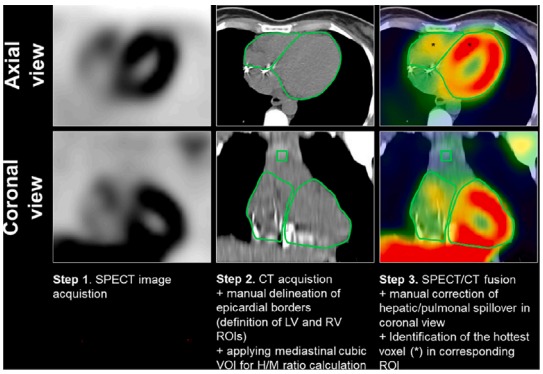

Fig. 7. An example of multi-modality cardiac image fusion. Here, cardiac CT and SPECT are fused to assess inherited arrhythmia syndromes.
Source: Image adapted from Siebermair et al. (2020) with permission.

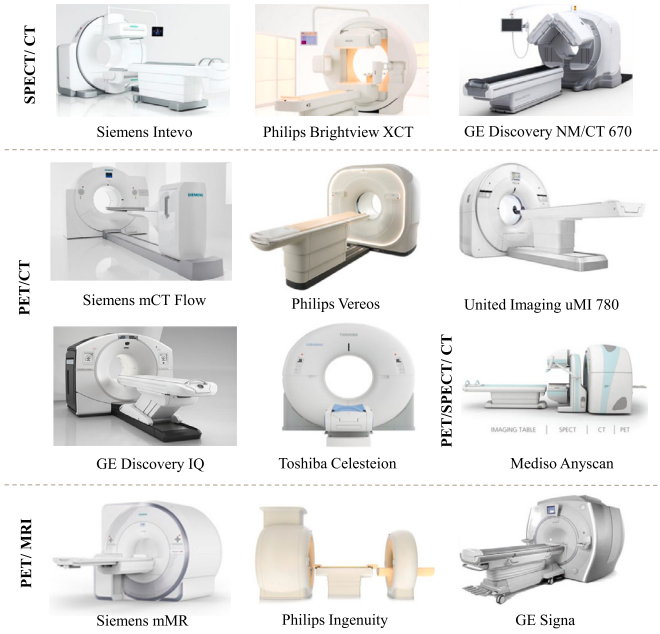

Fig. 8. Examples of commercially available hybrid imaging devices for clinical use.
Source: Image modified from Cal-Gonzalez et al. (2018) with permission.

their fusion is relatively rare and could be more challenging (Lawonn et al., 2018). Table 4 summarizes the applied modalities in cardiac image fusion with their applications in cardiac imaging studies. Note that as some of these reviewed papers provide limited details about fusion methodology, we classified image fusion works based on their applied modalities instead of the methodologies. Also, we only include parts of representative image fusion studies without pretending to be exhaustive.

3.2.1. PET/SPECT and CT/MRI fusion

Healthy cardiac function depends on a close interplay between anatomy and physiology, which is disrupted in many CVDs; thus, their joint evaluation can significantly boost a physician's ability to diagnose and plan treatment (Piccinelli, 2020). Initial attempts to fuse anatomical and functional information date back to the early 1990s and have gradually become established techniques, demonstrating the greater diagnostic power of fused images compared to single-mode or side-by-side interpretation (Peifer et al., 1990; Piccinelli et al., 2018). SPECT and PET can evaluate myocardial perfusion, metabolism, and regional absolute myocardial blood flow, while CT/MRI provides coronary anatomy and allows for multi-parametric evaluation of cardiac

Table 4
Summary of previously published works on the *multi-modality cardiac image fusion*. PVe: pulmonary vessel; PC: pulmonary conduit; PA: pulmonary artery; LSVC: left superior vena cava; MV: mitral valve; MyoI: myocardial infarction; RA: right atrium; CCAA: complex CA anomalies; PCI: percutaneous coronary intervention; AF: atrial fibrillation; TAVI: trans-aortic valve implantation; LAA: LA appendage; CHD: congenital heart disease; CRT: cardiac resynchronization therapy; MBF: myocardial blood flow; MFR: myocardial flow reserve; RFR: relative flow reserve; iAS: inherited arrhythmia syndromes; SHD: structural heart disease; EM: electromagnetic; STDME: simultaneous two-screen display of multidetector-CT and real-time echogram; TE: transendocardial; VNE: virtual native enhancement; MSF: multi-sequence MRI fusion.

	Study	Modality	Target	Method	Motivation/application
PET/SPECT and CT/MR fusion	Gräni et al. (2017)	PET, CT	CA	CardIQ fusion software	Assess the impact of CCAA on Myo perfusion
	Aguadé-Bruix et al. (2017)	PET, CT	Aorta	N/A	Diagnose and evaluate the extent of endocarditis
	Piccinelli et al. (2020)	PET, CTA	Myo	Rigid reg	Extract MBF, MFR and RFR along CAs
	Quail and Sinusas (2017)	PET, MRI	Myo	N/A	Visualize each CA and strain in its territory
	Izquierdo-Garcia et al. (2020)	PET, MRI	Myo	OsiriX DICOM viewer	Explore the effect of histone deacetylases on the heart
	Zandieh et al. (2018)	PET, MRI	Myo	Landmark based rigid reg	Diagnose patients with cardiac sarcoidosis
	Degrauwe et al. (2017)	PET, MRI, CT	Myo, PVe	N/A	Assess cardiac paragangliomas
	Gaemperli et al. (2007)	SPECT, CT	Myo	CardIQ fusion software	Combine information of CA and lesion
	Sazonova et al. (2017)	SPECT, CT	PC	Hybrid devices	Diagnose infectious endocarditis
	Siebermair et al. (2020)	SPECT, CT	LV, RV	N/A	Evaluate chamber-specific patterns of autonomic innervation in iAS
	Koukouraki et al. (2013)	SPECT, CTA	Myo	CardIQ fusion software	Clinical management of patients with suspected CAD
	Nakahara et al. (2016)	SPECT, CTA	Myo	Fusion based bull's eye	Determine hemodynamically relevant coronary vessels
	Kirişli et al. (2014)	SPECT, CTA	Myo	Point-cloud based reg	Allow Myo perfusion defect correlations with corresponding CA
	Piccinelli et al. (2018)	SPECT, CTA	Myo	Rigid reg	Detect and localize CAD
	Yoneyama et al. (2019)	SPECT, CTA	Myo	Manual registration	Defect correlations with corresponding CA
Echo and CT/MRI fusion	Maffessanti et al. (2017)	Echo, CT	CA	N/A	Visualize each CA and strain in its territory
	Tavard et al. (2014)	Echo, CT, EAM	LV	N/A	Extraction of local electro-mechanical delays
	Bruge et al. (2015)	Echo, CT, EAM	LV	N/A	Select the LV pacing sites
	Watanabe et al. (2021)	Echo, CT	CA	STDME technique	Assess conduit stenosis in complex adult CHD
	Kiss et al. (2011)	Echo, MRI	LV, RV, Myo	Landmark based reg	Assess Myo viability and diagnose ischemia
	Kiss et al. (2013)	Echo, MRI	LV	Landmark based rigid reg	Guide the echocardiographic acquisition
	Gomez et al. (2020)	Echo, MRI	WH	Landmark based reg	3D printed heart models
	Hatt et al. (2013)	Echo, MRI, X-ray	LV	N/A	Precise targeting for TE therapeutic delivery
X-ray and CT/MRI/Echo fusion	Zhou et al. (2014)	X-ray, SPECT	LV	Vessel-surface rigid reg	Guide LV lead implantation for CRT
	Ma et al. (2010b)	X-ray, (LGE) MRI	LV, scar	Manual reg	Guide LV lead implantation for CRT
	Dori et al. (2011)	X-ray, MRI	PA	Landmark based rigid reg	Facilitate cardiac catheterization of CHD
	Faranesh et al. (2013)	X-ray, MRI	AO, CA	Affine motion model	Facilitate cardiac interventions
	Abu Hazeem et al. (2014)	X-ray, MRI	PA, LSVC	Landmark based reg	Facilitate cardiac catheterization of CHD
	McGuirt et al. (2016)	X-ray, MRI	PA, LSVC	Landmark based reg	Facilitate cardiac catheterization of CHD
	Choi et al. (2016)	X-ray, MRI	LV	Edge based rigid reg	Guide LV lead implantation for CRT
	Grant et al. (2019)	X-ray, MRI	AO	Landmark based rigid reg	Select transcatheter CHD interventions
	Ma et al. (2010a)	X-ray, MRI	LV	2D-3D manual reg	Guide LV lead implantation for CRT
	Tomkowiak et al. (2011)	X-ray, (LGE) MRI	LV, scar	Custom software	Guide catheter-based TE delivery
	Ghoshhajra et al. (2017)	X-ray, CT	CA	Reg with manual correction	Guide chronic total occlusion of PCI
	Vernikouskaya et al. (2018)	X-ray, CTA	AO	Reg with manual correction	Facilitate TAVI procedures
	Ma et al. (2010c)	X-ray, Echo	LV, RV	Intensity-based rigid reg	Guide cardiac catheterization procedures
	Clegg et al. (2015)	X-ray, Echo	MV	Probe tracking	Guide percutaneous SHD interventions
	Housden et al. (2012)	X-ray, Echo	LA, RA	Probe based 2D-3D reg	Facilitate catheter ablation and TAVI
	Zorinas et al. (2017)	X-ray, Echo	AO	EchoNavigator system	Assist catheter-based cardiac operations
	Hadeed et al. (2018)	X-ray, Echo	N/A	EchoNavigator system	Guide interventional procedures for CHD
	Ebelt et al. (2020)	X-ray, Echo	LAA	TrueFusion technology	Improve the procedure of LAA closure
MSF	Cordero-Grande et al. (2012)	Cine, LGE MRI	Myo	Local entropy based reg	Assess MyoI
	Zhang et al. (2021a)	Cine, T1 mapping MRI	Myo	DL VNE generator	Generate gadolinium-free LGE-like MRI

morphology, ventricular function, myocardial perfusion, and viability. Integrated SPECT/PET and CT/MRI allow true simultaneous analysis of the structure and function of the heart and has been applied in clinical practice, as presented in the first row of Table 4. Compared to PET-CT, hybrid PET-MRI offers some advantages in that it does not require exposure to ionizing radiation from CT and iodinated contrast agents (Bergquist et al., 2017). It can be applied for the assessment of MyoI (Lee et al., 2012), cardiac sarcoidosis (Zandieh et al., 2018), atherosclerosis (Cuadrado et al., 2016), non-ischemic cardiomyopathies (Zhang et al., 2022), myocarditis (Nensa et al., 2018), vasculitis (Laurent et al., 2019), and cardiac tumors (Rinuncini et al., 2016). The fusion of SPECT with CT (especially CTA) images is regarded as the most successful example of fusion imaging (Kramer and Narula, 2010), and has been widely employed for the assessment of CAD (Koukouraki et al., 2013; Piccinelli et al., 2018).

3.2.2. Echo and CT/MRI fusion

Echo has great potential and offers clear benefits when complementing other modalities due to its ability to provide real-time information. The limited FOV and noise in Echo data could be alleviated by integrating it with additional imaging modalities. For example, TEE can be used for the assessment of morphology, function and hemodynamics in most adult congenital heart disease (CHD) patients, while CT enables extensive anatomical analysis due to its high spatial resolution. Several methods have been developed for synchronized display of real-time Echo images and multi-planar reconstruction images of CT or MRI (Watanabe et al., 2021). The fused images can provide additional findings, allowing accurate assessment of the diagnosis and severity of diseases, compared to Echo alone. For example, it can be employed in cardiac surgery, longitudinal studies, and to derive a more complete picture of the heart (motion from Echo and tissue perfusion from MRI) (Takaya and Ito, 2020).

3.2.3. X-ray and CT/MRI/echo fusion

X-ray fluoroscopy is commonly used for guiding minimally invasive cardiac interventions due to its excellent catheter and device visualization. However, it is limited by the 2D projection nature of the images, exposure to radiation, and poor soft-tissue contrast, which however can be solved with the use of diagnostic quality 3D images, such as MRI, CT and real-time 3D Echo. For example, the fusion of X-ray and MRI can be employed to facilitate cardiac catheterization of CHD patients with significant reductions in contrast and radiation exposure and decide the optimal pacing of the LV lead during CRT procedures. The introduction of additional LGE MRI during this fusion can further assist cardiologists to avoid scarring regions, as positioning an LV lead within the scarring areas may reduce response to CRT (Ma et al., 2010b). The fusion of X-ray and CT (or CTA) has been used to guide percutaneous procedures (Dori et al., 2011), guide chronic total occlusion of percutaneous coronary intervention (Ghoshhajra et al., 2017), and facilitate transaortic valve implantation (TAVI) procedures (Vernikouskaya et al., 2018). Real-time 3D stereo echocardiography (such as 3D TEE) can be fused with X-ray fluoroscopy to guide percutaneous structural heart disease interventions (Clegg et al., 2015) and facilitate AF catheter ablation as well as TAVI procedures (Housden et al., 2012). As opposed to fluoroscopy, 3D TEE provides excellent detail of 3D anatomy and soft tissue structures and offers "real-time" intraoperative guidance (Clegg et al., 2015). However, its advantages are limited by Echo shadowing, which reduces visualization of the catheters and metallic structures (Zorinas et al., 2017). Nevertheless, compared to CT and MRI, 3D Echo is widely available in hospitals at a much lower cost and provides real-time cardiac anatomical and function information for the fusion. With the recent availability of commercially available fusion packages on commercial X-ray systems, a wider range of clinical applications has been developed based on image fusion related to X-rays. Fig. 9 presents a clinical application example of X-ray and Echo image fusion.

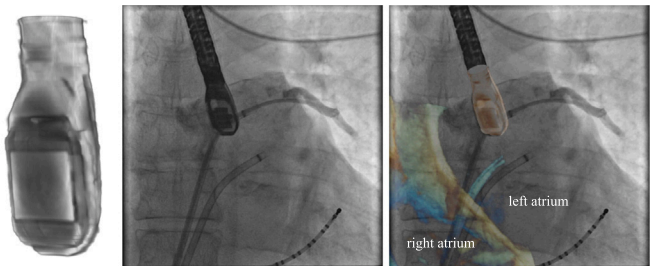

Fig. 9. A clinical application example of multi-modality cardiac image fusion for guiding AF catheter ablation and TAVI procedures. Here, X-ray image can present transesophageal Echo (TEE) probe, while TEE is better for visualizing cardiac anatomy. *Source:* Image adapted from Housden et al. (2012) with permission.

3.2.4. Multi-sequence MRI fusion

As MRI has different imaging sequences, one could fuse multi-sequence MRI to combine complementary information from different sequences. For example, Cordero-Grande et al. (2012) fused cine and LGE MRIs for precise representation of both the Myo boundaries and scars. Zhang et al. (2021a) fused cine and T1 mapping MRIs to generate gadolinium-free LGE-like MRI via a DL-based generator. Reducing the need for gadolinium can dramatically shorten scan times, lower the cost of associated consumables, minimize patient preparation time, and eliminate the need for physician presence. T1 mapping appears the most promising gadolinium-free technique but its clinical utility is still limited by the lack of standardized interpretation and post-processing. Therefore, one could combine T1 mapping and cine MRIs to exploit and enhance existing contrast and signals within them and display them in a standardized presentation.

3.2.5. Discussion

Image fusion typically includes two stages: (a) image registration (please refer to Table 3); (b) fusion of relevant features, which could be gray-level based or component-based analysis, from the aligned images. To avoid the registration step, several hybrid scanners have been developed to integrate multiple modalities (Sazonova et al., 2017; Lawonn et al., 2018). With the scanners, there still exist registration errors mainly due to cardiac or respiratory motion for cardiac imaging, so a post-alignment process remains desired (Garcia et al., 2009). The feature fusion involves the identification and selection of the features for specific clinical assessment purposes. In this study, we have found that the most common hybrid version is combining low-resolution molecular images (PET/SPECT) with anatomical context from high-resolution MR/CT; The most common target regions of fusion are LV Myo and LV, which are mainly involved with the management of CAD and the lead implantation for CRT, respectively.

Compared to other medical image fusion (brain, breast, liver, etc.) where many effective fusion schemes have been developed, cardiac image fusion is still at an early stage (James and Dasarathy, 2014). The works we surveyed did not provide many details on the fusion schemes, and most of them achieved static fusion. There were only a few software products commercially available for real-time fusion between dynamic images. For example, EchoNavigator is a software tool that enables real-time image synchronization and fusion of 2D and 3D TEE with fluoroscopy images. The coordinate system of the two imaging modalities can be aligned based on the localization and tracking of the TEE probe. This software might facilitate complex percutaneous procedures and decrease procedure length as well as radiation dose. Note that the software was installed only in a few hospitals at the time of publication (Biaggi et al., 2015), which limits the clinical evaluation of fusion images. Recently, many DL-based image fusion methods have been developed for brain image fusion (Zhang et al., 2021b), but they have not been applied to cardiac image fusion yet. Nevertheless, there are several DL-based works that achieved implicit cardiac image fusion

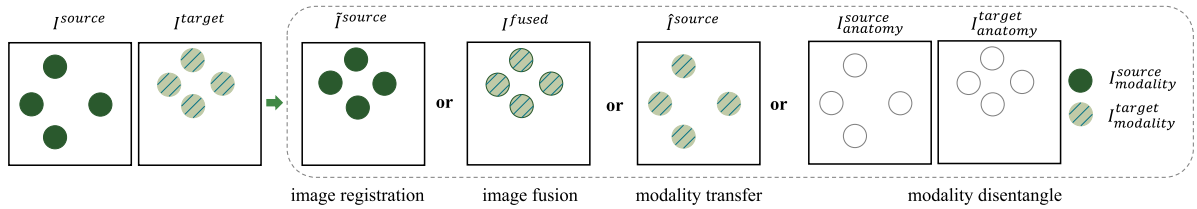

Fig. 10. Four typical multi-modality image processing schemes. Here, the distribution of the circles indicates the anatomical structure of the image, and the texture of the circles indicates the modality of the image. I^{target} and I^{source} denotes target image and source image, which exist both spatial misalignment and modality inconsistency. $\tilde{I}^{source}$, I^{fused}, and $\hat{I}^{source}$ are deformed source image, fused image, and target-style source image, respectively. $I_{anatomy}$ and $I_{modality}$ are the disentangled anatomy image and modality information, respectively. Note that in this illustration the modality fusion is performed on the pre-aligned images, i.e., $\tilde{I}^{source}$ and I^{target}.

in the latent space for multi-modality image segmentation (please c.f. Section 3.3.2 for details). Given a large amount of data, deep neural networks are powerful for learning hierarchical feature representations. Note that there are no general criteria for network architecture design, and the questions of what, when and how, applied to cardiac image fusion, remain unresolved. Moreover, current research mainly focuses on the fusion of two modalities, and the fusion of three or more modalities is rarely studied in literature (Tirupal et al., 2021). Despite extensive research and test applications, multi-modality image fusion techniques have not yet been extensively translated into clinical routine. In conclusion, fused imaging further increases the variety of cardiac imaging modalities (modality augmentation), but effective techniques are still under development.

3.3. Segmentation

Multi-modality cardiac image segmentation has received a substantial research attention, including both anatomical segmentation (Zhuang et al., 2022) and pathology segmentation (Zhuang and Li, 2020). It needs to solve the difference in data distribution among different modalities normally via registration, fusion, or domain adaptation (modality transfer or disentanglement). Fig. 10 provides the sketch maps of these modality processing schemes. The image registration employs spatial transformation parameters to align images of different modalities and then performs segmentation on the anatomy-aligned images (Luo and Zhuang, 2020; Zhuang, 2019). Based on the registration results, one could further fuse several modalities into a single one, and then perform segmentation on the integrated images/features (Zhuang and Shen, 2016). Moreover, one could utilize transfer learning to transfer different modalities to the target domain and then perform segmentation on the modality-aligned images/features (Chen et al., 2019c). Another similar idea is to disentangle the anatomy and modality information from cardiac images, and the target region can be directly segmented on the disentangled anatomy images/features (Chartsias et al., 2019a). Table 5 summarizes the representative multi-modality cardiac image segmentation methods, the applied modalities and the target substructures of the heart.

3.3.1. Registration based segmentation

A direct way to propagate anatomy knowledge between modalities is multi-modality registration, and these methods can be categorized as registration based segmentation. Among registration based segmentation methods, atlas registration based approaches are commonly used in multi-modality scenarios. They register one or multiple atlases to the target image, followed by propagation of (usually manual) labels. We refer the reader to Table 3 for multi-modality registration. If several atlases are available, labels from individual atlases can be combined into a final segmentation via a label fusion strategy (Zhuang and Shen, 2016; Ding et al., 2020). The number of atlases determines the potential optimal performance of multi-atlas segmentation (MAS), and thus considering multi-modality atlases is beneficial when they are available. Conventional multi-modality MAS based methods are generally computationally expensive. This is because these methods perform the registration step in an iterative fashion and typically employ patch-based label fusion (Bai et al., 2013; Zhuang and Shen, 2016; Sanroma et al., 2018). To solve this, one could achieve both image registration and label fusion by deep neural networks for a computationally efficient MAS framework (Ding et al., 2020).

However, these DL-based MAS frameworks cannot be optimized in an end-to-end fashion, as the image registration and label fusion are separated into two tasks. Recently, Luo and Zhuang (2020) proposed a probabilistic image registration framework based on a multivariate mixture model and neural network estimation. In their framework, MAS was unified by groupwise registration, and registration and segmentation of multi-modality cardiac images were achieved simultaneously. The joint distribution of multi-modality images was modeled as multivariant mixtures, and the model was formulated with transformation. Segmentation can be performed on a virtual common space, where all the images were simultaneously registered. Instead of the commonly used Expectation Maximization (EM) algorithm (Zhuang, 2019), they utilized neural networks to efficiently estimate the parameters of multivariate mixture model (Luo and Zhuang, 2020).

3.3.2. Fusion based segmentation

To the best of our knowledge, there are only a few works that employ image fusion for multi-modality cardiac segmentation. Most fusion based segmentation methods do not explicitly generate a new integrated image by image fusion (also namely *explicit fusion*), but only perform an *implicit fusion* at different levels. The only available explicit fusion based segmentation, up to our knowledge, is from Tong et al. (2017), where cardiac MRI and CT were fused based on their normalized mean intensity values. With the fused images, the size of the training set was increased, and therefore the segmentation model yielded better results. Overall, the reason for employing fusion-based segmentation methods for multi-modality images is to leverage complementary information from different modalities, leading to improved segmentation performance and potentially enhancing clinical utility in various medical imaging applications. Explicit fusion based segmentation offers advantages in terms of providing fine-grained control, enhancing interpretability, and enabling adaptability. Nevertheless, the contribution of each modality to the final segmentation may not always be easily quantifiable or visualizable, and the interpretation of the fused information may still require expert knowledge and experience. On the other hand, implicit fusion methods, where the fusion occurs automatically within DL-based models, mitigate the need for domain expertise, simplify the feature extraction steps, and can be optimized in an end-to-end style.

Fig. 11 presents the three typical types of DL-based modality fusion for multi-modality cardiac image segmentation. Many works simply concatenate different modalities into different channels and focus on the subsequent segmentation network architecture, namely input-level fusion (Wang et al., 2019b; Yu et al., 2020b; Zhang et al., 2020; Elif and Ilkay, 2020). Similarly, one could perform fusion by fusing the model outputs from different modality inputs, namely decision-level fusion. For the decision-level fusion, many fusion strategies can be used, such as averaging and majority voting (Rokach, 2010). Both input- and

Table 5
Summary of previously published representative works on *multi-modality cardiac segmentation*. MM-WHS: unpaired cardiac CT and MRI dataset from Multi-Modality Whole Heart Segmentation Challenge (Zhuang et al., 2022); MyoPS: paired cardiac bSSFP, T2-weighed, and LGE MRIs from Myocardial Pathology Segmentation Combining Multi-Sequence CMR Challenge (Li et al., 2023b); X-rayAI: X-ray angiography image; T1-CE: contrast-enhanced T1 imaging; MAS: multi-atlas segmentation; CNN: Convolutional neural network; MTL: multi-task learning; HM: histogram matching; UDA: unsupervised domain adaptation; FCNN: full convolutional neural network; MMD: maximum mean discrepancy.

	Study	Modality	Target	Method	Type
Registration based segmentation	Peters et al. (2010)	CT, MRI, X-rayAI	WH; LA	Simulated search	Supervised
	Zhuang and Shen (2016)	CT, MRI	WH	Multi-scale and modality MAS	Supervised
	Zheng et al. (2019)	MS-CMRSeg	LV, RV, Myo	Deep registration and segmentation	Supervised
	Ding et al. (2020)	MM-WHS	Myo	DL-based cross-modality MAS	Supervised
	Zhuang (2019)	MS-CMRSeg	Myo	Multivariate mixture model	Supervised
	Luo and Zhuang (2020)	MS-CMRSeg	LV, RV, Myo	Deep multivariate mixture model	Supervised
	Paknezhad et al. (2020)	Tagged, cine MRI	Myo	Deformation-based segmentation	Supervised
Fusion based segmentation	Mortazi et al. (2017)	MM-WHS	WH	Multi-planar network with an adaptive fusion strategy	Supervised
	Tong et al. (2017)	MM-WHS	WH	Modality normalization and fusion	Supervised
	Zhao et al. (2020)	MyoPS	LV scar and edema	Stacked and parallel U-Nets for fusion	Supervised
	Jiang et al. (2020)	MyoPS	LV scar and edema	Max-fusion U-net	Supervised
	Li et al. (2022c)	MS-CMRSeg, MyoPS	LV, RV, Myo; LV scar and edema	Deep co-training	Supervised
	Ankenbrand et al. (2020)	MyoPS	LV scar and edema	Ensemble U-net	Supervised
	Zhai et al. (2020)	MyoPS	LV scar and edema	Coarse-to-fine weighted ensemble model	Supervised
	Martín-Isla et al. (2020)	MyoPS	LV scar and edema	Stacked BCDU-net with MRI synthesis	Supervised
	Wang et al. (2022)	MyoPS	LV scar and edema	Auto-weighted attention ensemble model	Supervised
Domain adaptation based segmentation	Zhang et al. (2018)	CT, MRI	WH	Cycle- and shape-consistency GAN	Supervised
	Chen et al. (2019b)	MM-WHS	LA, LV, Myo, AO	Synergistic image and feature adaptation	Unsupervised
	Tao et al. (2019)	MS-CMRSeg	LV, RV, Myo	Shape-transfer GAN	Unsupervised
	Chen et al. (2019c)	MS-CMRSeg	LV, RV, Myo	Image-to-image translation	Unsupervised
	Ly et al. (2019)	MS-CMRSeg	LV, RV, Myo	Style data augmentation	Unsupervised
	Wang et al. (2019a)	MS-CMRSeg	LV, RV, Myo	HM and domain adversarial learning	Unsupervised
	Dou et al. (2019)	MM-WHS	LA, LV, Myo, AO	Plug-and-play adversarial UDA	Unsupervised
	Ouyang et al. (2019)	MM-WHS	LA, LV, Myo, AO	VAE-based feature prior matching	Unsupervised
	Chen et al. (2020b)	MM-WHS, MS-CMRSeg	LA, LV, RV, Myo, AO	Affinity-guide CNN	Supervised
	Liao et al. (2020)	MM-WHS	WH	Multi-modality transfer learning	Semi-supervised
	Yu et al. (2020a)	CT, MRI	Myo	MTL + adversarial reverse mapping	Supervised
	Liu and Du (2020)	MS-CMRSeg	LV, RV, Myo	CycleGAN with MMD constraints	Unsupervised
	Wu and Zhuang (2020)	MM-WHS, MS-CMRSeg	LV, RV, Myo	Explicit domain discrepancy	Unsupervised
	Li et al. (2020a)	MM-WHS	WH	Dual-teacher++	Semi-supervised
	Xue et al. (2020)	MM-WHS	WH	Dual-task and hierarchical learning	Unsupervised
	Bian et al. (2020)	MM-WHS[a]	LA, LV, Myo, AO	Uncertainty-aware domain alignment	Unsupervised
	Wu and Zhuang (2021)	MM-WHS, MS-CMRSeg	WH; LV, RV, Myo	Variational approximation	Unsupervised
	Wang et al. (2021)	MM-WHS	LA, LV, Myo, AO	Global and category-wise alignment	Unsupervised
	Bian et al. (2021)	MM-WHS[a]	LA, LV, Myo, AO	Zero-shot learning	Unsupervised
	Chen et al. (2021a)	MM-WHS[a]	LA, LV, Myo, AO	Information bottleneck GAN	Unsupervised
	Chen et al. (2021b)	MM-WHS[a]	LA, LV, Myo, AO	Diverse data augmentation GAN	Unsupervised
	Cui et al. (2021a)	MM-WHS	LA, LV, Myo, AO	Bidirectional UDA	Unsupervised
	Cui et al. (2021b)	MM-WHS	LA, LV, Myo, AO	Hybrid domain-invariant information	Unsupervised
	Tomar et al. (2021)	MM-WHS[a]	LA, LV, Myo, AO	Spatial adaptive normalization	Unsupervised
	Vesal et al. (2021)	MM-WHS, MS-CMRSeg	LV, RV, Myo	Point-cloud shape adaptation	Unsupervised
	Zeng et al. (2021)	MM-WHS[a]	LA, LV, Myo, AO	Semantic consistent UDA	Unsupervised
	Guo et al. (2021b)	MRI, CT, Echo	LV, Myo	Few-shot multi-level semantic adaptation	Semi-supervised
	Liu et al. (2021)	MM-WHS	LA, LV, Myo, AO	Symmetric FCNN with attention	Unsupervised
	Kots et al. (2021)	MM-WHS[a]	LA, LV, Myo, AO	Deep co-training	Semi-supervised
	Cai et al. (2016)	CT, MRI	LA, LV, Myo; WH	Groupwise; spectral decomposition	Unsupervised
	Dou et al. (2020)	MM-WHS[a]	LA, LV, Myo, AO	Knowledge distillation	Supervised
	Chartsias et al. (2019b)	bSSFP + LGE MRI	LV, Myo	Disentangled representation learning	Semi-supervised
	Chartsias et al. (2019a)	MM-WHS[a]	WH	Disentangled representation learning	Semi-supervised
	Chartsias et al. (2020)	bSSFP, LGE MRI[a]	LV, Myo	Disentangle align and fuse network	Semi-supervised
	Pei et al. (2021)	MM-WHS, MS-CMRSeg	LV, RV, Myo	Disentangle domain features	Unsupervised
	Wang and Zheng (2021)	MM-WHS, MS-CMRSeg	LV, RV, Myo	Cycle-consistent model	Unsupervised

[a]Denotes that the evaluation dataset also includes non-cardiac or single-modality dataset which is out of the scope of this study.

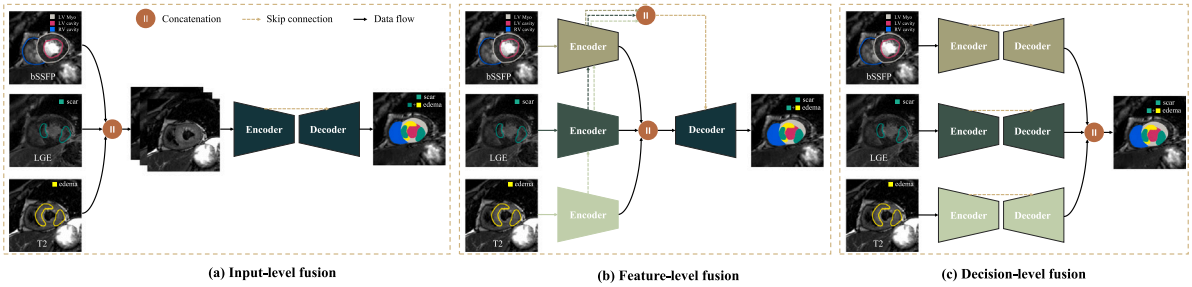

Fig. 11. An example of multi-modality cardiac image segmentation. Here, we present three different deep learning based fusion strategies for myocardial pathology segmentation combining multi-sequence MRIs. Note that here bSSFP, T2-weighed, and LGE MRIs have been aligned before fusion.

decision-level fusion are simple, but ignore the relationship among different modalities. A potential solution is to utilize two-stage networks which consider the prior spatial relationship between different modalities. One typical application is cardiac pathology segmentation, where anatomical information can be extracted from one modality (bSSFP MRI) at the first stage; with obtained segmentation masks from the first stage, the functional information can be learned by combining other modalities (LGE and T2-weighted MRIs) at the second stage (Zhuang and Li, 2020). Moreover, fusion can be performed on latent feature space (Mortazi et al., 2017; Jiang et al., 2020; Li et al., 2022c; Zhao et al., 2020), namely feature-level fusion, and multi-scale information fusion can be achieved via densely connected layers (Zhao et al., 2020). For example, Jiang et al. (2020) proposed a max-fusion U-Net for multi-sequence cardiac pathology segmentation, where the features from different modalities were fused via a pixel-wise maximum operator. The operator was expected to guide the network to keep informative features extracted by each modality. Furthermore, the contribution of each modality can be weighted via cross-modal convolutions (Tseng et al., 2017).

Compared with input/decision-level fusion, feature-level fusion can pay more attention to learning the complex relationship between different modalities (Zhou et al., 2019b). However, the features to be merged are not modality-invariant, and therefore may affect the multi-modality segmentation. To solve this, one could combine disentangled representation learning with fusion schemes for the segmentation. For example, Chartsias et al. (2020) disentangled modality and anatomy features from multi-modality images, and then fused the disentangled anatomy features for cardiac segmentation of bSSFP and LGE MRIs. Besides modality fusion, model ensemble scheme is also widely employed for multi-modality cardiac segmentation by integrating several predictions from different models (Ankenbrand et al., 2020; Zhai et al., 2020; Martín-Isla et al., 2020).

3.3.3. Domain adaptation based segmentation

For multi-modality cardiac analysis, the annotation of all modalities via supervised learning can be tedious, time-consuming, and significantly variable across imaging modalities. An intuitive solution is to transfer the knowledge from the annotation-rich modalities (denoted as source domain) to another annotation-poor modality (referred to as target domain). Note that here the source and target domains could be collected from the same or different subjects. Due to the existence of domain shift, the model trained on the source domain usually fails on the target domain (Wu and Zhuang, 2020; Li et al., 2022a). Domain adaptation is therefore proposed to generalize models from the source domain to the target domain without much performance degradation. This is normally achieved by aligning two domains into a common space, where their domain discrepancy can be minimized. Regarding the manner of domain alignments, current domain adaptation can be categorized into three kinds, i.e., discrepancy minimization-based strategies, adversarial learning-based algorithms and reconstruction-based methods (Liu et al., 2021). There are many applications of

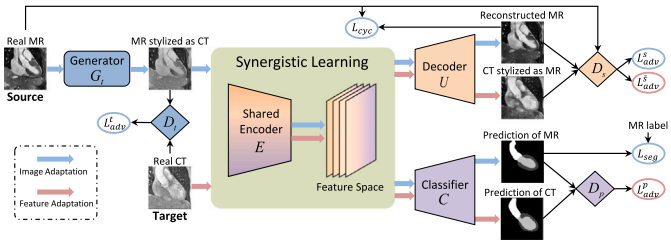

Fig. 12. An example of unsupervised domain adaptation based cross-modality cardiac image segmentation.
Source: Image adapted from Chen et al. (2019b) with permission.

domain adaptation, such as semantic segmentation, image classification, and object detection. Specific to the cardiology field, domain adaptation has been employed for cross-modality image segmentation (Pei et al., 2021), cross-axis MRI segmentation (Koehler et al., 2021), cardiac strain analysis of Echo (Lu et al., 2021), cross-individual ECG arrhythmia classification (Chen et al., 2020c), and comparison of cardiac simulation models (Duchateau et al., 2019). We mainly summarize the work of cross-modality cardiac image segmentation via domain adaptation, either by modality transfer or modality disentangle, as presented in the bottom part of Table 5. One can see cardiac cross-modality domain adaptation works emerge from 2019, with the release of two public cardiac multi-modality/sequence datasets. All these works are DL-based and are generally unsupervised, i.e., without using the target domain label. Fig. 12 presents an example where unsupervised domain adaptation is applied to segment cardiac CT with the assistance of MRI. Two unique semi-supervised works are based on dual-teacher++ (Li et al., 2020a) and few shot (Guo et al., 2021b), which both employed only limited target domain label.

Note that the domain shift between different modalities, such as CT and MRI, can be much larger compared to that between different sequences within the same modality, such as bSSFP, T2-weighed, and LGE MRIs (Courtial et al., 2019). Multi-sequence data is typically obtained from the same patient, further leading to smaller domain discrepancies (Pei et al., 2021). To quantitatively measure the domain discrepancies, one could employ statistical measures and domain discrepancy metrics, such as maximum mean discrepancy (MMD) (Chen et al., 2019d), Wasserstein distance (Shen et al., 2018), and correlation alignment (Xu et al., 2022). The domain shift between different modalities/sequences can result in performance degradation of DL-based models, but many other factors beyond the size of domain discrepancy also affect the extent of degradation (Wang and Zheng, 2021). Therefore, when applying domain-based adaptive segmentation, it may not be sufficient to predict performance degradation solely based on domain shifts.

3.3.4. Discussion

Multi-modality image segmentation benefits from both aforementioned image registration and fusion especially when involving a combination of multiple modalities. However, currently image registration

Table 6
Public multi-modality cardiac image datasets.

Reference	Dataset	Target	Disease	Type
Utah (2012)	155 bSSFP, LGE MRI	LA cavity and scar	AF	Paired
Tobon-Gomez et al. (2013)	15 MRI, 3D Echo	Myo	Healthy	Paired
Tobon-Gomez et al. (2015)	30 MRI, 30 CT	LA cavity	AF	Unpaired
Karim et al. (2018)	10 MRI, 10 CT	LA wall	AF	Unpaired
Zhuang et al. (2019)	60 MRI, 60 CT	WH	AF, CHD, others	Unpaired
Zhuang et al. (2022)	45 bSSFP, T2-weighted, LGE MRI	LV, RV, Myo	MyoI	Paired
Li et al. (2023b)	45 bSSFP, T2-weighted, LGE MRI	LV scar and edema	MyoI	Paired

or explicit image fusion is mostly used as a pre-processing step for structure segmentation (Li et al., 2023b; Tong et al., 2017). Only a few studies combined registration with segmentation in a unified framework for multi-modality cardiac images, namely *combined computing* (Zhuang, 2019; Luo and Zhuang, 2020, 2022). These combined computing methods often employed probabilistic models and formulated the estimation of both registration and segmentation parameters as a maximum likelihood estimation (MLE) problem. By maximizing the likelihood function, the parameters of both the registration and segmentation models can be estimated simultaneously, resulting in a joint estimation of the parameters for both tasks. In addition to probabilistic models, neural networks have also been used for combined computing of registration and segmentation tasks directly, without explicitly formulating them as MLE problems. For example, Ding et al. (2023) achieved combined computing of multi-sequence MRI registration and Myo segmentation for Myo pathology segmentation. However, they found that it is hard to achieve simultaneous multi-sequence registration, Myo segmentation and Myo pathology segmentation. This is because pathology segmentation task focused on the abnormal intensity information, which may not be directly compatible with the registration and anatomical segmentation tasks that are based on different sequences. In the future, it would be desirable to integrate the abnormal intensity information from pathology segmentation with the multi-sequence image registration and anatomical segmentation tasks in a unified framework. Unified registration and segmentation frameworks eliminate the need for a separate registration model, and segmentation can facilitate registration and vice versa.

Domain adaptation can be regarded as a new application of multi-modality imaging. It does not combine information from different modalities but transfers information across modalities, to assist the image segmentation of the target domain which usually has limited available annotated data. Modality information transfer can also be employed in cardiac image reconstruction, where cardiac motion priors can be obtained from other modalities for motion correction (Sang et al., 2021). An alternative idea to domain adaptation that appears in multi-modality image registration is the disentangled representation. It is reasonable as both multi-modality image registration and segmentation care about the structural information instead of the modality information. Moreover, compared to cardiac image registration and fusion, DL-based models have been widely employed for multi-modality cardiac image segmentation, thanks to the release of public datasets.

4. Data and evaluation measures

4.1. Public multi-modality cardiac datasets

TheCardiacAtlasProject provides a public imaging database for computational modeling and statistical atlases of the heart (Fonseca et al., 2011). It includes images targeted to different cardiac structures as well as diseases and acquired with different modalities from different centers. Other challenge events have released public multi-modality cardiac datasets, as summarized in Table 6. One can see that different from the computer vision datasets, there are a limited number of public multi-modality cardiac image datasets. Also, only some specific modalities are covered, including MRI, CT and Echo. Nevertheless, these datasets have already substantially facilitated the development of multi-modality cardiac imaging analysis, as we summarized in Section 3.3. In the future, more multi-modality cardiac images, either paired or unpaired, are expected to be released to boost the development of multi-modality cardiac image analysis.

4.2. Evaluation measures

Thorough validation is necessary for clinical acceptance. Verifying the accuracy of multi-modality image registration or fusion is a difficult task as a good quality gold standard is normally unavailable. Visual assessment, sometimes used to evaluate the accuracy, is subjective and thus not reproducible. For an objective evaluation, external labels, anatomical landmarks and/or external fiducial frames are required (Makela et al., 2002). In contrast, the evaluation of multi-modality image segmentation is relatively simple as manual segmentation can be used as the gold standard. Nevertheless, the comparison of measures from literature is difficult as different metrics can be applied to evaluate one method. Note that sometimes different evaluation metrics could lead to different conclusions regarding the performance of an algorithm, indicating the potential limitation of current metrics. In this section, we summarize several common measures employed in each multi-modality image computing task.

4.2.1. Image registration measures

For assessing the performance of cardiac multi-modality image registration, a range of different measures have been explored (Van de Kraats et al., 2005). The registration may involve different combinations of dimensions, with the most common combinations being 3D-to-3D and 2D-to-3D. For 3D-to-3D registration, one could employ mean landmark distance (mLD) (Sinha et al., 1995), mean target registration error (mTRE), and surface distance (Sturm et al., 2003; Mäkelä et al., 2001) for evaluation. Here, mLD can be defined as,

$$\mathrm{mLD}\left(\hat{T}\right) = \frac{1}{N_l}\sum_{i,j=1}^{N_l}\left\|\hat{T}(\mathbf{l}_i) - \mathbf{l}_j\right\|, \tag{1}$$

where $\hat{T}$ is the predicted transformation, N_l is the number of landmarks, and $\mathbf{l}_i$ and $\mathbf{l}_j$ are paired landmarks from source and target images, respectively. mTRE is computed as the mean 3D distance between the point $\mathbf{p}_j$ from the target image space and the corresponding point $\mathbf{p}_i$ from the source image space transformed with the predicted transformation $\hat{T}$,

$$\mathrm{mTRE}\left(\hat{T}\right) = \frac{1}{N_p}\sum_{i,j=1}^{N_p}\left\|\hat{T}(\mathbf{p}_i) - \mathbf{p}_j\right\|, \tag{2}$$

where N_p is the number of points. mTRE is a good measure for patient-to-image registration for navigation, as it calculates the misalignment on specific points of interest within the target volume where the operation will be performed. Surface distance can be defined as the mean 3D Euclidean distance, standard deviation, and root mean square distance between the transformed source image and target image surfaces (Sturm et al., 2003). Note that here the surface is sampled after registration in the format of paired corresponding points. Therefore, one could employ the percent number of overlapped point pairs as a registration measure. Checkerboard visualization for visual assessment is also commonly used (Mäkelä et al., 2003; Camara et al., 2009; Courtial et al., 2019), as presented in Fig. 13. Due to the absence of

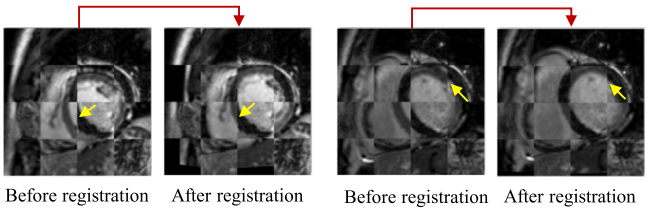

Fig. 13. Two examples of multi-modality cardiac image registration (bSSFP and LGE MRIs) visual evaluation via overlaid blocks. The representative visible fixed misalignment areas are highlighted by the yellow arrows.

the gold standard, one could instead evaluate the anatomical labels of transformed source images in terms of Dice and Hausdorff distance (HD) (Turco et al., 2016; Atehortúa et al., 2020), defined as,

$$\mathrm{Dice}(V_1, V_2) = \frac{2\left|V_1 \cap V_2\right|}{\left|V_1\right| + \left|V_2\right|}, \tag{3}$$

and

$$\mathrm{HD}(X, Y) = \max\left[\sup_{x\in X}\inf_{y\in Y} d(x, y), \sup_{y\in Y}\inf_{x\in X} d(x, y)\right], \tag{4}$$

where V_1 and V_2 denote the set of pixels in the target and transformed source labels, respectively; $|\cdot|$ refers to the number of pixels in set V; X and Y represent two sets of contour points; and $d(x, y)$ indicates the Euclidean distance between the two points x and y; Besides, one could randomly transform the source image with known transformations for the known gold standard to quantify registration accuracy (Pauna et al., 2003).

For 2D-to-3D registration, visual inspection (Aksoy et al., 2013), $\mathrm{mTRE}_{\mathrm{proj}}$ (Gouveia et al., 2017), and centerline 2D distance measure (Baka et al., 2013; Van de Kraats et al., 2005) have been utilized for evaluation. Here, $\mathrm{mTRE}_{\mathrm{proj}}$ refers to the mTRE in the projection direction and is defined as,

$$\mathrm{mTRE}_{\mathrm{proj}}\left(\hat{T}\right) = \frac{1}{N_p}\sum_{i,j=1}^{N_p}\left\|(\hat{T}(\mathbf{p}_i) - \mathbf{p}_j)\cdot\hat{\mathbf{n}}\right\|, \tag{5}$$

where $\hat{\mathbf{n}}$ is the normal to the projection plane. However, 2D error measures may be more appropriate than mTRE, as 2D-to-3D registration normally projects a 3D image onto a 2D image plane. Another solution is employing mean reprojection distance (mRPD), which calculates the minimum distance between the line (eg. centerline of CA) from 2D projected points to the corresponding 3D position of that point. Here, mRPD can be defined as,

$$\mathrm{mRPD}\left(\hat{T}\right) = \frac{1}{N_p}\sum_{i,j=1}^{N_p}\mathrm{Dist}(L_i(\hat{T}(source, \mathbf{p}_i)), \mathbf{p}_j), \tag{6}$$

where $\mathrm{Dist}(L_i, \mathbf{p}_j)$ denotes the minimum distance between the 3D point $\mathbf{p}_j$ and a line L_i through $\mathbf{p}_i$ and the source image (2D image) space.

Besides, the Jacobian determinant can measure the plausibility of estimated displacement fields for non-rigid registration (Ashburner, 2007). The Jacobian matrix of a displacement field $\mathbf{\Phi}$ at a spatial point $\mathbf{p}$ is defined as,

$$J_{\mathbf{\Phi}}(\mathbf{p}) = \nabla\mathbf{\Phi}(\mathbf{p}) \tag{7}$$

where $\mathbf{\Phi}(\mathbf{p})$ denotes the displacement value at $\mathbf{p}$. Jacobian determinant $\det(J_{\mathbf{\Phi}}(\mathbf{p})) \leq 0$ indicates that $\mathbf{\Phi}(\mathbf{p})$ is not topology-preserving, while the values near 1 represent smooth fields (Dalca et al., 2019).

4.2.2. Image fusion measures

Although there are several multi-modality cardiac image fusion works, most of them are performed in clinical studies generally with visual evaluation (Chauhan et al., 2021). There are many available objective evaluation measures for image fusion, including entropy, MI, standard deviation (SD), peak signal to noise ratio (PSNR), structural similarity index measure, average gradient, $\mathrm{Q}_{\mathrm{AB/F}}$metric, root mean square error (RMSE), edge intensity, visual information fidelity, spatial frequency, and spectral discrepancy (Tirupal et al., 2021; Bhavana and Krishnappa, 2015). This qualitative analysis mainly aims to check the quality of fused images from different perspectives. However, specific to the cardiology field, the measure of image fusion is mainly performed at the registration stage instead of the fusion stage, as to our knowledge. This may be due, at least in part, to the limited methodology development of image fusion in cardiology.

4.2.3. Image segmentation measures

The most commonly used measure for multi-modality cardiac image segmentation is the Dice score. Jaccard index, HD, and average surface distance (ASD) have also been used (Li et al., 2021b,a; Zhuang, 2019), defined as:

$$\mathrm{Jaccard}(V_{\mathrm{auto}}, V_{\mathrm{manual}}) = \frac{\left|V_{\mathrm{auto}} \cap V_{\mathrm{manual}}\right|}{\left|V_{\mathrm{auto}} \cup V_{\mathrm{manual}}\right|}, \tag{8}$$

and

$$\mathrm{ASD}(X, Y) = \frac{1}{2}\left(\frac{\sum_{x\in X}\min_{y\in Y} d(x, y)}{\sum_{x\in X} 1} + \frac{\sum_{y\in Y}\min_{x\in X} d(x, y)}{\sum_{y\in Y} 1}\right), \tag{9}$$

where V_{auto} and V_{manual} denote the set of pixels in the automatic and manual segmentation, respectively. Statistical measurements can also be employed (Li et al., 2021b; Mortazi et al., 2017), i.e., Accuracy (Acc), Specificity (Spe), Sensitivity (Sen), and Precision (Pre). Acc refers to the proportion of pixels that have received the correct label among the total number of subjects examined. Spe and Sen (also known as Recall) are utilized to reflect the success rates of algorithms for the background and the foreground segmentation, respectively. Precision (also called positive predictive value) indicates the fraction of relevant instances among the retrieved instances. These measures can appear in various combinations when evaluating multi-modality cardiac image segmentation, and Dice is usually included (Cai et al., 2016; Ding et al., 2020).

5. Discussion and future perspectives

The last decade has witnessed an enormous amount of efforts in the specific field of multi-modality image computing for cardiac analysis. Cardiac hybrid imaging can provide valuable diagnostic and prognostic information for patients with CVDs, compared with side-by-side evaluation from a single imaging modality (Gimelli and Liga, 2013). Table 7 summarizes the potential clinical applications of the developed computing algorithms. With the development of hybrid imaging devices, there has been a reduction in complex image processing through software. This is because the superposition of images using a hybrid device, although it may not be obtained simultaneously, is obtained by successive measurements. Nevertheless, many techniques have not yet been translated into clinical routine. This is, at least in part, attributed to the fact that the pre-processing step, i.e., registration, usually requires intensive manual interaction. In this discussion, we aim to identify the most important challenges that may drive future research in multi-modality cardiac image analysis.

5.1. Multi-modality cardiac computing with missing modality

In multi-modality cardiac studies, one or more sub-modalities may be missing due to poor image quality (e.g. imaging artifacts), failed acquisitions or counterindications (Qiu et al., 2023). However, current multi-modality learning algorithms generally assume that all modalities are available (Azad et al., 2022). Nevertheless, there exist a number of methods to deal with missing modalities, which can be roughly categorized into three types. Firstly, different models can be designed for every potential missing modality combination, which is

Table 7
Summary of potential clinical applications of combining multi-modality cardiac imaging for cardiac analysis. PAD: peripheral artery disease; ID: infectious endocarditis; DCM: dilated cardiomyopathy; HCM: hypertrophic cardiomyopathy; CS: cardiac sarcoidosis; DMR: degenerative mitral valve regurgitation; AS: aortic stenosis; MVD: mitral valve disease; AVS: aortic valve stenosis; TAVR: trans-aortic valve replacement.

Modality	Clinical application	Pathology	Representative study
CT, MRI	WH segmentation; LA cavity segmentation; LA wall thickness measurement; cardiac index estimation	AF, CHD, etc.	Zhuang et al. (2019), Tobon-Gomez et al. (2015), Karim et al. (2018) and Yu et al. (2020a)
CTA, MRI	CA quantification	CAD	Sturm et al. (2003)
CTA, SPECT	Myo/CA quantification	CAD, ID	Koukouraki et al. (2013), Piccinelli and Garcia (2013) and Sazonova et al. (2017)
CTA, X-ray	Angioplasty; TAVI guidance	CAD, AVS	Baka et al. (2013) and Gouveia et al. (2017)
MRI, X-ray	Invasive cardiovascular procedures (such as CRT); LV contour detection; target endomyocardial injections	PAD, CHD, MyoI	Oost et al. (2003), Gutiérrez et al. (2007), Ma et al. (2010a), Faranesh et al. (2013), Abu Hazeem et al. (2014), De Silva et al. (2006) and Choi et al. (2016)
CT, Echo	LA wall thickness measurement; real-time surgical navigation; ablation/TAVI/TAVR guidance	AF, AS, MVD, CHD	Karim et al. (2018), Huang et al. (2009), Sandoval and Dillenseger (2013), Khalil et al. (2017a,c) and Watanabe et al. (2021)
MRI, Echo	Cardiac motion estimation; Echo acquisition guidance; Myo viability assessment	DCM, HCM, MyoI	Puyol-Anton et al. (2017), Atehortúa et al. (2020), Kiss et al. (2013, 2011) and Mäkelä et al. (2003)
MRI, PET	Practical MRI acquisition; Myo viability, perfusion and metabolism assessment; cardiac motion correction	MyoI, CAD, CS	Kolbitsch et al. (2017), Sinha et al. (1995), Mäkelä et al. (2001), Zandieh et al. (2018) and Polycarpou et al. (2021)
X-ray, Echo	LAA closure procedure guidance; ablation and TAVI guidance	CHD, AF, SHD	Housden et al. (2012), Hadeed et al. (2018) and Ebelt et al. (2020)
bSSFP, T2-weighted, LGE MRIs	LV (scar and edema), RV, Myo segmentation	MyoI	Zhuang et al. (2022), Li et al. (2023b) and Wang et al. (2022)
bSSFP, T2 mapping MRIs	Generate gadolinium-free LGE-like MRI	MyoI	Zhang et al. (2021a)
bSSFP, LGE MRIs	LA fibrosis and scar segmentation	AF	Li et al. (2020b) and Wu et al. (2018)
Tagged, cine MRIs	Myo strain analysis; motion estimation	DMR	Paknezhad et al. (2020) and Shi et al. (2012)

complicated and time-consuming. Secondly, many works attempt to impute or synthesize missing modalities to obtain the complete imaging modalities (Havaei et al., 2016). However, an additional network is normally required for synthesis, and the model might be sensitive to the synthesized image quality. Thirdly, one could learn a shared feature representation through all sub-modalities and then project it to a single model (Zhou et al., 2019a). The third solution is more efficient than the previous two approaches though it is difficult to learn a shared latent representation. The most straightforward way is employing a mean function to map all available sub-modalities into a unified representation, though this may lose important information (Lau et al., 2019). Feature disentanglement and domain adaptation can also be utilized to generate a shared feature representation for missing modalities (Chen et al., 2019a; Shen and Gao, 2019). However, current studies mainly focus on segmentation (especially brain tumor segmentation), while the issue of missing modalities occurring in multi-modality cardiac analysis has not been well investigated. Only one recent study, by Qiu et al. (2023), has addressed this issue by proposing an effective and flexible architecture that can extract and fuse cross-modality features. Their architecture learned a shared feature representation, to handle different numbers of cardiac MRIs and complex combinations of modalities, with output branches targeting specific pathologies.

There exist several studies that attempt to find alternative cardiac imaging modalities for missing modalities, namely modality replacement. Modality replacement aims to find "cheap" modalities (such as CTA and cine/T1 mapping MRIs) to replace the "expensive" ones (such as LGE MRI) by employing the inter-relationship among multi-modality images. For example, the LV scarring areas presented in LGE MRI are correlated to LV Myo thicknesses measured by CTA (Takigawa et al., 2019). Zhang et al. (2019) found that LV myocardial wall motion present in non-enhanced cine MRI could be used to predict chronic MyoI areas. Therefore, one could employ CTA or cine MRI to detect scar regions instead of LGE MRI which is time-consuming to acquire and requires contrast agents (O'Brien et al., 2021). Also, native T1 mapping MRI can be utilized to replace LGE MRI as it exhibits sensitivity to a variety of cardiac diseases (Zhang et al., 2021a). So far, only a few modality replacement works (Zhang et al., 2021a; Takigawa et al., 2019) have been proposed and are mainly devoted to LV Myo pathology analysis. It would be desirable to continue the study of modality relationships and develop modality replacement technologies for other cardiac substructure analyses.

5.2. Optimizing modality selection for cost-effective multi-modality cardiac imaging

Despite the potential benefits of combining multiple modalities, the optimal combination of imaging modality is an important but under-researched field (Bernardino et al., 2022). Although adding new imaging modalities in multi-modality cardiac imaging normally can provide valuable complementary information, it also introduces additional costs including economic costs as well as patient comfort and safety (Hadian et al., 2021). Economic costs can include the cost of equipment, infrastructure, personnel, and imaging contrast agents, which may vary depending on the modality or sequence being added. Some imaging modalities may be more uncomfortable or invasive for patients, leading to increased patient anxiety or discomfort. For example, MRI may be challenging for patients with claustrophobia or other conditions that limit their ability to tolerate the exam. Similarly, imaging modalities that involve ionizing radiation, such as PET and SPECT, may pose potential risks to patients, particularly in pediatric or young patients, and should be minimized whenever possible. These costs need to be weighed against the potential benefits of new imaging modalities in terms of improved diagnostic accuracy and patient outcomes, and thus optimize modality selection.

Therefore, it is important to quantitatively evaluate the incremental addition of new imaging modalities. For example, Ding et al. (2023) found that the contribution of different MRI sequences is varied for multi-sequence based myocardial pathology segmentation. Walker et al. (2013) tested eight different imaging modality combinations of SPECT, MRI and coronary angiography (CA), to evaluate their cost-effectiveness for coronary heart disease (CHD). Their experimental results confirmed the necessity of MRI in the investigation of patients with CHD. Although machine learning has achieved remarkable success in quantitative analysis and diagnosis of cardiac images, the assessment of the appropriateness of modality selection has been overlooked, as data are typically considered an immutable input of the algorithms.

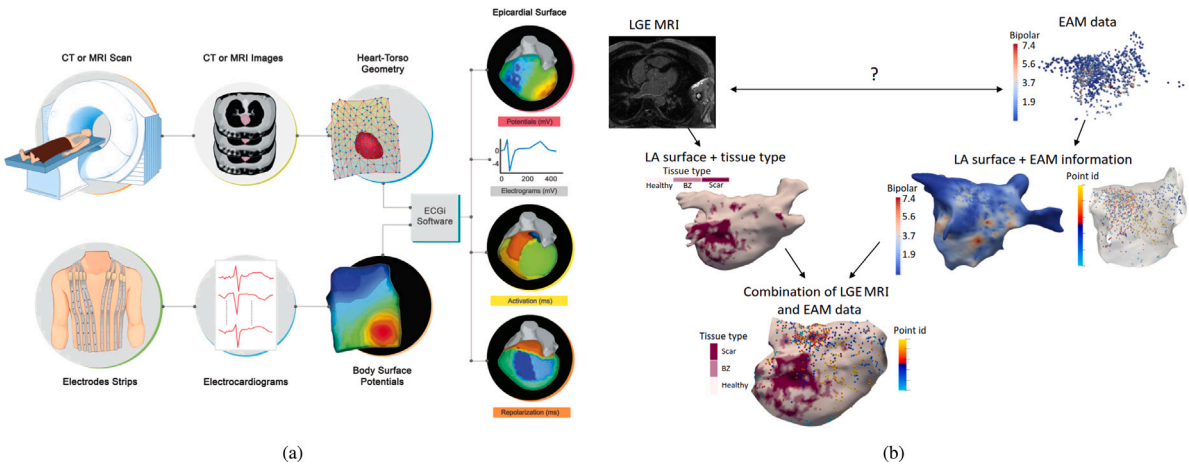

Fig. 14. Two examples of combining cardiac imaging with non-imaging datasets. (a) The procedure of electrocardiographic imaging (ECGi), which combines CT/MRI with ECG signal using mathematical algorithms. Here, body surface potentials are recorded from several electrodes, while the patient-specific heart-torso geometry is obtained from thoracic CT or MRI. Image adapted from Pereira et al. (2020) with permission; (b) The procedure of combining LGE MRI and EAM data for LA scar and border zone (BZ) localization and visualization. Image adapted from Núñez García et al. (2018) with permission.

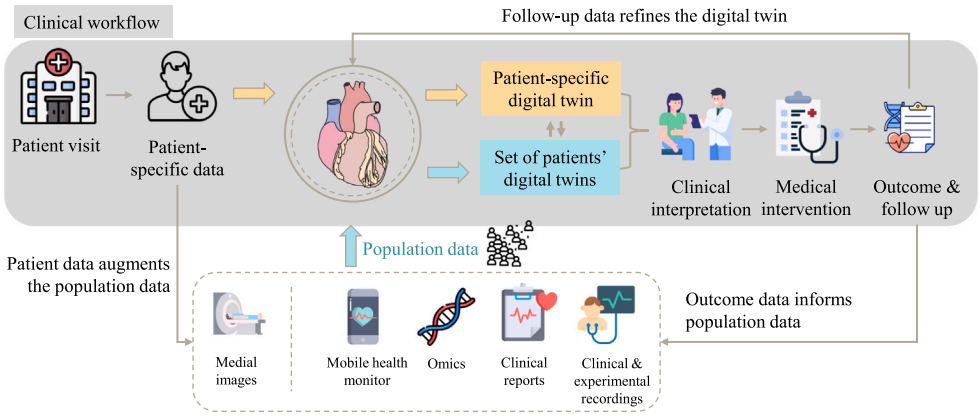

Fig. 15. The procedure of combining imaging and non-imaging data to create cardiac "digital twins", enabling personalized therapies in precision medicine. *Source:* Image designed referring to Corral-Acero et al. (2020).

A recent study by Bernardino et al. (2022) is the only known deep learning-based approach that employs reinforcement learning to sequentially assess the incremental addition of new imaging modalities until sufficient confidence is attained for producing a diagnosis. In the future, with the advancements in deep learning, there is a potential for developing more sophisticated approaches to dynamically select the most appropriate imaging modality (combination) based on the clinical scenario.

5.3. Integration of cardiac imaging with non-imaging information

In addition to multi-modality images, there are many available non-imaging information sources associated with CVDs (Bai et al., 2020; Meyer et al., 2020). Take UK Biobank data as an example, which provides gender, age, BMI, biological information, heart and lung function measures, etc. Bycroft et al. (2018). Among these non-imaging modalities, ECGs can provide a substantial amount of information through its indirect recording of the electrical activity of the heart. This includes scar regions after MyoI, different arrhythmias, the effects of hypertension, as well as information about recovery and cardiac motion. However, its interpretation requires considerable human expertise, and ECGs are limited in their ability to spatially locate and characterize CVDs. The structural information from cardiac imaging data may be complementary to the information provided by ECGs. Body surface ECG mapping data, which provides a larger amount of measurements and includes more spatial information, may be preferable for this purpose (Cochet et al., 2014; Pereira et al., 2020). As presented in Fig. 14(a), one could combine cardiac geometry obtained from CT/MRI with body surface potentials for a more comprehensive noninvasive assessment of cardiac arrhythmias. Specifically, the combined multi-modality information might be able to identify the mechanism of the arrhythmia and locate the circuit or source based on cardiac anatomy and myocardial substrate (Cochet et al., 2014; Li et al., 2023a). It could then be embedded into a 3D mapping system to assist in catheter ablation therapy for atrial or ventricular arrhythmias. Electroanatomical mapping (EAM) can also be integrated with cardiac imaging, such as CT (Itoh et al., 2010), MRI (Reddy et al., 2004), X-ray (Scaglione et al., 2011), to guide ablation procedures (see Fig. 14(b)). Wang et al. (2018) combined cine MRI with intra-ventricular pressure recording data to estimate diastolic myocardial stiffness and stress for personalized biomechanical analysis. Non-imaging information can also be integrated to diagnose cardiac abnormalities, for example, combining ECG and phonocardiogram signals (Chakir et al., 2020; Li et al., 2020d).

Integrating imaging and non-imaging data to generate cardiac "digital twins" is essential for developing personalized therapies (Gillette et al., 2021). Cardiac "digital twins" are virtual representations of an individual's heart that are created using computational models based on data from various sources, such as medical imaging, physiological measurements, genetic Data, and clinical data (see Fig. 15). By combining these diverse data types, the virtual models can simulate the behavior

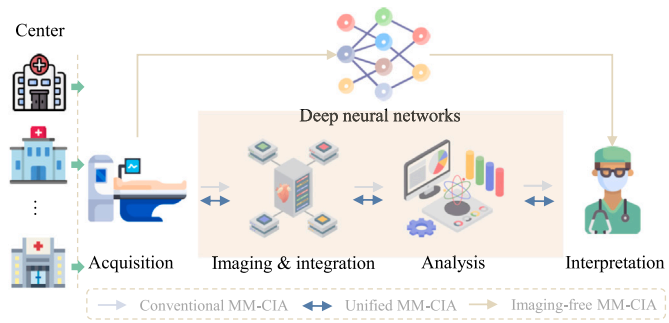

Fig. 16. Traditional vs. future expected multi-center multi-modality cardiac image analysis (MM-CIA) procedures. Conventional MM-CIA is usually only optimized in a single direction and usually not for a clinical endpoint, while unified MM-CIA can transfer information in both directions. Imaging-free MM-CIA even can directly achieve CVD diagnosis from imaging acquisition in the absence of actual imaging.

and function of the real heart in a dynamic and personalized manner, allowing for a holistic understanding of the individual's cardiac physiology, pathology, and response to treatments (Corral-Acero et al., 2020). However, it could be more challenging than the integration of different imaging modalities. This is because it brings a data format variation, resulting in the requirement of intermediate conversion steps for each data. For example, cardiac imaging data usually needs to be converted into a surface, while ECG normally needs to be recorded on a body surface via a multi-electrode vest. It is necessary to develop algorithmic techniques to learn high-level features from two types of data sources for a more elegant combination (Bacoyannis et al., 2021).

5.4. Unified framework for multi-center multi-modality cardiac image analysis

Current multi-modality image processing steps do not include much user interaction, resulting in the limited ability to adjust upstream processing steps based on downstream requirements. Furthermore, these processing stages are not optimized for a clinical endpoint. We therefore expect a unified framework for joint optimization of the whole pipeline with respect to a clinical endpoint, as shown in Fig. 16. For example, Pan et al. (2021) recently developed a joint image synthesis and disease diagnosis framework using incomplete multi-modality neuroimages. This study emphasized the importance of performing a disease-image-oriented joint optimization for disease identification and prediction.

Due to different clinical acquisition protocols across hospitals, acquiring all modalities from all centers is costly and often impossible in clinical settings. Federated learning (also referred to as collaborative learning) is a promising technique that can train models on multiple distributed centers that hold local data samples (Li et al., 2020c). It ensures data sharing while protecting patient data privacy, which would increase the number of available cardiac imaging with different modalities. However, different centers may own misaligned imaging modalities, which raises a realistic challenge for federated learning. Recently, Chang et al. (2022) designed a privacy secure decentralized multi-modality adaptive learning architecture, namely ModalityBank. ModalityBank consists of a domain-specific modulation parameters bank, a central generator, and multiple distributed discriminators located in a variety of medical centers. It can synthesize multi-modality images by switching different sets of configurations to complete missing modalities across data centers. Nevertheless, the domain generalization ability of current DL-based models needs to be significantly improved to handle multi-center multi-modality cardiac datasets (Li et al., 2021c). In the future, with deep neural networks we even could achieve direct CVD diagnosis from imaging acquisition without the requirement of imaging, which however could be too ambitious for now.

5.5. Unified representation of multi-modality cardiac images

The representation of multi-modality images requires a common coordinate system, where the spatial information about cardiac anatomy and physiology from different modalities can be combined. 2D polar maps offer cardiac regional features, permits a comparison of spatial data across patients, and allow a standardized analysis across different imaging modalities. The most popular application of polar maps to the heart is the shaped LV, which is often mapped into a planar bull's-eye plot (Cerqueira et al., 2002). In the bull's-eye polar map, the LV can be divided into different segments (AHA-16, 17 or 18) for simplification and standardization (Lang et al., 2015). Fig. 17(a) presents the most common AHA-17 map, which can be used to visualize regional function information about the LV, including wall motion, perfusion and distribution of scars and edema. Bull's eye maps have also been applied to visualize the CA (Nakahara et al., 2016; Fukushima et al., 2020) and coronary sinus (Ma et al., 2012). Specific to multi-modality image analysis, Nakahara et al. (2016) proposed a fusion based bull's eye map to describe the SPECT-coronary CTA data in a single image. Tavard et al. (2014) employed a bull's eye map to visualize the fused anatomical, functional and electrical data acquired from CT, speckle tracking Echo, and EAM. Although easy to apply in practice, bull's-eye polar map allow only a discrete, coarse representation of LV. To solve this, Paun et al. (2017) provided more general continuous representations of both LV and RV. Compared to the ventricles, it is more challenging to generate a standard planar mapping for the atria which usually have more complex shapes (Li et al., 2022b). There are only a few studies targeting atrial polar mapping (Williams et al., 2017; Nuñez-Garcia et al., 2019, 2020). Their templates were all designed for the most common LA topology with four pulmonary veins and are sensitive to LA topological variants. Fig. 17 (b) presents a universal atrial coordinate mapping system for 2D visualization of both the LA and right atrium.

Polar maps have the advantage of displaying the entire cardiac surface and the coronary anatomy in a single 2D image, but it comes at the expense of undesired geometric distortions. In contrast, a unified 3D cardiac visualization offers a more comprehensive and intuitive representation of the cardiac anatomy and function, allowing for a more accurate and holistic understanding of the cardiac structure and function. For unified 3D biventricular representation, universal ventricular coordinates (UVC) (Bayer et al., 2018) and consistent biventricular coordinate (Cobiveco) (Schuler et al., 2021) has been proposed. Fig. 18 illustrates the basic concept of Cobiveco, where the transmural coordinate increases from the center of the septum, the apicobasal coordinate starts from the bottom and center of the septum, and the rotational coordinate is counter-rotating in the LV and RV free walls and unifies at the septum. All three coordinates have been normalized to range from 0 to 1. For unified 3D atrial representation, universal atrial coordinate (UAC) has been developed for multi-modality cardiac image analysis (Roney et al., 2019). In the future, we expect more comprehensive and robust cardiac polar maps, which can cover more substructures of the heart and adapt for cardiac variations across patients.

6. Conclusion

The development of cardiac multi-modality imaging has already refined clinical decision-making and improved the treatment of patients with CVD. Many studies have been proposed to integrate multiple imaging modalities, to facilitate our understanding of the complex anatomy of the heart and its behavior and a move to more patient-specific interpretation. This review summarizes recent advances in multi-modality cardiac imaging techniques, computing algorithms, public datasets, evaluation measures, clinical applications and future perspectives. We conclude that although the development of machine learning, especially deep learning, has promoted multi-modality cardiac image analysis, there are still many unresolved issues. Note that although the

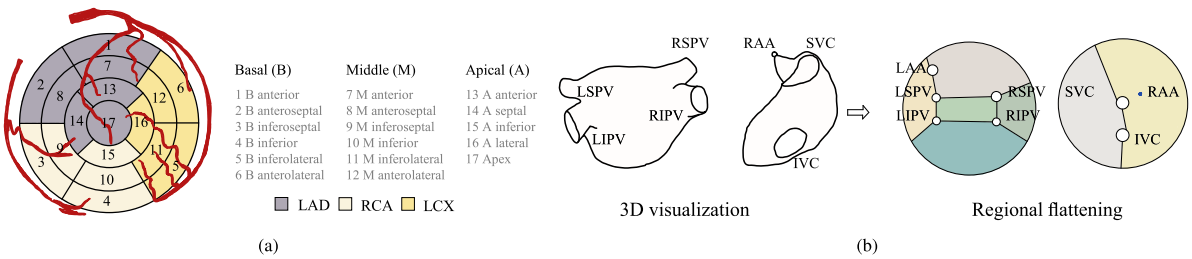

Fig. 17. Illustration of 2D unified representation of the heart for multi-modality cardiac images. (a) LV AHA-17 bull's-eye plot and the coronary arteries (CA) regions with corresponding names (LAD: left anterior descending; RCA: right CA; LCX: left circumflex); (b) Regional flattening of the LA and RA. RAA: RA appendage; SVC/IVC: superior/inferior vena cava; PV: pulmonary vein; LSPV: left superior PV; LIPV: left inferior PV; RSPV: right superior PV; RIPV: right inferior PV.
Source: Image designed referring to Nuñez-Garcia et al. (2019).

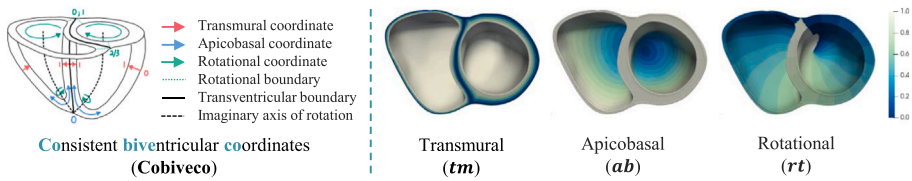

Fig. 18. Illustration of 3D unified representation of the heart for multi-modality cardiac images. Here, we employ the biventricles as example, which can be represented using consistent biventricular coordinates, i.e., the transmural, apicobasal, and rotational coordinates.

review focuses on the multi-modality cardiac image computing, the key issues and obstacles of the computing techniques can be generalized to other medical image analysis applications and utilized in mainstream clinical practice.

Declaration of competing interest

The authors declare that they have no known competing financial interests or personal relationships that could have appeared to influence the work reported in this paper.

Data availability

No data was used for the research described in the article.

Acknowledgments

This work was funded by the CompBioMed 2 Centre of Excellence in Computational Biomedicine (European Commission Horizon 2020 research and innovation programme, grant agreement No. 823712). L. Li was partially supported by the SJTU 2021 Outstanding Doctoral Graduate Development Scholarship, China. X. Zhuang was supported by the National Natural Science Foundation of China (grant no. 61971142, 62111530195 and 62011540404) and the development fund for Shanghai talents, China (no. 2020015).

References

Abu Hazeem, A.A., Dori, Y., Whitehead, K.K., Harris, M.A., Fogel, M.A., Gillespie, M.J., Rome, J.J., Glatz, A.C., 2014. X-ray magnetic resonance fusion modality may reduce radiation exposure and contrast dose in diagnostic cardiac catheterization of congenital heart disease. Catheter. Cardiovasc. Interv. 84 (5), 795–800.

Aguadé-Bruix, S., Pizzi, M., Roque, A., Calabria, H.C., Fernández-Hidalgo, N., Alujas, M.G., 2017. Diagnostic value of 18F-FDG PET/cardiac CT in late prosthetic aortic endocarditis with periprosthetic abscess. Rev. Esp. Med. Nucl. Imagen Mol. 36 (1), 59–60.

Aksoy, T., Unal, G., Demirci, S., Navab, N., Degertekin, M., 2013. Template-based CTA to x-ray angio rigid registration of coronary arteries in frequency domain with automatic x-ray segmentation. Med. Phys. 40 (10), 101903.

Alessio, A.M., Bindschadler, M., Busey, J.M., Shuman, W.P., Caldwell, J.H., Branch, K.R., 2019. Accuracy of myocardial blood flow estimation from dynamic contrast-enhanced cardiac CT compared with PET. Circ.: Cardiovasc. Imaging 12 (6), e008323.

Ammari, A., Mahmoudi, R., Hmida, B., Saouli, R., Bedoui, M.H., 2021. A review of approaches investigated for right ventricular segmentation using short-axis cardiac MRI. IET Image Process..

Angelidis, G., Giamouzis, G., Karagiannis, G., Butler, J., Tsougos, I., Valotassiou, V., Giannakoulas, G., Dimakopoulos, N., Xanthopoulos, A., Skoularigis, J., et al., 2017. SPECT and PET in ischemic heart failure. Heart Fail. Rev. 22 (2), 243–261.

Ankenbrand, M.J., Lohr, D., Schreiber, L.M., 2020. Exploring ensemble applications for multi-sequence myocardial pathology segmentation. In: Myocardial Pathology Segmentation Combining Multi-Sequence CMR Challenge. Springer, pp. 60–67.

Arar, M., Ginger, Y., Danon, D., Bermano, A.H., Cohen-Or, D., 2020. Unsupervised multi-modal image registration via geometry preserving image-to-image translation. In: Proceedings of the IEEE/CVF Conference on Computer Vision and Pattern Recognition. pp. 13410–13419.

Ashburner, J., 2007. A fast diffeomorphic image registration algorithm. Neuroimage 38 (1), 95–113.

Atehortúa, A., Garreau, M., Simon, A., Donal, E., Lederlin, M., Romero, E., 2020. Fusion of 3D real-time echocardiography and cine MRI using a saliency analysis. Int. J. Comput. Assist. Radiol. Surg. 15 (2), 277–285.

Azad, R., Khosravi, N., Dehghanmanshadi, M., Cohen-Adad, J., Merhof, D., 2022. Medical image segmentation on MRI images with missing modalities: A review. arXiv preprint arXiv:2203.06217.

Bacoyannis, T., Ly, B., Cedilnik, N., Cochet, H., Sermesant, M., 2021. Deep learning formulation of electrocardiographic imaging integrating image and signal information with data-driven regularization. EP Eur. 23 (Supplement_1), i55–i62.

Bai, W., Shi, W., O'regan, D.P., Tong, T., Wang, H., Jamil-Copley, S., Peters, N.S., Rueckert, D., 2013. A probabilistic patch-based label fusion model for multi-atlas segmentation with registration refinement: application to cardiac MR images. IEEE Trans. Med. Imaging 32 (7), 1302–1315.

Bai, W., Suzuki, H., Huang, J., Francis, C., Wang, S., Tarroni, G., Guitton, F., Aung, N., Fung, K., Petersen, S.E., et al., 2020. A population-based phenome-wide association study of cardiac and aortic structure and function. Nat. Med. 26 (10), 1654–1662.

Baka, N., Metz, C., Schultz, C., Neefjes, L., van Geuns, R.J., Lelieveldt, B.P., Niessen, W.J., van Walsum, T., de Bruijne, M., 2013. Statistical coronary motion models for 2D+ t/3D registration of X-ray coronary angiography and CTA. Med. Image Anal. 17 (6), 698–709.

Bauer, R.W., Kerl, J.M., Fischer, N., Burkhard, T., Larson, M.C., Ackermann, H., Vogl, T.J., 2010. Dual-energy CT for the assessment of chronic myocardial infarction in patients with chronic coronary artery disease: comparison with 3-T MRI. Am. J. Roentgenol. 195 (3), 639–646.

Bayer, J., Prassl, A.J., Pashaei, A., Gomez, J.F., Frontera, A., Neic, A., Plank, G., Vigmond, E.J., 2018. Universal ventricular coordinates: A generic framework for describing position within the heart and transferring data. Med. Image Anal. 45, 83–93.

Bergquist, P.J., Chung, M.S., Jones, A., Ahlman, M.A., White, C.S., Jeudy, J., 2017. Cardiac applications of PET-MR. Curr. Cardiol. Rep. 19 (5), 1–10.

Bernardino, G., Jonsson, A., Loncaric, F., Martí Castellote, P.-M., Sitges, M., Clarysse, P., Duchateau, N., 2022. Reinforcement learning for active modality selection during diagnosis. In: Medical Image Computing and Computer Assisted Intervention–MICCAI 2022: 25th International Conference, Singapore, September 18–22, 2022, Proceedings, Part I. Springer, pp. 592–601.

Betancur, J., Simon, A., Halbert, E., Tavard, F., Carré, F., Hernández, A., Donal, E., Schnell, F., Garreau, M., 2016. Registration of dynamic multiview 2D ultrasound and late gadolinium enhanced images of the heart: Application to hypertrophic cardiomyopathy characterization. Med. Image Anal. 28, 13–21.

Bhavana, V., Krishnappa, H., 2015. Multi-modality medical image fusion using discrete wavelet transform. Procedia Comput. Sci. 70, 625–631.

Biaggi, P., Fernandez-Golfín, C., Hahn, R., Corti, R., 2015. Hybrid imaging during transcatheter structural heart interventions. Curr. Cardiovasc. Imaging Rep. 8 (9), 1–14.

Bian, C., Yuan, C., Ma, K., Yu, S., Wei, D., Zheng, Y., 2021. Domain adaptation meets zero-shot learning: An annotation-efficient approach to multi-modality medical image segmentation. IEEE Trans. Med. Imaging.

Bian, C., Yuan, C., Wang, J., Li, M., Yang, X., Yu, S., Ma, K., Yuan, J., Zheng, Y., 2020. Uncertainty-aware domain alignment for anatomical structure segmentation. Med. Image Anal. 64, 101732.

Boveiri, H.R., Khayami, R., Javidan, R., Mehdizadeh, A., 2020. Medical image registration using deep neural networks: A comprehensive review. Comput. Electr. Eng. 87, 106767.

Bruge, S., Simon, A., Lederlin, M., Betancur, J., Hernandez, A., Donal, E., Leclercq, C., Garreau, M., 2015. Multi-modal data fusion for cardiac resynchronization therapy planning and assistance. In: 2015 37th Annual International Conference of the IEEE Engineering in Medicine and Biology Society. EMBC, IEEE, pp. 2391–2394.

de Bruijn, S.F., Agema, W.R., Lammers, G.J., van der Wall, E.E., Wolterbeek, R., Holman, E.R., Bollen, E.L., Bax, J.J., 2006. Transesophageal echocardiography is superior to transthoracic echocardiography in management of patients of any age with transient ischemic attack or stroke. Stroke 37 (10), 2531–2534.

Bycroft, C., Freeman, C., Petkova, D., Band, G., Elliott, L.T., Sharp, K., Motyer, A., Vukcevic, D., Delaneau, O., O'Connell, J., et al., 2018. The UK biobank resource with deep phenotyping and genomic data. Nature 562 (7726), 203–209.

Cai, Y., Islam, A., Bhaduri, M., Chan, I., Li, S., 2016. Unsupervised freeview groupwise cardiac segmentation using synchronized spectral network. IEEE Trans. Med. Imaging 35 (9), 2174–2188.

Cal-Gonzalez, J., Rausch, I., Shiyam Sundar, L.K., Lassen, M.L., Muzik, O., Moser, E., Papp, L., Beyer, T., 2018. Hybrid imaging: instrumentation and data processing. Front. Phys. 6, 47.

Camara, O., Oubel, E., Piella, G., Balocco, S., De Craene, M., Frangi, A., 2009. Multi-sequence registration of cine, tagged and delay-enhancement MRI with shift correction and steerable pyramid-based detagging. In: International Conference on Functional Imaging and Modeling of the Heart. Springer, pp. 330–338.

Cao, X., Yang, J., Gao, Y., Guo, Y., Wu, G., Shen, D., 2017. Dual-core steered non-rigid registration for multi-modal images via bi-directional image synthesis. Med. Image Anal. 41, 18–31.

Cerqueira, M.D., Weissman, N.J., Dilsizian, V., Jacobs, A.K., Kaul, S., Laskey, W.K., Pennell, D.J., Rumberger, J.A., Ryan, T., et al., 2002. Standardized myocardial segmentation and nomenclature for tomographic imaging of the heart: a statement for healthcare professionals from the cardiac imaging committee of the council on clinical cardiology of the American heart association. Circulation 105 (4), 539–542.

Chakir, F., Jilbab, A., Nacir, C., Hammouch, A., 2020. Recognition of cardiac abnormalities from synchronized ECG and PCG signals. Phys. Eng. Sci. Med. 43 (2), 673–677.

Chang, Q., Qu, H., Yan, Z., Gao, Y., Baskaran, L., Metaxas, D., 2022. Modality bank: Learn multi-modality images across data centers without sharing medical data. In: 2022 44th Annual International Conference of the IEEE Engineering in Medicine & Biology Society (EMBC). pp. 4758–4763.

Chartsias, A., Joyce, T., Papanastasiou, G., Semple, S., Williams, M., Newby, D.E., Dharmakumar, R., Tsaftaris, S.A., 2019a. Disentangled representation learning in cardiac image analysis. Med. Image Anal. 58, 101535.

Chartsias, A., Papanastasiou, G., Wang, C., Semple, S., Newby, D.E., Dharmakumar, R., Tsaftaris, S.A., 2020. Disentangle, align and fuse for multimodal and semi-supervised image segmentation. IEEE Trans. Med. Imaging 40 (3), 781–792.

Chartsias, A., Papanastasiou, G., Wang, C., Stirrat, C., Semple, S., Newby, D., Dharmakumar, R., Tsaftaris, S.A., 2019b. Multimodal cardiac segmentation using disentangled representation learning. In: International Workshop on Statistical Atlases and Computational Models of the Heart. Springer, pp. 128–137.

Chauhan, K., Chauhan, R.K., Saini, A., 2021. Medical image fusion methods: Review and application in cardiac diagnosis. Image Process. Autom. Diagn. Cardiac Dis. 195–215.

Chen, C., Biffi, C., Tarroni, G., Petersen, S., Bai, W., Rueckert, D., 2019a. Learning shape priors for robust cardiac MR segmentation from multi-view images. In: International Conference on Medical Image Computing and Computer-Assisted Intervention. Springer, pp. 523–531.

Chen, M., Carass, A., Jog, A., Lee, J., Roy, S., Prince, J.L., 2017. Cross contrast multi-channel image registration using image synthesis for MR brain images. Med. Image Anal. 36, 2–14.

Chen, C., Dou, Q., Chen, H., Qin, J., Heng, P.-A., 2019b. Synergistic image and feature adaptation: Towards cross-modality domain adaptation for medical image segmentation. In: Proceedings of the AAAI Conference on Artificial Intelligence. pp. 865–872.

Chen, J., Li, W., Li, H., Zhang, J., 2020b. Deep class-specific affinity-guided convolutional network for multimodal unpaired image segmentation. In: International Conference on Medical Image Computing and Computer-Assisted Intervention. Springer, pp. 187–196.

Chen, X., Lian, C., Wang, L., Deng, H., Kuang, T., Fung, S.H., Gateno, J., Shen, D., Xia, J.J., Yap, P.-T., 2021b. Diverse data augmentation for learning image segmentation with cross-modality annotations. Med. Image Anal. 71, 102060.

Chen, C., Ouyang, C., Tarroni, G., Schlemper, J., Qiu, H., Bai, W., Rueckert, D., 2019c. Unsupervised multi-modal style transfer for cardiac MR segmentation. In: International Workshop on Statistical Atlases and Computational Models of the Heart. Springer, pp. 209–219.

Chen, C., Qin, C., Qiu, H., Tarroni, G., Duan, J., Bai, W., Rueckert, D., 2020a. Deep learning for cardiac image segmentation: a review. Front. Cardiovasc. Med. 7, 25.

Chen, Y., Song, S., Li, S., Wu, C., 2019d. A graph embedding framework for maximum mean discrepancy-based domain adaptation algorithms. IEEE Trans. Image Process. 29, 199–213.

Chen, M., Wang, G., Ding, Z., Li, J., Yang, H., 2020c. Unsupervised domain adaptation for ECG arrhythmia classification. In: 2020 42nd Annual International Conference of the IEEE Engineering in Medicine & Biology Society. EMBC, IEEE, pp. 304–307.

Chen, J., Zhang, Z., Xie, X., Li, Y., Xu, T., Ma, K., Zheng, Y., 2021a. Beyond mutual information: Generative adversarial network for domain adaptation using information bottleneck constraint. IEEE Trans. Med. Imaging.

Choi, J., Radau, P., Xu, R., Wright, G.A., 2016. X-ray and magnetic resonance imaging fusion for cardiac resynchronization therapy. Med. Image Anal. 31, 98–107.

Çimen, S., Gooya, A., Grass, M., Frangi, A.F., 2016. Reconstruction of coronary arteries from X-ray angiography: A review. Med. Image Anal. 32, 46–68.

Clegg, S.D., Chen, S.J., Nijhof, N., Kim, M.S., Salcedo, E.E., Quaife, R.A., Messenger, J.C., Bracken, J., Carroll, J.D., 2015. Integrated 3D echo-x ray to optimize image guidance for structural heart intervention. Cardiovasc. Imaging 8 (3), 371–374.

Clough, J.R., Oksuz, I., Puyol-Antón, E., Ruijsink, B., King, A.P., Schnabel, J.A., 2019. Global and local interpretability for cardiac MRI classification. In: Medical Image Computing and Computer Assisted Intervention–MICCAI 2019: 22nd International Conference, Shenzhen, China, October 13–17, 2019, Proceedings, Part IV 22. Springer, pp. 656–664.

Cochet, H., Dubois, R., Sacher, F., Derval, N., Sermesant, M., Hocini, M., Montaudon, M., Haïssaguerre, M., Laurent, F., Jaïs, P., 2014. Cardiac arrythmias: multimodal assessment integrating body surface ECG mapping into cardiac imaging. Radiology 271 (1), 239–247.

Cordero-Grande, L., Merino-Caviedes, S., Albà, X., i Ventura, R.F., Frangi, A.F., Alberola-López, C., 2012. 3D fusion of cine and late-enhanced cardiac magnetic resonance images. In: 2012 9th IEEE International Symposium on Biomedical Imaging. ISBI, IEEE, pp. 286–289.

Corral-Acero, J., Margara, F., Marciniak, M., Rodero, C., Loncaric, F., Feng, Y., Gilbert, A., Fernandes, J.F., Bukhari, H.A., Wajdan, A., et al., 2020. The 'digital twin'to enable the vision of precision cardiology. Eur. Heart J. 41 (48), 4556–4564.

Courtial, N., Simon, A., Donal, E., Lederlin, M., Garreau, M., 2019. Cardiac cine-MRI/CT registration for interventions planning. In: 2019 IEEE 16th International Symposium on Biomedical Imaging (ISBI 2019). IEEE, pp. 776–779.

Cremers, D., Guetter, C., Xu, C., 2006. Nonparametric priors on the space of joint intensity distributions for non-rigid multi-modal image registration. In: 2006 IEEE Computer Society Conference on Computer Vision and Pattern Recognition (CVPR'06), Vol. 2. IEEE, pp. 1777–1783.

Cuadrado, I., Saura, M., Castejón, B., Martin, A.M., Herruzo, I., Balatsos, N., Zamorano, J.L., Zaragoza, C., 2016. Preclinical models of atherosclerosis. The future of hybrid PET/MR technology for the early detection of vulnerable plaque. Expert Rev. Mol. Med. 18.

Cui, Z., Li, C., Du, Z., Chen, N., Wei, G., Chen, R., Yang, L., Shen, D., Wang, W., 2021b. Structure-driven unsupervised domain adaptation for cross-modality cardiac segmentation. IEEE Trans. Med. Imaging 40 (12), 3604–3616.

Cui, H., Yuwen, C., Jiang, L., Xia, Y., Zhang, Y., 2021a. Bidirectional cross-modality unsupervised domain adaptation using generative adversarial networks for cardiac image segmentation. Comput. Biol. Med. 136, 104726.

Dalca, A., Rakic, M., Guttag, J., Sabuncu, M., 2019. Learning conditional deformable templates with convolutional networks. Adv. Neural Inf. Process. Syst. 32.

De Silva, R., Gutierrez, L.F., Raval, A.N., McVeigh, E.R., Ozturk, C., Lederman, R.J., 2006. X-ray fused with magnetic resonance imaging (XFM) to target endomyocardial injections: validation in a swine model of myocardial infarction. Circulation 114 (22), 2342–2350.

de Vos, B.D., Berendsen, F.F., Viergever, M.A., Sokooti, H., Staring, M., Išgum, I., 2019. A deep learning framework for unsupervised affine and deformable image registration. Med. Image Anal. 52, 128–143.

Degrauwe, S., Monney, P., Qanadli, S.D., Prior, J., Beigelmann-Aubry, C., Masci, P.-G., Eeckhout, E., Muller, O., Iglesias, J.F., 2017. Intrapericardial paraganglioma: the role of integrated advanced multi-modality cardiac imaging for the assessment and management of rare primary cardiac tumors. Cardiol. J. 24 (4), 447–449.

Dewey, M., Siebes, M., Kachelrieß, M., Kofoed, K.F., Maurovich-Horvat, P., Nikolaou, K., Bai, W., Kofler, A., Manka, R., Kozerke, S., et al., 2020. Clinical quantitative cardiac imaging for the assessment of myocardial ischaemia. Nat. Rev. Cardiol. 17 (7), 427–450.

Dey, J., Konik, A., Segars, W.P., King, M.A., 2012. Multi-modal rigid and non-rigid registration for attenuation correction in cardiac SPECT/CT using emission scatter to CT conversion. In: 2012 IEEE Nuclear Science Symposium and Medical Imaging Conference Record (NSS/MIC). IEEE, pp. 2859–2866.

Ding, W., Li, L., Qiu, J., Wang, S., Huang, L., Chen, Y., Yang, S., Zhuang, X., 2023. Aligning multi-sequence CMR towards fully automated myocardial pathology segmentation.

Ding, W., Li, L., Zhuang, X., Huang, L., 2020. Cross-modality multi-atlas segmentation using deep neural networks. In: International Conference on Medical Image Computing and Computer-Assisted Intervention. Springer, pp. 233–242.

Ding, W., Li, L., Zhuang, X., Huang, L., 2021. Unsupervised multi-modality registration network based on spatially encoded gradient information. In: International Workshop on Statistical Atlases and Computational Models of the Heart. pp. 151–159.

Dori, Y., Sarmiento, M., Glatz, A.C., Gillespie, M.J., Jones, V.M., Harris, M.A., Whitehead, K.K., Fogel, M.A., Rome, J.J., 2011. X-ray magnetic resonance fusion to internal markers and utility in congenital heart disease catheterization. Circ.: Cardiovasc. Imaging 4 (4), 415–424.

Döring, M., Braunschweig, F., Eitel, C., Gaspar, T., Wetzel, U., Nitsche, B., Hindricks, G., Piorkowski, C., 2013. Individually tailored left ventricular lead placement: lessons from multimodality integration between three-dimensional echocardiography and coronary sinus angiogram. Europace 15 (5), 718–727.

Dou, Q., Liu, Q., Heng, P.A., Glocker, B., 2020. Unpaired multi-modal segmentation via knowledge distillation. IEEE Trans. Med. Imaging 39 (7), 2415–2425.

Dou, Q., Ouyang, C., Chen, C., Chen, H., Glocker, B., Zhuang, X., Heng, P.-A., 2019. Pnp-AdaNet: Plug-and-play adversarial domain adaptation network at unpaired cross-modality cardiac segmentation. IEEE Access 7, 99065–99076.

Duchateau, N., Rumindo, K., Clarysse, P., 2019. Domain adaptation via dimensionality reduction for the comparison of cardiac simulation models. In: International Conference on Functional Imaging and Modeling of the Heart. Springer, pp. 276–284.

Earls, J.P., Ho, V.B., Foo, T.K., Castillo, E., Flamm, S.D., 2002. Cardiac MRI: recent progress and continued challenges. J. Magn. Reson. Imaging: Off. J. Int. Soc. Magn. Reson. Med. 16 (2), 111–127.

Ebelt, H., Domagala, T., Offhaus, A., Wiora, M., Schwenzky, A., Hoyme, M., Anacker, J., Röhl, P., 2020. Fusion imaging of X-ray and transesophageal echocardiography improves the procedure of left atrial appendage closure. Cardiovasc. Drugs Ther. 34 (6), 781–787.

El-Gamal, F.E.-Z.A., Elmogy, M., Atwan, A., 2016. Current trends in medical image registration and fusion. Egypt. Inform. J. 17 (1), 99–124.

Elif, A., Ilkay, O., 2020. Accurate myocardial pathology segmentation with residual U-net. In: Myocardial Pathology Segmentation Combining Multi-Sequence CMR Challenge. Springer, pp. 128–137.

Faber, T.L., McColl, R.W., Opperman, R.M., Corbett, J.R., Peshock, R.M., 1991. Spatial and temporal registration of cardiac SPECT and MR images: methods and evaluation.. Radiology 179 (3), 857–861.

Faranesh, A.Z., Kellman, P., Ratnayaka, K., Lederman, R.J., 2013. Integration of cardiac and respiratory motion into MRI roadmaps fused with x-ray. Med. Phys. 40 (3), 032302.

Fields, J.M., Davis, J., Girson, L., Au, A., Potts, J., Morgan, C.J., Vetter, I., Riesenberg, L.A., 2017. Transthoracic echocardiography for diagnosing pulmonary embolism: a systematic review and meta-analysis. J. Am. Soc. Echocardiogr. 30 (7), 714–723.

Fonseca, C.G., Backhaus, M., Bluemke, D.A., Britten, R.D., Chung, J.D., Cowan, B.R., Dinov, I.D., Finn, J.P., Hunter, P.J., Kadish, A.H., et al., 2011. The cardiac atlas project—an imaging database for computational modeling and statistical atlases of the heart. Bioinformatics 27 (16), 2288–2295.

Fukushima, K., Matsuo, Y., Nagao, M., Sakai, A., Kihara, N., Onishi, K., Sakai, S., 2020. Patient based bull's eye map display of coronary artery and ventricles from coronary computed tomography angiography. J. Comput. Assist. Tomogr. 44 (1), 26–31.

Gaemperli, O., Schepis, T., Kalff, V., Namdar, M., Valenta, I., Stefani, L., Desbiolles, L., Leschka, S., Husmann, L., Alkadhi, H., et al., 2007. Validation of a new cardiac image fusion software for three-dimensional integration of myocardial perfusion SPECT and stand-alone 64-slice CT angiography. Eur. J. Nucl. Med. Mol. Imaging 34 (7), 1097–1106.

Garcia, J.A., Bhakta, S., Kay, J., Chan, K.-C., Wink, O., Ruijters, D., Carroll, J.D., 2009. On-line multi-slice computed tomography interactive overlay with conventional X-ray: a new and advanced imaging fusion concept. Int. J. Cardiol. 133 (3), e101–e105.

Ghoshhajra, B.B., Takx, R.A., Stone, L.L., Girard, E.E., Brilakis, E.S., Lombardi, W.L., Yeh, R.W., Jaffer, F.A., 2017. Real-time fusion of coronary CT angiography with x-ray fluoroscopy during chronic total occlusion PCI. Eur. Radiol. 27 (6), 2464–2473.

Giannoglou, G.D., Chatzizisis, Y.S., Sianos, G., Tsikaderis, D., Matakos, A., Koutkias, V., Diamantopoulos, P., Maglaveras, N., Parcharidis, G.E., Louridas, G.E., 2006. Integration of multi-modality imaging for accurate 3D reconstruction of human coronary arteries in vivo. Nucl. Instrum. Methods Phys. Res. A 569 (2), 310–313.

Gilardi, M.C., Rizzo, G., Savi, A., Landoni, C., Bettinardi, V., Rossetti, C., Striano, G., Fazio, F., 1998. Correlation of SPECT and PET cardiac images by a surface matching registration technique. Comput. Med. Imaging Graph. 22 (5), 391–398.

Gillette, K., Gsell, M.A., Prassl, A.J., Karabelas, E., Reiter, U., Reiter, G., Grandits, T., Payer, C., Štern, D., Urschler, M., et al., 2021. A framework for the generation of digital twins of cardiac electrophysiology from clinical 12-leads ECGs. Med. Image Anal. 71, 102080.

Gimelli, A., Liga, R., 2013. Clinical applications of multimodality cardiac imaging. Clin. Transl. Imaging 1 (5), 297–304.

Goitein, O., Matetzky, S., Beinart, R., Di Segni, E., Hod, H., Bentancur, A., Konen, E., 2009. Acute myocarditis: noninvasive evaluation with cardiac MRI and transthoracic echocardiography. Am. J. Roentgenol. 192 (1), 254–258.

Gomez, A., Gomez, G., Simpson, J., Valverde, I., 2020. 3D hybrid printed models in complex congenital heart disease: 3D echocardiography and cardiovascular magnetic resonance imaging fusion. Eur. Heart J. 41 (43), 4214.

Gouveia, A.R., Metz, C., Freire, L., Almeida, P., Klein, S., 2017. Registration-by-regression of coronary CTA and X-ray angiography. Comput. Methods Biomech. Biomed. Eng.: Imaging & Vis. 5 (3), 208–220.

Gräni, C., Benz, D.C., Possner, M., Clerc, O.F., Mikulicic, F., Vontobel, J., Stehli, J., Fuchs, T.A., Pazhenkottil, A.P., Gaemperli, O., et al., 2017. Fused cardiac hybrid imaging with coronary computed tomography angiography and positron emission tomography in patients with complex coronary artery anomalies. Congenit. Heart Dis. 12 (1), 49–57.

Grant, E.K., Kanter, J.P., Olivieri, L.J., Cross, R.R., Campbell-Washburn, A., Faranesh, A.Z., Cronin, I., Hamann, K.S., O'Byrne, M.L., Slack, M.C., et al., 2019. X-ray fused with MRI guidance of pre-selected transcatheter congenital heart disease interventions. Catheter. Cardiovasc. Interv. 94 (3), 399–408.

Grau, V., Becher, H., Noble, J.A., 2007. Registration of multiview real-time 3-D echocardiographic sequences. IEEE Trans. Med. Imaging 26 (9), 1154–1165.

Guetter, C., Wacker, M., Xu, C., Hornegger, J., 2007. Registration of cardiac SPECT/CT data through weighted intensity co-occurrence priors. In: International Conference on Medical Image Computing and Computer-Assisted Intervention. Springer, pp. 725–733.

Guetter, C., Xu, C., Sauer, F., Hornegger, J., 2005. Learning based non-rigid multi-modal image registration using Kullback-Leibler divergence. In: International Conference on Medical Image Computing and Computer-Assisted Intervention. Springer, pp. 255–262.

Guo, F., Krahn, P.R., Escartin, T., Roifman, I., Wright, G., 2021a. Cine and late gadolinium enhancement MRI registration and automated myocardial infarct heterogeneity quantification. Magn. Reson. Med. 85 (5), 2842–2855.

Guo, S., Xu, L., Feng, C., Xiong, H., Gao, Z., Zhang, H., 2021b. Multi-level semantic adaptation for few-shot segmentation on cardiac image sequences. Med. Image Anal. 73, 102170.

Gutiérrez, L.F., Silva, R.d., Ozturk, C., Sonmez, M., Stine, A.M., Raval, A.N., Raman, V.K., Sachdev, V., Aviles, R.J., Waclawiw, M.A., et al., 2007. Technology preview: X-ray fused with magnetic resonance during invasive cardiovascular procedures. Catheter. Cardiovasc. Interv. 70 (6), 773–782.

Habijan, M., Babin, D., Galić, I., Leventić, H., Romić, K., Velicki, L., Pižurica, A., 2020. Overview of the whole heart and heart chamber segmentation methods. Cardiovasc. Eng. Technol. 1–23.

Hadeed, K., Hascoët, S., Karsenty, C., Ratsimandresy, M., Dulac, Y., Chausseray, G., Alacoque, X., Fraisse, A., Acar, P., 2018. Usefulness of echocardiographic-fluoroscopic fusion imaging in children with congenital heart disease. Arch. Cardiovasc. Dis. 111 (6–7), 399–410.

Hadian, M., Jabbari, A., Mazaheri, E., Norouzi, M., 2021. What is the impact of clinical guidelines on imaging costs? J. Educ. Health Promot. 10.

Hascoet, S., Hadeed, K., Marchal, P., Dulac, Y., Alacoque, X., Heitz, F., Acar, P., 2015. The relation between atrial septal defect shape, diameter, and area using three-dimensional transoesophageal echocardiography and balloon sizing during percutaneous closure in children. Eur. Heart J.-Cardiovasc. Imaging 16 (7), 747–755.

Hascoët, S., Warin-Fresse, K., Baruteau, A.-E., Hadeed, K., Karsenty, C., Petit, J., Guérin, P., Fraisse, A., Acar, P., 2016. Cardiac imaging of congenital heart diseases during interventional procedures continues to evolve: pros and cons of the main techniques. Arch. Cardiovasc. Dis. 109 (2), 128–142.

Hatt, C.R., Jain, A.K., Parthasarathy, V., Lang, A., Raval, A.N., 2013. MRI—3D ultrasound—X-ray image fusion with electromagnetic tracking for transendocardial therapeutic injections: In-vitro validation and in-vivo feasibility. Comput. Med. Imaging Graph. 37 (2), 162–173.

Havaei, M., Guizard, N., Chapados, N., Bengio, Y., 2016. Hemis: Hetero-modal image segmentation. In: International Conference on Medical Image Computing and Computer-Assisted Intervention. Springer, pp. 469–477.

Housden, R.J., Arujuna, A., Ma, Y., Nijhof, N., Gijsbers, G., Bullens, R., O'Neill, M., Cooklin, M., Rinaldi, C.A., Gill, J., et al., 2012. Evaluation of a real-time hybrid three-dimensional echo and X-ray imaging system for guidance of cardiac catheterisation procedures. In: International Conference on Medical Image Computing and Computer-Assisted Intervention. Springer, pp. 25–32.

Huang, X., Moore, J., Guiraudon, G., Jones, D.L., Bainbridge, D., Ren, J., Peters, T.M., 2009. Dynamic 2D ultrasound and 3D CT image registration of the beating heart. IEEE Trans. Med. Imaging 28 (8), 1179–1189.

Itoh, T., Sasaki, S., Kimura, M., Owada, S., Horiuchi, D., Sasaki, K., Okumura, K., 2010. Three-dimensional cardiac image integration of electroanatomical mapping of only left atrial posterior wall with CT image to guide circumferential pulmonary vein ablation. J. Interv. Cardiac Electrophysiol. 29 (3), 167–173.

Izquierdo-Garcia, D., Hooker, J.M., Schroeder, F.A., Mekkaoui, C., Gilbert, T.M., Panagia, M., Cero, C., Rogers, L., Bhanot, A., Wang, C., et al., 2020. Epigenetic signatures of human myocardium and brown adipose tissue revealed with simultaneous positron emission tomography and magnetic resonance of class I histone deacetylases. MedRxiv.

Jamart, K., Xiong, Z., Talou, G.D.M., Stiles, M.K., Zhao, J., 2020. Mini review: Deep learning for atrial segmentation from late gadolinium-enhanced MRIs. Front. Cardiovasc. Med. 7.

James, A.P., Dasarathy, B.V., 2014. Medical image fusion: A survey of the state of the art. Inf. Fusion 19, 4–19.

Jia, D., Zhuang, X., 2021. Learning-based algorithms for vessel tracking: A review. Comput. Med. Imaging Graph. 101840.

Jiang, H., Wang, C., Chartsias, A., Tsaftaris, S.A., 2020. Max-fusion U-net for multi-modal pathology segmentation with attention and dynamic resampling. In: Myocardial Pathology Segmentation Combining Multi-Sequence CMR Challenge. Springer, pp. 68–81.

Kalidas, V., Tamil, L., 2016. Cardiac arrhythmia classification using multi-modal signal analysis. Physiol. Meas. 37 (8), 1253.

Kang, D., Woo, J., Kuo, C.J., Slomka, P.J., Dey, D., Germano, G., 2012. Heart chambers and whole heart segmentation techniques. J. Electron. Imaging 21 (1), 010901.

Karim, R., Blake, L.-E., Inoue, J., Tao, Q., Jia, S., Housden, R.J., Bhagirath, P., Duval, J.-L., Varela, M., Behar, J.M., et al., 2018. Algorithms for left atrial wall segmentation and thickness–evaluation on an open-source CT and MRI image database. Med. Image Anal. 50, 36–53.

Kaufmann, P.A., Di Carli, M.F., 2009. Hybrid SPECT/CT and PET/CT imaging: the next step in noninvasive cardiac imaging. In: Seminars in Nuclear Medicine, Vol. 39. Elsevier, pp. 341–347.

Khalil, A., Faisal, A., Lai, K.W., Ng, S.C., Liew, Y.M., 2017a. 2D to 3D fusion of echocardiography and cardiac CT for TAVR and TAVI image guidance. Med. Biol. Eng. Comput. 55 (8), 1317–1326.

Khalil, A., Faisal, A., Ng, S.-C., Liew, Y.M., Lai, K.W., 2017b. Mitral valve rigid registration using 2D echocardiography and cardiac computed tomography. In: 2017 International Conference on Applied System Innovation. ICASI, IEEE, pp. 629–632.

Khalil, A., Faisal, A., Ng, S.-C., Liew, Y.M., Lai, K.W., 2017c. Multimodality registration of two-dimensional echocardiography and cardiac CT for mitral valve diagnosis and surgical planning. J. Med. Imaging 4 (3), 037001.

Khalil, A., Ng, S.-C., Liew, Y.M., Lai, K.W., 2018. An overview on image registration techniques for cardiac diagnosis and treatment. Cardiol. Res. Pract. 2018.

Kholiavchenko, M., Sirazitdinov, I., Kubrak, K., Badrutdinova, R., Kuleev, R., Yuan, Y., Vrtovec, T., Ibragimov, B., 2020. Contour-aware multi-label chest X-ray organ segmentation. Int. J. Comput. Assist. Radiol. Surg. 15 (3), 425–436.

Kim, H.W., Farzaneh-Far, A., Kim, R.J., 2009. Cardiovascular magnetic resonance in patients with myocardial infarction: current and emerging applications. J. Am. Coll. Cardiol. 55 (1), 1–16.

Kirişli, H.A., Gupta, V., Shahzad, R., Al Younis, I., Dharampal, A., van Geuns, R.-J., Scholte, A.J., de Graaf, M.A., Joemai, R.M., Nieman, K., et al., 2014. Additional diagnostic value of integrated analysis of cardiac CTA and SPECT MPI using the SMARTVis system in patients with suspected coronary artery disease. J. Nucl. Med. 55 (1), 50–57.

Kiss, G., Åsen, J.P., Bogaert, J., Amundsen, B., Claus, P., D'hooge, J., Torp, H.G., 2011. Multi-modal cardiac image fusion and visualization on the GPU. In: 2011 IEEE International Ultrasonics Symposium. IEEE, pp. 254–257.

Kiss, G., Ford, S., Claus, P., D'hooge, J., Torp, H., 2013. Fusion of 3D echo and cardiac magnetic resonance volumes during live scanning. In: 2013 IEEE International Ultrasonics Symposium. IUS, IEEE, pp. 832–835.

Klaassen, S.H., van Veldhuisen, D.J., Nienhuis, H.L., van den Berg, M.P., Hazenberg, B.P., van der Meer, P., 2020. Cardiac transthyretin-derived amyloidosis: An emerging target in heart failure with preserved ejection fraction? Cardiac Fail. Rev. 6.

Koehler, S., Hussain, T., Blair, Z., Huffaker, T., Ritzmann, F., Tandon, A., Pickardt, T., Sarikouch, S., Latus, H., Greil, G., et al., 2021. Unsupervised domain adaptation from axial to short-axis multi-slice cardiac MR images by incorporating pretrained task networks. IEEE Trans. Med. Imaging.

Kolbitsch, C., Ahlman, M.A., Davies-Venn, C., Evers, R., Hansen, M., Peressutti, D., Marsden, P., Kellman, P., Bluemke, D.A., Schaeffter, T., 2017. Cardiac and respiratory motion correction for simultaneous cardiac PET/MR. J. Nucl. Med. 58 (5), 846–852.

Kots, M., Pozigun, M., Konstantinov, A., Chukanov, V., 2021. Semi-supervised learning for medical image segmentation. In: Proceedings of International Scientific Conference on Telecommunications, Computing and Control. Springer, pp. 245–253.

Koukouraki, S., Pagonidis, K., Perisinakis, K., Klinaki, I., Stathaki, M., Damilakis, J., Karantanas, A., Karkavitsas, N., 2013. Hybrid cardiac imaging: insights in the dilemma of the appropriate clinical management of patients with suspected coronary artery disease. Eur. J. Radiol. 82 (2), 281–287.

Kouw, W.M., Loog, M., 2019. A review of domain adaptation without target labels. IEEE Trans. Pattern Anal. Mach. Intell. 43 (3), 766–785.

Van de Kraats, E.B., Penney, G.P., Tomazevic, D., Van Walsum, T., Niessen, W.J., 2005. Standardized evaluation methodology for 2-D-3-D registration. IEEE Trans. Med. Imaging 24 (9), 1177–1189.

Kramer, C.M., Narula, J., 2010. Fusion images: more informative than the sum of individual images?

Kwan, A.C., Salto, G., Cheng, S., Ouyang, D., 2021. Artificial intelligence in computer vision: Cardiac MRI and multimodality imaging segmentation. Curr. Cardiovasc. Risk Rep. 15 (9), 1–8.

Laczay, B., Patel, D., Grimm, R., Xu, B., 2021. State-of-the-art narrative review: multimodality imaging in electrophysiology and cardiac device therapies. Cardiovasc. Diag. Ther. 11 (3), 881.

Lamare, F., Le Maitre, A., Dawood, M., Schäfers, K., Fernandez, P., Rimoldi, O., Visvikis, D., 2014. Evaluation of respiratory and cardiac motion correction schemes in dual gated PET/CT cardiac imaging. Med. Phys. 41 (7), 072504.

Lang, R.M., Badano, L.P., Mor-Avi, V., Afilalo, J., Armstrong, A., Ernande, L., Flachskampf, F.A., Foster, E., Goldstein, S.A., Kuznetsova, T., et al., 2015. Recommendations for cardiac chamber quantification by echocardiography in adults: an update from the American society of echocardiography and the European association of cardiovascular imaging. Eur. Heart J.-Cardiovasc. Imaging 16 (3), 233–271.

Lau, K., Adler, J., Sjölund, J., 2019. A unified representation network for segmentation with missing modalities. arXiv preprint arXiv:1908.06683.

Laurent, C., Ricard, L., Fain, O., Buvat, I., Adedjouma, A., Soussan, M., Mekinian, A., 2019. PET/MRI in large-vessel vasculitis: clinical value for diagnosis and assessment of disease activity. Sci. Rep. 9 (1), 1–7.

Lawonn, K., Smit, N.N., Bühler, K., Preim, B., 2018. A survey on multimodal medical data visualization. In: Computer Graphics Forum. Wiley Online Library, pp. 413–438.

Lee, W.W., Marinelli, B., Van Der Laan, A.M., Sena, B.F., Gorbatov, R., Leuschner, F., Dutta, P., Iwamoto, Y., Ueno, T., Begieneman, M.P., et al., 2012. PET/MRI of inflammation in myocardial infarction. J. Am. Coll. Cardiol. 59 (2), 153–163.

Li, L., Camps, J., Banerjee, A., Rodriguez, B., Grau, V., et al., 2023a. Influence of myocardial infarction on QRS properties: A simulation study. In: International Conference on Functional Imaging and Modeling of the Heart. pp. 223–232.

Li, P., Hu, Y., Liu, Z.-P., 2021d. Prediction of cardiovascular diseases by integrating multi-modal features with machine learning methods. Biomed. Signal Process. Control 66, 102474.

Li, F.Y., Li, W., Gao, X., Xiao, B., 2021b. A novel framework with weighted decision map based on convolutional neural network for cardiac MR segmentation. IEEE J. Biomed. Health Inf..

Li, F., Li, W., Qin, S., Wang, L., 2021a. MDFA-Net: Multiscale dual-path feature aggregation network for cardiac segmentation on multi-sequence cardiac MR. Knowl.-Based Syst. 215, 106776.

Li, X.-C., Liu, X.-H., Liu, L.-B., Li, S.-M., Wang, Y.-Q., Mead, R.H., 2020d. Evaluation of left ventricular systolic function using synchronized analysis of heart sounds and the electrocardiogram. Heart Rhythm 17 (5), 876–880.

Li, F.P., Rajchl, M., White, J.A., Goela, A., Peters, T.M., 2013. Generation of synthetic 4D cardiac CT images for guidance of minimally invasive beating heart interventions. In: International Conference on Information Processing in Computer-Assisted Interventions. Springer, pp. 11–20.

Li, T., Sahu, A.K., Talwalkar, A., Smith, V., 2020c. Federated learning: Challenges, methods, and future directions. IEEE Signal Process. Mag. 37 (3), 50–60.

Li, W., Wang, L., Li, F., Qin, S., Xiao, B., 2022c. Myocardial pathology segmentation of multi-modal cardiac MR images with a simple but efficient siamese U-shaped network. Biomed. Signal Process. Control 71, 103174.

Li, K., Wang, S., Yu, L., Heng, P.A., 2020a. Dual-teacher++: Exploiting intra-domain and inter-domain knowledge with reliable transfer for cardiac segmentation. IEEE Trans. Med. Imaging 40 (10), 2771–2782.

Li, L., Wu, F., Wang, S., Luo, X., Martín-Isla, C., Zhai, S., Zhang, J., Liu, Y., Zhang, Z., Ankenbrand, M.J., et al., 2023b. MyoPS: a benchmark of myocardial pathology segmentation combining three-sequence cardiac magnetic resonance images. Med. Image Anal. 102808.

Li, L., Wu, F., Yang, G., Xu, L., Wong, T., Mohiaddin, R., Firmin, D., Keegan, J., Zhuang, X., 2020b. Atrial scar quantification via multi-scale CNN in the graph-cuts framework. Med. Image Anal. 60, 101595.

Li, L., Zimmer, V.A., Schnabel, J.A., Zhuang, X., 2021c. AtrialGeneral: Domain generalization for left atrial segmentation of multi-center LGE MRIs. In: International Conference on Medical Image Computing and Computer-Assisted Intervention. Springer, pp. 557–566.

Li, L., Zimmer, V.A., Schnabel, J.A., Zhuang, X., 2022a. AtrialJSQnet: a new framework for joint segmentation and quantification of left atrium and scars incorporating spatial and shape information. Med. Image Anal. 76, 102303.

Li, L., Zimmer, V.A., Schnabel, J.A., Zhuang, X., 2022b. Medical image analysis on left atrial LGE MRI for atrial fibrillation studies: A review. Med. Image Anal. 102360.

Liao, R., Guetter, C., Xu, C., Sun, Y., Khamene, A., Sauer, F., 2006. Learning-based 2D/3D rigid registration using jensen-Shannon divergence for image-guided surgery. In: International Workshop on Medical Imaging and Virtual Reality. Springer, pp. 228–235.

Liao, X., Qian, Y., Chen, Y., Xiong, X., Wang, Q., Heng, P.-A., 2020. MMTLNet: Multi-modality transfer learning network with adversarial training for 3D whole heart segmentation. Comput. Med. Imaging Graph. 85, 101785.

Liu, Y., Du, X., 2020. DUDA: Deep unsupervised domain adaptation learning for multi-sequence cardiac MR image segmentation. In: Chinese Conference on Pattern Recognition and Computer Vision. PRCV, Springer, pp. 503–515.

Liu, J., Liu, H., Gong, S., Tang, Z., Xie, Y., Yin, H., Niyoyita, J.P., 2021. Automated cardiac segmentation of cross-modal medical images using unsupervised multi-domain adaptation and spatial neural attention structure. Med. Image Anal. 102135.

Lu, A., Ahn, S.S., Ta, K., Parajuli, N., Stendahl, J.C., Liu, Z., Boutagy, N.E., Jeng, G.-S., Staib, L.H., O'Donnell, M., et al., 2021. Learning-based regularization for cardiac strain analysis via domain adaptation. IEEE Trans. Med. Imaging 40 (9), 2233–2245.

Luo, X., Zhuang, X., 2020. MvMM-Regnet: A new image registration framework based on multivariate mixture model and neural network estimation. In: International Conference on Medical Image Computing and Computer-Assisted Intervention. Springer, pp. 149–159.

Luo, X., Zhuang, X., 2022. $\mathcal{A}$-Metric: An N-dimensional information-theoretic framework for groupwise registration and deep combined computing. IEEE Trans. Pattern Anal. Mach. Intell..

Ly, B., Cochet, H., Sermesant, M., 2019. Style data augmentation for robust segmentation of multi-modality cardiac MRI. In: International Workshop on Statistical Atlases and Computational Models of the Heart. Springer, pp. 197–208.

Ma, Y., Duckett, S., Chinchapatnam, P., Gao, G., Shetty, A., Rinaldi, C.A., Schaeffter, T., Rhode, K.S., 2010a. MRI to X-ray fluoroscopy overlay for guidance of cardiac resynchronization therapy procedures. In: 2010 Computing in Cardiology. IEEE, pp. 229–232.

Ma, Y., Duckett, S., Chinchapatnam, P., Shetty, A., Rinaldi, C.A., Schaeffter, T., Rhode, K.S., 2010b. Image and physiological data fusion for guidance and modelling of cardiac resynchronization therapy procedures. In: International Workshop on Statistical Atlases and Computational Models of the Heart. Springer, pp. 105–113.

Ma, Y., Karim, R., Housden, R.J., Gijsbers, G., Bullens, R., Rinaldi, C.A., Razavi, R., Schaeffter, T., Rhode, K.S., 2012. Cardiac unfold: a novel technique for image-guided cardiac catheterization procedures. In: International Conference on Information Processing in Computer-Assisted Interventions. Springer, pp. 104–114.

Ma, Y., Penney, G.P., Bos, D., Frissen, P., Rinaldi, C.A., Razavi, R., Rhode, K.S., 2010c. Hybrid echo and x-ray image guidance for cardiac catheterization procedures by using a robotic arm: a feasibility study. Phys. Med. Biol. 55 (13), N371.

Ma, H., Smal, I., Daemen, J., van Walsum, T., 2020. Dynamic coronary roadmapping via catheter tip tracking in X-ray fluoroscopy with deep learning based Bayesian filtering. Med. Image Anal. 61, 101634.

Maes, F., Collignon, A., Vandermeulen, D., Marchal, G., Suetens, P., 1997. Multimodality image registration by maximization of mutual information. IEEE Trans. Med. Imaging 16 (2), 187–198.

Maffessanti, F., Patel, A.R., Patel, M.B., Walter, J.J., Mediratta, A., Medvedofsky, D., Kachenoura, N., Lang, R.M., Mor-Avi, V., 2017. Non-invasive assessment of the haemodynamic significance of coronary stenosis using fusion of cardiac computed tomography and 3D echocardiography. Eur. Heart J.-Cardiovasc. Imaging 18 (6), 670–680.

Mäkelä, T., Clarysse, P., Lötjönen, J., Sipilä, O., Lauerma, K., Hänninen, H., Pyökkimies, E.-P., Nenonen, J., Knuuti, J., Katila, T., et al., 2001. A new method for the registration of cardiac PET and MR images using deformable model based segmentation of the main thorax structures. In: International Conference on Medical Image Computing and Computer-Assisted Intervention. Springer, pp. 557–564.

Makela, T., Clarysse, P., Sipila, O., Pauna, N., Pham, Q.C., Katila, T., Magnin, I.E., 2002. A review of cardiac image registration methods. IEEE Trans. Med. Imaging 21 (9), 1011–1021.

Mäkelä, T., Pham, Q.C., Clarysse, P., Nenonen, J., Lötjönen, J., Sipilä, O., Hänninen, H., Lauerma, K., Knuuti, J., Katila, T., et al., 2003. A 3-D model-based registration approach for the PET, MR and MCG cardiac data fusion. Med. Image Anal. 7 (3), 377–389.

Marinelli, M., Positano, V., Tucci, F., Neglia, D., Landini, L., 2012. Automatic PET-CT image registration method based on mutual information and genetic algorithms. Sci. World J. 2012.

Martin, R., Hascoët, S., Dulac, Y., Peyre, M., Mejean, S., Hadeed, K., Cazavet, A., Leobon, B., Acar, P., 2013. Comparison of two-and three-dimensional transthoracic echocardiography for measurement of aortic annulus diameter in children. Arch. Cardiovasc. Dis. 106 (10), 492–500.

Martín-Isla, C., Asadi-Aghbolaghi, M., Gkontra, P., Campello, V.M., Escalera, S., Lekadir, K., 2020. Stacked BCDU-Net with semantic CMR synthesis: Application to myocardial pathology segmentation challenge. In: Myocardial Pathology Segmentation Combining Multi-Sequence CMR Challenge. Springer, pp. 1–16.

Martinez-Möller, A., Souvatzoglou, M., Navab, N., Schwaiger, M., Nekolla, S.G., 2007. Artifacts from misaligned CT in cardiac perfusion PET/CT studies: frequency, effects, and potential solutions. J. Nucl. Med. 48 (2), 188–193.

McGuirt, D., Mazal, J., Rogers, T., Faranesh, A.Z., Schenke, W., Stine, A., Grant, L., Lederman, R.J., 2016. X-ray fused with magnetic resonance imaging to guide endomyocardial biopsy of a right ventricular mass. Radiol. Technol. 87 (6), 622–626.

Meyer, H.V., Dawes, T.J., Serrani, M., Bai, W., Tokarczuk, P., Cai, J., de Marvao, A., Henry, A., Lumbers, R.T., Gierten, J., et al., 2020. Genetic and functional insights into the fractal structure of the heart. Nature 584 (7822), 589–594.

Mieres, J., Makaryus, A.N., Redberg, R., Shaw, L., 2007. Noninvasive cardiac imaging. Am. Fam. Phys. 75 (8), 1219–1228.

Ming, C.T., Omar, Z., Mahmood, N.H., Kadiman, S., 2015. A literature survey of ultrasound and computed tomography-based cardiac image registration. J. Teknol. 74 (6).

Mortazi, A., Burt, J., Bagci, U., 2017. Multi-planar deep segmentation networks for cardiac substructures from MRI and CT. In: International Workshop on Statistical Atlases and Computational Models of the Heart. Springer, pp. 199–206.

Mylonas, I., Alam, M., Amily, N., Small, G., Chen, L., Yam, Y., Hibbert, B., Chow, B.J., 2014. Quantifying coronary artery calcification from a contrast-enhanced cardiac computed tomography angiography study. Eur. Heart J. Cardiovasc. Imaging 15 (2), 210–215.

Nakahara, T., Iwabuchi, Y., Murakami, K., 2016. Diagnostic performance of 3D bull's eye display of SPECT and coronary CTA fusion. JACC: Cardiovasc. Imaging 9 (6), 703–711.

Nensa, F., Kloth, J., Tezgah, E., Poeppel, T.D., Heusch, P., Goebel, J., Nassenstein, K., Schlosser, T., 2018. Feasibility of FDG-PET in myocarditis: comparison to CMR using integrated PET/MRI. J. Nucl. Cardiol. 25 (3), 785–794.

Núñez García, M., et al., 2018. Left atrial parameterisation and multi-modal data analysis: application to atrial fibrillation (Ph.D. thesis). Universitat Pompeu Fabra.

Nuñez-Garcia, M., Bernardino, G., Alarcón, F., Caixal, G., Mont, L., Camara, O., Butakoff, C., 2020. Fast quasi-conformal regional flattening of the left atrium. IEEE Trans. Vis. Comput. Graphics 26 (8), 2591–2602.

Nuñez-Garcia, M., Bernardino, G., Doste, R., Zhao, J., Camara, O., Butakoff, C., 2019. Standard quasi-conformal flattening of the right and left atria. In: International Conference on Functional Imaging and Modeling of the Heart. Springer, pp. 85–93.

O'Brien, H., Whitaker, J., Sidhu, B.S., Gould, J., Kurzendorfer, T., O'Neill, M.D., Rajani, R., Grigoryan, K., Rinaldi, C.A., Taylor, J., et al., 2021. Automated left ventricle ischemic scar detection in CT using deep neural networks. Front. Cardiovasc. Med. 8.

Oktay, O., Schuh, A., Rajchl, M., Keraudren, K., Gomez, A., Heinrich, M.P., Penney, G., Rueckert, D., 2015. Structured decision forests for multi-modal ultrasound image registration. In: International Conference on Medical Image Computing and Computer-Assisted Intervention. Springer, pp. 363–371.

Olsen, F.J., Bertelsen, L., de Knegt, M.C., Christensen, T.E., Vejlstrup, N., Svendsen, J.H., Jensen, J.S., Biering-Sørensen, T., 2016. Multimodality cardiac imaging for the assessment of left atrial function and the association with atrial arrhythmias. Circ.: Cardiovasc. Imaging 9 (10), e004947.

Oost, C., Lelieveldt, B.P., Üzümcü, M., Lamb, H., Reiber, J.H., Sonka, M., 2003. Multi-view active appearance models: application to X-ray LV angiography and cardiac MRI. In: Biennial International Conference on Information Processing in Medical Imaging. Springer, pp. 234–245.

Ouyang, J., Adeli, E., Pohl, K.M., Zhao, Q., Zaharchuk, G., 2021. Representation disentanglement for multi-modal brain MRI analysis. In: International Conference on Information Processing in Medical Imaging. Springer, pp. 321–333.

Ouyang, C., Kamnitsas, K., Biffi, C., Duan, J., Rueckert, D., 2019. Data efficient unsupervised domain adaptation for cross-modality image segmentation. In: International Conference on Medical Image Computing and Computer-Assisted Intervention. Springer, pp. 669–677.

Paknezhad, M., Brown, M.S., Marchesseau, S., 2020. Improved tagged cardiac MRI myocardium strain analysis by leveraging cine segmentation. Comput. Methods Programs Biomed. 184, 105128.

Pan, Y., Liu, M., Xia, Y., Shen, D., 2021. Disease-image-specific learning for diagnosis-oriented neuroimage synthesis with incomplete multi-modality data. IEEE Trans. Pattern Anal. Mach. Intell..

Papp, L., Zuhayra, M., Koch, R., 2009. Triple-modality normalized mutual information based medical image registration of cardiac PET/CT and SPECT images. In: Bildverarbeitung Für Die Medizin 2009. Springer, pp. 386–389.

Partington, S.L., Kwong, R.Y., Dorbala, S., 2011. Multimodality imaging in the assessment of myocardial viability. Heart Fail. Rev. 16 (4), 381–395.

Paun, B., Bijnens, B., Iles, T., Iaizzo, P.A., Butakoff, C., 2017. Patient independent representation of the detailed cardiac ventricular anatomy. Med. Image Anal. 35, 270–287.

Pauna, N., Croisille, P., Costes, N., Reilhac, A., Mäkelä, T., Cozar, O., Janier, M., Clarysse, P., 2003. A strategy to quantitatively evaluate MRI/PET cardiac rigid registration methods using a Monte Carlo simulator. In: International Workshop on Functional Imaging and Modeling of the Heart. Springer, pp. 194–204.

Pei, C., Wu, F., Huang, L., Zhuang, X., 2021. Disentangle domain features for cross-modality cardiac image segmentation. Med. Image Anal. 71, 102078.

Peifer, J.W., Ezquerra, N.F., Cooke, C.D., Mullick, R., Klein, L., Hyche, M.E., Garcia, E., 1990. Visualization of multimodality cardiac imagery. IEEE Trans. Biomed. Eng. 37 (8), 744–756.

Peng, P., Lekadir, K., Gooya, A., Shao, L., Petersen, S.E., Frangi, A.F., 2016. A review of heart chamber segmentation for structural and functional analysis using cardiac magnetic resonance imaging. Magn. Reson. Mater. Phys. Biol. Med. 29 (2), 155–195.

Peoples, J.J., Bisleri, G., Ellis, R.E., 2019. Deformable multimodal registration for navigation in beating-heart cardiac surgery. Int. J. Comput. Assist. Radiol. Surg. 14 (6), 955–966.

Pereira, H., Niederer, S., Rinaldi, C.A., 2020. Electrocardiographic imaging for cardiac arrhythmias and resynchronization therapy. EP Eur. 22 (10), 1447–1462.

Peters, J., Ecabert, O., Meyer, C., Kneser, R., Weese, J., 2010. Optimizing boundary detection via simulated search with applications to multi-modal heart segmentation. Med. Image Anal. 14 (1), 70–84.

Petitjean, C., Dacher, J.-N., 2011. A review of segmentation methods in short axis cardiac MR images. Med. Image Anal. 15 (2), 169–184.

Piccinelli, M., 2020. Multimodality image fusion, moving forward.

Piccinelli, M., Cho, S.-G., Garcia, E.V., Alexanderson, E., Lee, J.M., Cooke, C.D., Goyal, N., Sanchez, M.S., Folks, R.D., Chen, Z., et al., 2020. Vessel-specific quantification of absolute myocardial blood flow, myocardial flow reserve and relative flow reserve by means of fused dynamic 13NH3 PET and CCTA: ranges in a low-risk population and abnormality criteria. J. Nucl. Cardiol. 27 (5), 1756–1769.

Piccinelli, M., Garcia, E., 2013. Multimodality image fusion for diagnosing coronary artery disease. J. Biomed. Res. 27 (6), 439.

Piccinelli, M., Santana, C., Sirineni, G.K.R., Folks, R.D., Cooke, C.D., Arepalli, C.D., Aguade-Bruix, S., Keidar, Z., Frenkel, A., Israel, O., et al., 2018. Diagnostic performance of the quantification of myocardium at risk from MPI SPECT/CTA 2G fusion for detecting obstructive coronary disease: A multicenter trial. J. Nucl. Cardiol. 25 (4), 1376–1386.

Pluim, J.P., Maintz, J.A., Viergever, M.A., 2003. Mutual-information-based registration of medical images: a survey. IEEE Trans. Med. Imaging 22 (8), 986–1004.

Polycarpou, I., Soultanidis, G., Tsoumpas, C., 2021. Synergistic motion compensation strategies for positron emission tomography when acquired simultaneously with magnetic resonance imaging. Phil. Trans. R. Soc. A 379 (2204), 20200207.

Pontecorboli, G., Figueras i Ventura, R.M., Carlosena, A., Benito, E., Prat-Gonzales, S., Padeletti, L., Mont, L., 2017. Use of delayed-enhancement magnetic resonance imaging for fibrosis detection in the atria: a review. EP Eur. 19 (2), 180–189.

Puyol-Antón, E., Sidhu, B.S., Gould, J., Porter, B., Elliott, M.K., Mehta, V., Rinaldi, C.A., King, A.P., 2022. A multimodal deep learning model for cardiac resynchronisation therapy response prediction. 79, p. 102465,

Puyol-Anton, E., Sinclair, M., Gerber, B., Amzulescu, M.S., Langet, H., De Craene, M., Aljabar, P., Piro, P., King, A.P., 2017. A multimodal spatiotemporal cardiac motion atlas from MR and ultrasound data. Med. Image Anal. 40, 96–110.

Qin, C., Shi, B., Liao, R., Mansi, T., Rueckert, D., Kamen, A., 2019. Unsupervised deformable registration for multi-modal images via disentangled representations. In: International Conference on Information Processing in Medical Imaging. Springer, pp. 249–261.

Qiu, J., Li, L., Wang, S., Zhang, K., Chen, Y., Yang, S., Zhuang, X., 2023. MyoPS-Net: Myocardial pathology segmentation with flexible combination of multi-sequence CMR images. Med. Image Anal. 84, 102694.

Quail, M.A., Sinusas, A.J., 2017. PET-CMR in heart failure-synergistic or redundant imaging? Heart Fail. Rev. 22 (4), 477–489.

Reddy, V.Y., Malchano, Z.J., Holmvang, G., Schmidt, E.J., d'Avila, A., Houghtaling, C., Chan, R.C., Ruskin, J.N., 2004. Integration of cardiac magnetic resonance imaging with three-dimensional electroanatomic mapping to guide left ventricular catheter manipulation: feasibility in a porcine model of healed myocardial infarction. J. Am. Coll. Cardiol. 44 (11), 2202–2213.

Rinuncini, M., Zuin, M., Scaranello, F., Fejzo, M., Rampin, L., Rubello, D., Faggian, G., Roncon, L., 2016. Differentiation of cardiac thrombus from cardiac tumor combining cardiac MRI and 18f-FDG-PET/CT imaging. Int. J. Cardiol. 212, 94–96.

Rischpler, C., Nekolla, S.G., Dregely, I., Schwaiger, M., 2013. Hybrid PET/MR imaging of the heart: potential, initial experiences, and future prospects. J. Nucl. Med. 54 (3), 402–415.

Roche, A., Pennec, X., Malandain, G., Ayache, N., 2001. Rigid registration of 3-D ultrasound with MR images: a new approach combining intensity and gradient information. IEEE Trans. Med. Imaging 20 (10), 1038–1049.

Rokach, L., 2010. Ensemble-based classifiers. Artif. Intell. Rev. 33 (1), 1–39.

Roney, C.H., Pashaei, A., Meo, M., Dubois, R., Boyle, P.M., Trayanova, N.A., Cochet, H., Niederer, S.A., Vigmond, E.J., 2019. Universal atrial coordinates applied to visualisation, registration and construction of patient specific meshes. Med. Image Anal. 55, 65–75.

Sandoval, Z.L., Dillenseger, J.-L., 2013. Evaluation of computed tomography to ultrasound 2D image registration for atrial fibrillation treatment. In: Computing in Cardiology 2013. IEEE, pp. 245–248.

Sang, Y., Cao, M., Mcnitt-Gray, M., Gao, Y., Hu, P., Yan, R., Yang, Y., Ruan, D., 2021. Inter-phase 4D cardiac MRI registration with a motion prior derived from CTA. IEEE Trans. Biomed. Eng..

Sanroma, G., Benkarim, O.M., Piella, G., Camara, O., Wu, G., Shen, D., Gispert, J.D., Molinuevo, J.L., Ballester, M.A.G., Initiative, A.D.N., et al., 2018. Learning non-linear patch embeddings with neural networks for label fusion. Med. Image Anal. 44, 143–155.

Santarelli, M., Positano, V., Marcheschi, P., Landini, L., Marzullo, P., Benassi, A., 2001. Multimodal cardiac image fusion by geometrical features registration and warping. In: Computers in Cardiology 2001. Vol. 28 (Cat. No. 01CH37287). IEEE, pp. 277–280.

Savi, A., Gilardi, M.C., Rizzo, G., Pepi, M., Landoni, C., Rossetti, C., Lucignani, G., Bartorelli, A., Fazio, F., 1995. Spatial registration of echocardiographic and positron emission tomographic heart studies. Eur. J. Nucl. Med. 22 (3), 243–247.

Sazonova, S.I., Nikolaevna Ilyushenkova, J., Valer'evich Zavadovsky, K., Borisovich Lishmanov, Y., 2017. 99 m tc-HMPAO-labeled autologous leukocyte SPECT/CT for diagnosis of bacterial endocarditis of the prosthetic pulmonary conduit: A clinical case. Iran. J. Radiol. 14 (1).

Scaglione, M., Biasco, L., Caponi, D., Anselmino, M., Negro, A., Di Donna, P., Corleto, A., Montefusco, A., Gaita, F., 2011. Visualization of multiple catheters with electroanatomical mapping reduces X-ray exposure during atrial fibrillation ablation. Europace 13 (7), 955–962.

Schuler, S., Pilia, N., Potyagaylo, D., Loewe, A., 2021. Cobiveco: Consistent biventricular coordinates for precise and intuitive description of position in the heart–with matlab implementation. Med. Image Anal. 74, 102247.

Scott, K., Stuart, D., Peoples, J.J., Bisleri, G., Ellis, R.E., 2021. Efficient automatic 2D/3D registration of cardiac ultrasound and CT images. Comput. Methods Biomech. Biomed. Eng.: Imaging Vis. 9 (4), 438–446.

Shade, J.K., Prakosa, A., Popescu, D.M., Yu, R., Okada, D.R., Chrispin, J., Trayanova, N.A., 2021. Predicting risk of sudden cardiac death in patients with cardiac sarcoidosis using multimodality imaging and personalized heart modeling in a multivariable classifier. Sci. Adv. 7 (31), eabi8020.

Shen, Y., Gao, M., 2019. Brain tumor segmentation on MRI with missing modalities. In: International Conference on Information Processing in Medical Imaging. Springer, pp. 417–428.

Shen, J., Qu, Y., Zhang, W., Yu, Y., 2018. Wasserstein distance guided representation learning for domain adaptation. In: Proceedings of the AAAI Conference on Artificial Intelligence, Vol. 32.

Shi, W., Zhuang, X., Wang, H., Duckett, S., Luong, D.V., Tobon-Gomez, C., Tung, K., Edwards, P.J., Rhode, K.S., Razavi, R.S., et al., 2012. A comprehensive cardiac motion estimation framework using both untagged and 3-D tagged MR images based on nonrigid registration. IEEE Trans. Med. Imaging 31 (6), 1263–1275.

Siebermair, J., Kholmovski, E.G., Marrouche, N., 2017. Assessment of left atrial fibrosis by late gadolinium enhancement magnetic resonance imaging: methodology and clinical implications. JACC: Clin. Electrophysiol. 3 (8), 791–802.

Siebermair, J., Lehner, S., Sattler, S.M., Rizas, K.D., Beckmann, B.-M., Becker, A., Schiller, J., Metz, C., Zacherl, M., Vonderlin, N., et al., 2020. Left-ventricular innervation assessed by 123I-SPECT/CT is associated with cardiac events in inherited arrhythmia syndromes. Int. J. Cardiol. 312, 129–135.

Sinha, S., Sinha, U., Czernin, J., Porenta, G., Schelbert, H., 1995. Noninvasive assessment of myocardial perfusion and metabolism: feasibility of registering gated MR and PET images.. AJR. Am. J. Roentgenol. 164 (2), 301–307.

Slomka, P.J., Baum, R.P., 2009. Multimodality image registration with software: state-of-the-art. Eur. J. Nucl. Med. Mol. Imaging 36 (1), 44–55.

Slomka, P.J., Patton, J.A., Berman, D.S., Germano, G., 2009. Advances in technical aspects of myocardial perfusion SPECT imaging. J. Nucl. Cardiol. 16 (2), 255–276.

Smith, M.F., Gibert-Serra, X., Arrate, F., Chellappa, R., Chodnicki, K., Tian, J., Dickfeld, T., Dilsizian, V., 2014. CardioViewer: a novel modular software tool for integrating cardiac electrophysiology voltage measurements and PET/SPECT data. In: 2014 IEEE Nuclear Science Symposium and Medical Imaging Conference (NSS/MIC). IEEE, pp. 1–3.

Spagnolo, P., Giglio, M., Di Marco, D., Cannaò, P.M., Della Bella, P.E., Monti, C.B., Sardanelli, F., et al., 2021. Diagnosis of left atrial appendage thrombus in patients with atrial fibrillation: delayed contrast-enhanced cardiac CT. Eur. Radiol. 31 (3), 1236–1244.

Sturm, B., Powell, K.A., Stillman, A.E., White, R.D., 2003. Registration of 3D CT angiography and cardiac MR images in coronary artery disease patients. Int. J. Cardiovasc. Imaging 19 (4), 281–293.

Takaya, Y., Ito, H., 2020. New horizon of fusion imaging using echocardiography: its progress in the diagnosis and treatment of cardiovascular disease. J. Echocardiogr. 18 (1), 9–15.

Takigawa, M., Martin, R., Cheniti, G., Kitamura, T., Vlachos, K., Frontera, A., Martin, C.A., Bourier, F., Lam, A., Pillois, X., et al., 2019. Detailed comparison between the wall thickness and voltages in chronic myocardial infarction. J. Cardiovasc. Electrophysiol. 30 (2), 195–204.

Tao, X., Wei, H., Xue, W., Ni, D., 2019. Segmentation of multimodal myocardial images using shape-transfer GAN. In: International Workshop on Statistical Atlases and Computational Models of the Heart. Springer, pp. 271–279.

Tavakoli, V., Amini, A.A., 2013. A survey of shaped-based registration and segmentation techniques for cardiac images. Comput. Vis. Image Underst. 117 (9), 966–989.

Tavard, F., Simon, A., Leclercq, C., Donal, E., Hernández, A.I., Garreau, M., 2014. Multimodal registration and data fusion for cardiac resynchronization therapy optimization. IEEE Trans. Med. Imaging 33 (6), 1363–1372.

Tayebi, R.M., Wirza, R., Sulaiman, P.S., Dimon, M.Z., Khalid, F., Al-Surmi, A., Mazaheri, S., 2015. 3D multimodal cardiac data reconstruction using angiography and computerized tomographic angiography registration. J. Cardiothorac. Surg. 10 (1), 1–25.

Tirupal, T., Mohan, B.C., Kumar, S.S., 2021. Multimodal medical image fusion techniques–a review. Curr. Signal Transduct. Ther. 16 (2), 142–163.

Tobon-Gomez, C., De Craene, M., Mcleod, K., Tautz, L., Shi, W., Hennemuth, A., Prakosa, A., Wang, H., Carr-White, G., Kapetanakis, S., et al., 2013. Benchmarking framework for myocardial tracking and deformation algorithms: An open access database. Med. Image Anal. 17 (6), 632–648.

Tobon-Gomez, C., Geers, A.J., Peters, J., Weese, J., Pinto, K., Karim, R., Ammar, M., Daoudi, A., Margeta, J., Sandoval, Z., et al., 2015. Benchmark for algorithms segmenting the left atrium from 3D CT and MRI datasets. IEEE Trans. Med. Imaging 34 (7), 1460–1473.

Tomar, D., Lortkipanidze, M., Vray, G., Bozorgtabar, B., Thiran, J.-P., 2021. Self-attentive spatial adaptive normalization for cross-modality domain adaptation. IEEE Trans. Med. Imaging.

Tomkowiak, M.T., Klein, A.J., Vigen, K.K., Hacker, T.A., Speidel, M.A., VanLysel, M.S., Raval, A.N., 2011. Targeted transendocardial therapeutic delivery guided by MRI—x-ray image fusion. Catheter. Cardiovasc. Interv. 78 (3), 468–478.

Tong, Q., Ning, M., Si, W., Liao, X., Qin, J., 2017. 3D deeply-supervised U-net based whole heart segmentation. In: International Workshop on Statistical Atlases and Computational Models of the Heart. Springer, pp. 224–232.

Tseng, K.-L., Lin, Y.-L., Hsu, W., Huang, C.-Y., 2017. Joint sequence learning and cross-modality convolution for 3D biomedical segmentation. In: Proceedings of the IEEE Conference on Computer Vision and Pattern Recognition. pp. 6393–6400.

Turco, A., Gheysens, O., Nuyts, J., Duchenne, J., Voigt, J.-U., Claus, P., Vunckx, K., 2016. Impact of CT-based attenuation correction on the registration between dual-gated cardiac PET and high-resolution CT. IEEE Trans. Nucl. Sci. 63 (1), 180–192.

Utah, 2012. Cardiac MRI data from the comprehensive arrhythmia research and management (CARMA) center at the university of utah. http://insight-journal.org/midas/%20collection/view/197/.

Valsangiacomo Buechel, E.R., Mertens, L.L., 2012. Imaging the right heart: the use of integrated multimodality imaging. Eur. Heart J. 33 (8), 949–960.

Vernikouskaya, I., Rottbauer, W., Seeger, J., Gonska, B., Rasche, V., Wöhrle, J., 2018. Patient-specific registration of 3D CT angiography (CTA) with X-ray fluoroscopy for image fusion during transcatheter aortic valve implantation (TAVI) increases performance of the procedure. Clin. Res. Cardiol. 107 (6), 507–516.

Vesal, S., Gu, M., Kosti, R., Maier, A., Ravikumar, N., 2021. Adapt everywhere: Unsupervised adaptation of point-clouds and entropy minimisation for multi-modal cardiac image segmentation. IEEE Trans. Med. Imaging.

Wachinger, C., Navab, N., 2012. Entropy and Laplacian images: Structural representations for multi-modal registration. Med. Image Anal. 16 (1), 1–17.

Walimbe, V., Zagrodsky, V., Raja, S., Jaber, W.A., DiFilippo, F.P., Garcia, M.J., Brunken, R.C., Thomas, J.D., Shekhar, R., 2003. Mutual information-based multimodality registration of cardiac ultrasound and SPECT images: a preliminary investigation. Int. J. Cardiovasc. Imaging 19 (6), 483–494.

Walker, S., Girardin, F., McKenna, C., Ball, S.G., Nixon, J., Plein, S., Greenwood, J.P., Sculpher, M., 2013. Cost-effectiveness of cardiovascular magnetic resonance in the diagnosis of coronary heart disease: an economic evaluation using data from the CE-MARC study. Heart 99 (12), 873–881.

Wang, J., Huang, H., Chen, C., Ma, W., Huang, Y., Ding, X., 2019a. Multi-sequence cardiac MR segmentation with adversarial domain adaptation network. In: International Workshop on Statistical Atlases and Computational Models of the Heart. Springer, pp. 254–262.

Wang, Z.J., Wang, V.Y., Bradley, C.P., Nash, M.P., Young, A.A., Cao, J.J., 2018. Left ventricular diastolic myocardial stiffness and end-diastolic myofibre stress in human heart failure using personalised biomechanical analysis. J. Cardiovasc. Transl. Res. 11 (4), 346–356.

Wang, K.-N., Yang, X., Miao, J., Li, L., Yao, J., Zhou, P., Xue, W., Zhou, G.-Q., Zhuang, X., Ni, D., 2022. AWSnet: An auto-weighted supervision attention network for myocardial scar and edema segmentation in multi-sequence cardiac magnetic resonance images. Med. Image Anal. 102362.

Wang, X., Yang, S., Tang, M., Wei, Y., Han, X., He, L., Zhang, J., 2019b. SK-Unet: an improved U-net model with selective kernel for the segmentation of multi-sequence cardiac MR. In: International Workshop on Statistical Atlases and Computational Models of the Heart. Springer, pp. 246–253.

Wang, R., Zheng, G., 2021. CyCMIS: Cycle-consistent cross-domain medical image segmentation via diverse image augmentation. Med. Image Anal. 102328.

Wang, X., Zhu, F., Peng, Y., Shen, C., Ye, Z., Zhou, C., 2021. Semantic constraint based unsupervised domain adaptation for cardiac segmentation. Adv. Pure Math. 11 (6), 628–643.

Watanabe, N., Toh, N., Takaya, Y., Nakayama, R., Yokohama, F., Osawa, K., Miyoshi, T., Akagi, T., Kanazawa, S., Ito, H., 2021. Usefulness of cardiac fusion imaging with computed tomography and Doppler echocardiography in the assessment of conduit stenosis in complex adult congenital heart disease. J. Cardiol. 78 (6), 473–479.

Williams, S.E., Tobon-Gomez, C., Zuluaga, M.A., Chubb, H., Butakoff, C., Karim, R., Ahmed, E., Camara, O., Rhode, K.S., 2017. Standardized unfold mapping: a technique to permit left atrial regional data display and analysis. J. Interv. Card. Electrophysiol. 50 (1), 125–131.

Woo, J., Slomka, P.J., Dey, D., Cheng, V.Y., Hong, B.-W., Ramesh, A., Berman, D.S., Karlsberg, R.P., Kuo, C.-C.J., Germano, G., 2009. Geometric feature-based multimodal image registration of contrast-enhanced cardiac CT with gated myocardial perfusion SPECT. Med. Phys. 36 (12), 5467–5479.

Wu, F., Li, L., Yang, G., Wong, T., Mohiaddin, R., Firmin, D., Keegan, J., Xu, L., Zhuang, X., 2018. Atrial fibrosis quantification based on maximum likelihood estimator of multivariate images. In: International Conference on Medical Image Computing and Computer-Assisted Intervention. Springer, pp. 604–612.

Wu, Y., Tang, Z., Li, B., Firmin, D., Yang, G., 2021. Recent advances in fibrosis and scar segmentation from cardiac MRI: A state-of-the-art review and future perspectives. Front. Physiol. 12.

Wu, F., Zhuang, X., 2020. CF distance: A new domain discrepancy metric and application to explicit domain adaptation for cross-modality cardiac image segmentation. IEEE Trans. Med. Imaging 39 (12), 4274–4285.

Wu, F., Zhuang, X., 2021. Unsupervised domain adaptation with variational approximation for cardiac segmentation. IEEE Trans. Med. Imaging.

Xu, Y., Cao, H., Mao, K., Chen, Z., Xie, L., Yang, J., 2022. Aligning correlation information for domain adaptation in action recognition. IEEE Trans. Neural Netw. Learn. Syst..

Xue, Y., Feng, S., Zhang, Y., Zhang, X., Wang, Y., 2020. Dual-task self-supervision for cross-modality domain adaptation. In: International Conference on Medical Image Computing and Computer-Assisted Intervention. Springer, pp. 408–417.

Yoneyama, H., Nakajima, K., Taki, J., Wakabayashi, H., Matsuo, S., Konishi, T., Okuda, K., Shibutani, T., Onoguchi, M., Kinuya, S., 2019. Ability of artificial intelligence to diagnose coronary artery stenosis using hybrid images of coronary computed tomography angiography and myocardial perfusion SPECT. Eur. J. Hybrid Imaging 3 (1), 1–14.

Yu, C., Gao, Z., Zhang, W., Yang, G., Zhao, S., Zhang, H., Zhang, Y., Li, S., 2020a. Multitask learning for estimating multitype cardiac indices in MRI and CT based on adversarial reverse mapping. IEEE Trans. Neural Netw. Learn. Syst. 32 (2), 493–506.

Yu, H., Zha, S., Huangfu, Y., Chen, C., Ding, M., Li, J., 2020b. Dual attention U-net for multi-sequence cardiac MR images segmentation. In: Myocardial Pathology Segmentation Combining Multi-Sequence CMR Challenge. Springer, pp. 118–127.

Zandieh, S., Bernt, R., Mirzaei, S., Haller, J., Hergan, K., 2018. Image fusion between 18F-FDG PET and MRI in cardiac sarcoidosis: a case series. J. Nucl. Cardiol. 25 (4), 1128–1134.

Zeng, G., Lerch, T.D., Schmaranzer, F., Zheng, G., Burger, J., Gerber, K., Tannast, M., Siebenrock, K., Gerber, N., 2021. Semantic consistent unsupervised domain adaptation for cross-modality medical image segmentation. In: International Conference on Medical Image Computing and Computer-Assisted Intervention. Springer, pp. 201–210.

Zhai, S., Gu, R., Lei, W., Wang, G., 2020. Myocardial edema and scar segmentation using a coarse-to-fine framework with weighted ensemble. In: Myocardial Pathology Segmentation Combining Multi-Sequence CMR Challenge. Springer, pp. 49–59.

Zhang, Q., Burrage, M.K., Lukaschuk, E., Shanmuganathan, M., Popescu, I.A., Nikolaidou, C., Mills, R., Werys, K., Hann, E., Barutcu, A., et al., 2021a. Toward replacing late gadolinium enhancement with artificial intelligence virtual native enhancement for gadolinium-free cardiovascular magnetic resonance tissue characterization in hypertrophic cardiomyopathy. Circulation 144 (8), 589–599.

Zhang, Z., Chen, X., Wan, Q., Wang, H., Qi, N., You, Z., Yuan, J., Hu, L., Sun, H., Wang, Z., et al., 2022. A two-stage cardiac PET and late gadolinium enhancement MRI co-registration method for improved assessment of non-ischemic cardiomyopathies using integrated PET/MR. Eur. J. Nucl. Med. Mol. Imaging 1–10.

Zhang, W., Noble, J.A., Brady, J.M., 2006. Real time 3-D ultrasound to MR cardiovascular image registration using a phase-based approach. In: 3rd IEEE International Symposium on Biomedical Imaging: Nano To Macro, 2006. IEEE, pp. 666–669.

Zhang, X., Noga, M., Punithakumar, K., 2020. Fully automated deep learning based segmentation of normal, infarcted and edema regions from multiple cardiac MRI sequences. In: Myocardial Pathology Segmentation Combining Multi-Sequence CMR Challenge. Springer, pp. 82–91.

Zhang, Y., Sidibé, D., Morel, O., Mériaudeau, F., 2021b. Deep multimodal fusion for semantic image segmentation: A survey. Image Vis. Comput. 105, 104042.

Zhang, N., Yang, G., Gao, Z., Xu, C., Zhang, Y., Shi, R., Keegan, J., Xu, L., Zhang, H., Fan, Z., et al., 2019. Deep learning for diagnosis of chronic myocardial infarction on nonenhanced cardiac cine MRI. Radiology 291 (3), 606–617.

Zhang, Z., Yang, L., Zheng, Y., 2018. Translating and segmenting multimodal medical volumes with cycle-and shape-consistency generative adversarial network. In: Proceedings of the IEEE Conference on Computer Vision and Pattern Recognition. pp. 9242–9251.

Zhao, Z., Boutry, N., Puybareau, É., 2020. Stacked and parallel U-nets with multi-output for myocardial pathology segmentation. In: Myocardial Pathology Segmentation Combining Multi-Sequence CMR Challenge. Springer, pp. 138–145.

Zheng, Y., Lu, X., Georgescu, B., Littmann, A., Mueller, E., Comaniciu, D., 2009. Robust object detection using marginal space learning and ranking-based multi-detector aggregation: Application to left ventricle detection in 2D MRI images. In: 2009 IEEE Conference on Computer Vision and Pattern Recognition. IEEE, pp. 1343–1350.

Zheng, R., Zhao, X., Zhao, X., Wang, H., 2019. Deep learning based multi-modal cardiac MR image segmentation. In: International Workshop on Statistical Atlases and Computational Models of the Heart. Springer, pp. 263–270.

Zhou, C., Chan, H.-P., Chughtai, A., Patel, S., Hadjiiski, L.M., Wei, J., Kazerooni, E.A., 2012. Automated coronary artery tree extraction in coronary CT angiography using a multiscale enhancement and dynamic balloon tracking (MSCAR-DBT) method. Comput. Med. Imaging Graph. 36 (1), 1–10.

Zhou, W., Hou, X., Piccinelli, M., Tang, X., Tang, L., Cao, K., Garcia, E.V., Zou, J., Chen, J., 2014. 3D fusion of LV venous anatomy on fluoroscopy venograms with epicardial surface on SPECT myocardial perfusion images for guiding CRT LV lead placement. JACC: Cardiovasc. Imaging 7 (12), 1239–1248.

Zhou, T., Liu, M., Thung, K.-H., Shen, D., 2019a. Latent representation learning for Alzheimer's disease diagnosis with incomplete multi-modality neuroimaging and genetic data. IEEE Trans. Med. Imaging 38 (10), 2411–2422.

Zhou, T., Ruan, S., Canu, S., 2019b. A review: Deep learning for medical image segmentation using multi-modality fusion. Array 3, 100004.

Zhuang, X., 2013. Challenges and methodologies of fully automatic whole heart segmentation: a review. J. Healthc. Eng. 4 (3), 371–407.

Zhuang, X., 2019. Multivariate mixture model for myocardial segmentation combining multi-source images. IEEE Trans. Pattern Anal. Mach. Intell. 41 (12), 2933–2946.

Zhuang, X., Li, L., 2020. Myocardial Pathology Segmentation Combining Multi-Sequence Cardiac Magnetic Resonance Images: First Challenge, MyoPS 2020, Held in Conjunction with MICCAI 2020, Lima, Peru, October 4, 2020, Proceedings, Vol. 12554. Springer Nature.

Zhuang, X., Li, L., Payer, C., Štern, D., Urschler, M., Heinrich, M.P., Oster, J., Wang, C., Smedby, Ö., Bian, C., et al., 2019. Evaluation of algorithms for multi-modality whole heart segmentation: an open-access grand challenge. Med. Image Anal. 58, 101537.

Zhuang, X., Shen, J., 2016. Multi-scale patch and multi-modality atlases for whole heart segmentation of MRI. Med. Image Anal. 31, 77–87.

Zhuang, X., Xu, J., Luo, X., Chen, C., Ouyang, C., Rueckert, D., Campello, V.M., Lekadir, K., Vesal, S., RaviKumar, N., et al., 2022. Cardiac segmentation on late gadolinium enhancement MRI: a benchmark study from multi-sequence cardiac MR segmentation challenge. 81, p. 102528,

Zorinas, A., Janusauskas, V., Davidavicius, G., Puodziukaite, L., Zakarkaite, D., Kramena, R., Čypienė, R., Bilkis, V., Rucinskas, K., Aidietis, A., et al., 2017. Fusion of real-time 3D transesophageal echocardiography and cardiac fluoroscopy imaging in transapical catheter-based mitral paravalvular leak closure. Adv. Interv. Cardiol. 13 (3), 263.